FLUOROUS-PHASE PURIFICATION OF ^{99m}Tc RADIOPHARMACEUTICALS

FLUOROUS-PHASE PURIFICATION OF ^{99m}Tc RADIOPHARMACEUTICALS

By

Justin W Hicks, H.B.Sc.

A Thesis

Submitted to the School of Graduate Studies

In Partial Fulfillment of the Requirements

For the Degree

Masters of Science

McMaster University

MASTERS OF SCIENCE (2010)
(Chemistry)

McMASTER UNIVERSITY
Hamilton, Ontario

Title:	FLUOROUS-PHASE PURIFICATION OF ^{99m}Tc RADIOPHARMACEUTICALS
Author:	Justin W Hicks, H.B.Sc. (Mount Allison University)
Supervisor:	Professor John F Valliant
Number of Pages:	xvi, 128

Abstract

To produce Tc-based radiopharmaceuticals in high effective specific activity the excess precursor ligand must be removed. A new and convenient solid-phase ligand capture method of a resin-bound Cu chelate was recently developed to remove unlabeled ligand.[1] Herein, the impact of size on the purification was evaluated using three well-defined resin sizes and a model chelate system, where the average capture efficiency was 89.1 ± 3.3% and loss due to non-specific binding was 23.4 ± 1.6%.

A complementary solution-phase strategy was developed employing fluorous chemistry to remove unlabeled chelate-derivatives with less loss of product. The novel fluorous analog to the solid-phase copper chelate was synthesized in three steps (70% overall yield). Using the same model Tc(I) chelate, >99% of the ligand was captured by the fluorous ligand capture (FLC) method and the extent of non-specific binding was 65% lower than the solid-phase equivalent. A peptide conjugate was then used to further test the general utility of the FLC method with comparable ligand removal (95.1 ±0.8%) and non-specific binding (12.1 ± 1.2%).

Attempts were made to automate the FLC method using a microfluidic device with no detrimental effect to either the radiochemical yield (4.15 ± 1.0% non-specific binding) or the efficiency of ligand capture (99.74 ± 0.04%). A second strategy involved preloading the FLC agent onto fluorous silica and capturing the excess ligand (99.85 ± 0.02%) and peptide (95± 1%) as the radiolabeling mixture was washed over the cartridge with 2.25 ± 0.55% and 33.3 ± 3.2% product lost, respectively. This approach can now be incorporated into a new generation of instant kits or an integrated microfluidic preparation of molecular imaging probes in high effective specific activity.

Acknowledgements

Even though he may be the busiest man I have ever met, John was always there to help and for that I am forever grateful. From attending conference to conversations over coffee or pints, his advice was invaluable and I only hope that I can remember every word. Thanks to him, I am leaving McMaster with a great education. Luckily, other members of the group, past and present, have also gained from the example he has set. Their help with small and large problems could never be replaced. Although conversations were not always scientific, they were more often than not a delight.

The past two and a half years has been full of ups and scattered with downs. Whether times were good or bad, many lessons were learned. For their constant support, I have to thank my family and friends. My family is always there to tell me how proud they are of me and push me back up from a low. My friends in ABB keep a smile on my face even on the darkest, most frustrating days in the lab. My fiancée Emily has seen and heard it all. She has been there for each step I've taken and is the driving force in my life. Each day she tells me how proud she is of me and more than once it has given me the confidence to come back in the next day.

Furthermore, I'd like to thank my other committee member, Dr. Brennan, for all of his assistance and valuable input during my studies. I owe a debt of gratitude to all of the members of the facility services, especially Drs. Hughes and Green for all their help with NMR and MS. Lastly, I'd like to thank NSERC, Biotage, Molecular Insight Pharmaceuticals, and the OICR for funding my research herein.

Table of Contents

List of Figures

List of Schemes

List of Tables

List of Abbreviations

Ar	aryl
B_{max}	maximum expression of receptor
BPV	bispyridyl valeric acid
Bq	Becquerel(s)
br	broad
calcd.	calculated
cm^{-1}	wavenumbers
CT	computed tomography
d	doublet
δ	chemical shift in ppm
DCM	dimethylchloride
DIPEA	diisopropylethyl amine
DMF	dimethylformamide
DTV	dithiazole valeric acid
ErbB2	human epidermal growth factor
ESI	electrospray ionization
Et	ethyl
EtOH	ethanol
keV	kiloelectron volts
FC-72	perfluorinated hexanes
FDG	fluorodeoxyglucose
FLC	fluorous ligand capture
F-SPE	fluorous solid-phase extraction
FT	Fourier transformed
γ	gamma

HRMS	high-resolution mass spectroscopy
HPLC	high performance liquid chromatography
Hz	hertz
IPA	isopropanol
IR	infrared
J	coupling constant
K_D	equilibrium dissociation constant
m	multiplet (NMR), medium (IR)
Me	methyl
MeCN	acetonitrile
MeOH	methanol
MHz	megahertz
MIBG	*meta*-iodobenzlguanidine
mol	moles
mp	melting point
MRI	magnetic resonance imaging
MS	mass spectroscopy
NMR	nuclear magnetic resonance
PDMS	poly(dimethyl)siloxane
PET	positron emission tomography
Ph	phenyl
ppm	parts per million
q	quartet
RCP	radiochemical purity
RCY	radiochemical yield
s	singlet (NMR), strong (IR)

SAAC	single amino acid chelate
SPECT	single photon emission computed tomography
t	triplet
THF	tetrahydrofuran
TLC	thin layer chromatography
T:NT	target to non-target ratio
t_R	retention time
US	ultrasound
UV	ultraviolet
w	weak

Chapter 1

1. Introduction

1.1 - Molecular Imaging

In medicine, early diagnosis is a key to effectively treating most diseases.[2] Molecular imaging enables the non-invasive visualization of biochemical processes *in vivo*, resulting in the detection of a disease prior to a major physiological change.[3] Identifying the disease on a biochemical basis leads to selecting ideal treatment options and eliminates potentially unnecessary biopsies or interventions.[4] Currently, there is a suite of non-invasive diagnostic imaging modalities which are used to identify diseases or injuries *in vivo*. Examples of these modalities are computed tomography (CT),[5] magnetic resonance imaging (MRI),[6] optical,[7] ultrasound (US),[8] nuclear imaging methods [9], and combinations of these techniques. CT, MRI, and US are effective at distinguishing anatomical abnormalities from healthy tissue, however, such changes occur after the disease has had time to progress, generally leading to a poor prognosis. As mentioned, a more attractive situation would be the detection of disease at a molecular level and at the genesis of disease emergence. As such, the ability to visualize biochemical changes may lead to earlier diagnosis but can also be used as an indicator of aggressiveness or malignancy of the disease.[2] Another benefit to molecular imaging, beyond solely disease detection, is the application of personalized therapeutic pathways to suit the individual patient pathology.[3, 10]

While there are some examples of molecular imaging using MRI and US contrast agents, nuclear medicine techniques, which include of positron emission tomography (PET)[11] and single photon emission computed tomography (SPECT) are the most widely used molecular imaging methods.[12] These modalities detect radiation emitted from radioactive probes which targets changes in tissue function or biomarker concentration. The detection of systems is very sensitive and, therefore, only a minute amount of probe (pmol) is needed to generate an image. Because such a small mass is used, the biochemical process being studied is not perturbed.[13] This makes PET and SPECT sensitive enough to visualize changes in biochemistry that precede the appearance of anatomical changes.

1.2 – PET and SPECT

While both PET and SPECT detect the emission of radiation from an internal probe, the detection method and isotopes used differ between the two techniques. Positron emission tomography uses a circular array of detectors to reconstruct images from coincidence detection of the gamma emissions.[14] Positron emitting radionuclides include halogens (^{18}F, ^{76}Br, or ^{124}I), transition metals (^{64}Cu), and main group elements (^{11}C, ^{15}O, ^{13}N or ^{68}Ga).[9, 11, 15] As these nuclei decay, they emit positrons which travel a short distance before colliding with an electron, leading to annihilation. Two gamma rays with 511 keV are then emitted at 180° which are detected by the PET scanner.

Single photon emission computed tomography is similar to PET in its detection of gamma emission except the radionuclei are gamma emitting. Like PET, there are a variety of nuclides which may be used however with SPECT probes, each has unique

gamma energy. Some examples of gamma emitting isotopes include iodine isotopes (^{123}I and ^{125}I), ^{99m}Tc, and ^{111}In.[9, 16, 17] Akin to 2D x-ray images converted into a 3D reconstruction for CT images, a rotating gamma camera records multiple projections at difference angles which become 3D images by calculating where the gamma rays originated. Because PET scanners detect gamma emissions in coincidence, the technique is more sensitive than SPECT, has a higher practical resolution, and images can be readily quantified.[18] SPECT imaging's main advantage is that SPECT isotopes are readily obtainable and generally longer lived (i.e., longer $t_{1/2}$). This fact, coupled with the low cost of conventional gamma cameras makes SPECT more affordable than PET.[2]

In diagnostic nuclear medicine, the most widely used radionuclide is technetium-99m, accounting for 80% of the scans conducted in the clinic.[19] One of the advantages of this isotope is its commercial availability from a ^{99}Mo/^{99m}Tc generator, allowing for widespread distribution and accessibility. ^{99m}Tc also has ideal nuclear properties for SPECT which makes it a desirable radionuclide to use in molecular imaging. The primary gamma ray emission of 140 keV (generated during the isomeric transition of ^{99m}Tc to ^{99g}Tc) falls into the optimal range for SPECT detectors.[20] Fortuitously, the half life of 6.02 hours is sufficient to synthesize the agent, administer the radiotracer to the patient, and obtain the images without burdening the patient with a large dose of radiation.

There are two broad classes of ^{99m}Tc compounds: Tc-essential and Tc-tagged.[19] In the case of the former classification, the metal is an essential part of targeting and the pharmacokinetic properties of the compound. For example, the myocardial perfusion imaging agent Cardiolite® (^{99m}Tc-sestamibi, Figure 1.1) is a hexa-coordinate isonitrile

Tc(I) complex which is unipositively charged, lipophilic, and mimics potassium in terms of its size. This allows for Cardiolite® to accumulate in the heart tissue *via* a diffusion mechanism and electrostatic binding because of high mitochondrial membrane potential.[21] This is also an example of a generalist (perfusion-based) agent in that its distribution is based largely on physical processes (in this case, blood flow). For Tc-tagged compounds the metal itself does not dictate pharmacokinetic properties, rather the metal is linked to a targeting vector which imparts specificity.

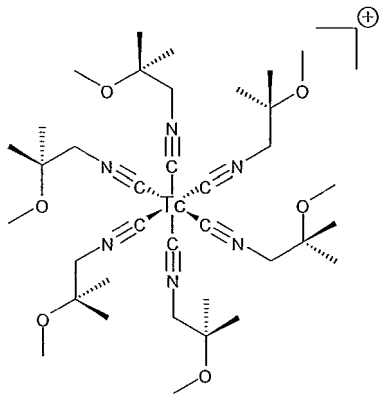

Figure 1.1 – Cardiolite® (^{99m}Tc-Sestamibi)

1.3 – ^{99m}Tc-based Molecular Imaging Probes

Metal-based radiopharmaceuticals typically are comprised of three components: a targeting vector, a chelate to coordinate with the metal, and a linker between these two components (Figure 1.2). The targeting vector can be peptides,[22, 23] small molecules,[24] nucleosides,[25] or monoclonal antibodies.[26] Octreoscan, for example, is an agent for imaging neuroendocrine tumors and was the first FDA clinically approved targeted peptide and radiometal-based imaging agent.[23, 27-29] It consists of a targeting vector for somatostatin receptors which has been derivatized with a chelate that binds

^{111}In. Depending on the radioactive isotope used, radiopharmaceuticals like Octreoscan can be used for both imaging and treatment.[21, 30]

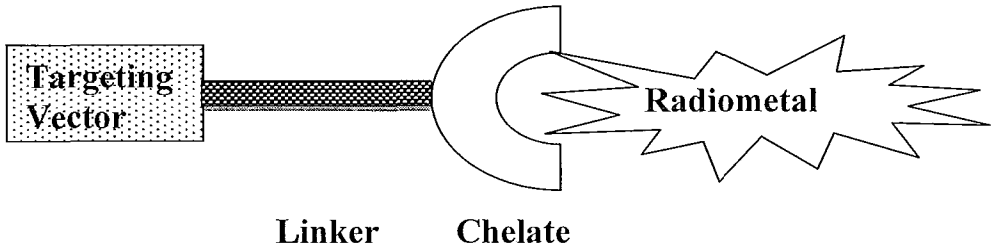

Figure 1.2 - General schematic of metal-based radiopharmaceuticals

Key properties for an effective targeted metal-based radiopharmaceutical are selectivity for the target, rapid clearance from the blood and non-target tissue, metabolic stability *in vivo*, and efficient transportation and penetration at the target site.[21, 28-31] Each of these properties can be affected by the both the targeting vector and the metal complex. While the theory is that a metal-chelate plays no role in the biodistribution of targeted agents, the truth is that adding a bulky or lipophilic Tc chelate to a small molecule or peptide can have a large impact on the pharmacokinetics of the agent. For instance, when Taylor *et al.* designed an iminodiacetic acid myocardial imaging agent based on lidocaine, the coordination to ^{99m}Tc changed the molecule so drastically that the complex had no uptake in the heart but was cleared rapidly through the hepatobiliary pathway.[32] Not only can size affect the biodistribution but changes to lipophilicity can also have an significant impact on the selectivity, clearance, and metabolic stability.[19]

The stability of the imaging agents *in vivo* is important to minimize the background signal seen from metabolites and to minimize the dose to organs such as the

liver and kidneys.[17] Chemical inertness is a desired property of the chelate-metal complexes as this prevents premature loss of the radionuclide from the targeting vector which would result in poor image quality and unnecessary radiation exposure to the patient.[33] There are two options for incorporating Tc into a targeting vector; either directly (i.e., labeling with existing functional groups) or using a bifunctional chelate. While direct coordination using donating group within the targeting ligand will avoid the need to add a bulky chelator, the strength of the metal-ligand complex might not be sufficient to preserve the metal *in vivo* nor may the activity of the targeting vector be retained once the metal is added. [17] This can be avoided by the addition of a bifunctional chelate to the molecule. Bifunctional chelates contain two components; one for coordination of a metal and the other for incorporation into the targeting vector. A few examples of such chelates include marcocyclic chelators and heteroatomic N_xS_{4-x} type ligands.[33, 34] Different chelates are used for different oxidation states of the Tc and to obtain the desired pharmacokinetics.

While there are numerous oxidation states of Tc (VII to –I), Tc(I) when attached to three carbonyl groups (the $[^{99m}Tc(CO)_3]^+$ core) is particularly attractive as it can form inert, d^6 octahedral complexes with a variety of donor atoms.[17] The tricarbonyl Tc(I) core is readily obtained from $[TcO_4]^-$ eluted from the generator thanks to an aqueous reduction reaction developed by Alberto *et al.* which forms $[^{99m}Tc(CO)_3(OH_2)_3]^+$.[35] The Tc(I) precursor is produced using boranocarbonate which acts as a reductant and a source of CO. The three water molecules are labile and easily replaced by donors from a chelate.

A more expedient microwave method for producing the $[^{99m}Tc(CO)_3]^+$ core was recently reported (Scheme 1.1).[1]

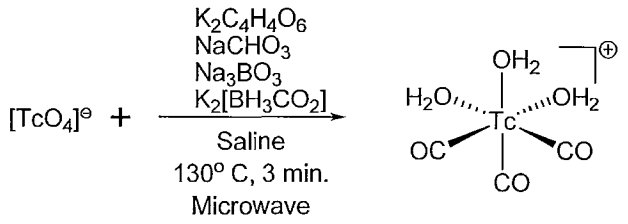

Scheme 1.1- Reduction of pertechnetate to triaquatricarbonyl technetium(I)

In an attempt to make it easier to label peptides with this Tc(I) species, single amino acid chelates (SAAC) were developed. These are modified lysine molecules containing tridentate groups formed at the ε – nitrogen atom.[36] Because these ligands were lysine derivatives, they could be easily placed anywhere within a peptide. The quintessential SAAC ligand is the dipyridyl group (ligand in Scheme 1.2) where electrons from the N of the pyridine rings and the N_ε replace the water ligands on $[^{99m}Tc(CO)_3(OH_2)_3]^+$ to form stable Tc(I) complexes (Scheme 1.2). Technetium SAAC compounds have been extensively studied [37] and successfully linked to a range of targeting vectors.

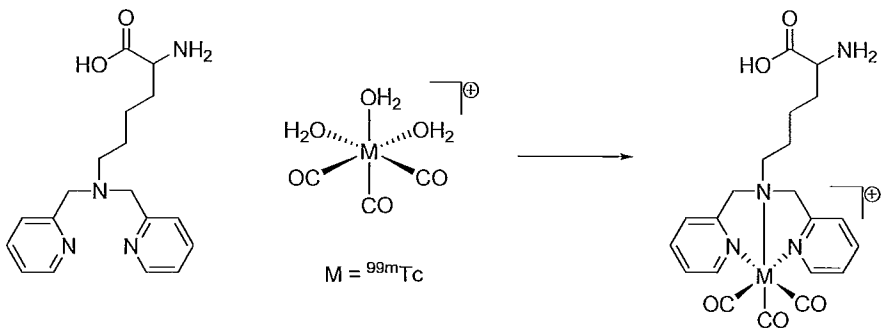

Scheme 1.2 - Reaction of SAAC ligand with $[^{99m}Tc(CO)_3(OH_2)_3]^+$

1.4 – Selectivity of Targeted Molecular Imaging Probes

In order for molecular radioimaging agents to be effective they must selectively bind to the target of interest and rapidly clear from non-targets tissues.[30] The highest theoretical target to non-target (T:NT) ratios for target specific radiopharmaceuticals are often governed by the expression level of the target (B_{max}) versus the affinity of the agent for the target (K_D) (Equation 1.1).[38] Factors which may lower the T:NT ratio from the theoretical value may include binding to targets not associated with the diseased tissue and non-specific binding of radioactive impurities. In many cases the T:NT ratio can be improved when agents are prepared in high effective specific activity because the precursor ligand often has comparable affinity for the target of interest.[39, 40]

$$T{:}NT = \frac{B_{max}}{K_D} \qquad \text{Equation 1.1}$$

With traditional radiolabeling protocols, the chelating ligand is added in large excess compared to the radioisotope, resulting in a mixture of labeled and unlabeled ligands (Scheme 1.3). Addition of the radiometal to the chelate can be either prior to, or after, inclusion of the chelating moiety into the targeting vector, depending on the conditions under which radiolabeling is taking place. If the targeting vector is stable to the labeling conditions, the metal would be added after the chelate has been attached. By adding the metal as the final step, there is still a need for a purification step to remove excess targeting vector from the conjugation reaction between the chelate and targeting vector.

For targeted radiopharmaceuticals both the labeled and unlabeled compounds contain the same targeting vector, consequently they often have similar affinities for the target of interest. The large excess of unlabeled ligand is problematic in that is can prevent the labeled compound from binding the target and this can decrease the T:NT ratio, leading to poor image quality.[41] As a result, there is a need for the development of methods to produce molecules in high effective specific activity.

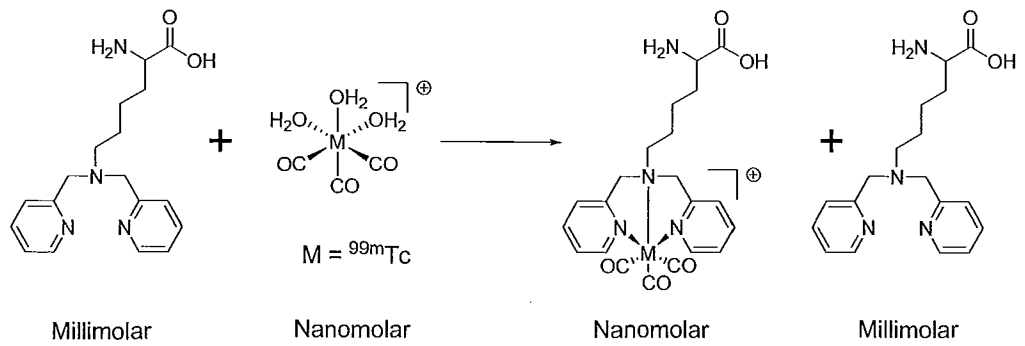

Scheme 1.3 – A typical radiolabeling reaction showing relative amounts of starting materials and products

1.5 – Separation Procedures

The ideal labeling reaction would be one in which two reagents react quantitatively eliminating any other side products and requiring no purification.[42] As this is never the case in radiochemistry, different methods for removing byproducts or excess starting material can be used. Classical purification methods such as crystallization, distillation, extraction, or sublimation are excellent means to isolating non-radioactive compounds but are not effective for radiochemists because the amounts of material used are so small.

High performance liquid chromatography (HPLC) is widely used to separate precursor ligands from labeled products. On the time scale needed for producing labeled compounds, chromatography is time consuming and furthermore requires operators to handle radioactive samples, thereby potentially increasing their dose. Phase-switching chemistry (other than acid/base extractions) has arisen as a potential facile and efficient means to isolate products in high effective specific activity from traditional labeling mixtures.

1.6 – Solid-Phase Purification Strategies for Radiolabeling Reactions

Clinically approved Tc-based agents are commonly prepared using kit formulations because they are reproducible methods that follow simple standard operating procedures. In instant kits, the precursor and appropriate reducing agent are prepackaged into a vial such that after the addition of $[^{99m}TcO_4]^-$ from the generator, the desired compound is formed in a single step. After precipitates are removed by filtration, the probe is administered to the patient awaiting a SPECT scan. The agents produced using instant kits are, however, mostly perfusion-based (i.e., Tc-essential) and the concentration of precursor remaining in the product has no effect on the image quality as there are no specific targets to block and thusly do not require purification. In order to apply the kit formulation strategy to targeted agents, a facile purification method that can be integrated with instant kit labeling methods is needed.

Solid-supported reagents can be easily separated from reaction mixtures by filtration. Solid-phase labeling takes advantage of this by attaching the substrate which is being radiolabeled to an insoluble support (such as a polystyrene resin) in such a manner

that upon reacting with the radioisotope, the cleaved product moves into solution and the resin collected by filtration. One of the most effective solid-phase labeling methods uses isotopes of iodine (^{123}I, $t_{½}$ = 13.2 hr, E_{γ} = 159 keV and ^{131}I, $t_{½}$ = 8 d, β^- = 606 keV, γ = 364 keV) and a polymer supported tin substrate. This strategy was used to prepare *meta*-iodobenzyl guanidine (MIBG, Scheme 1.4) in high effective specific activity (18.5 GBq/mol).[43] Upon reaction with iodine, the radioiodinated product is cleaved from the solid and separated from any precursor by simple filtration.

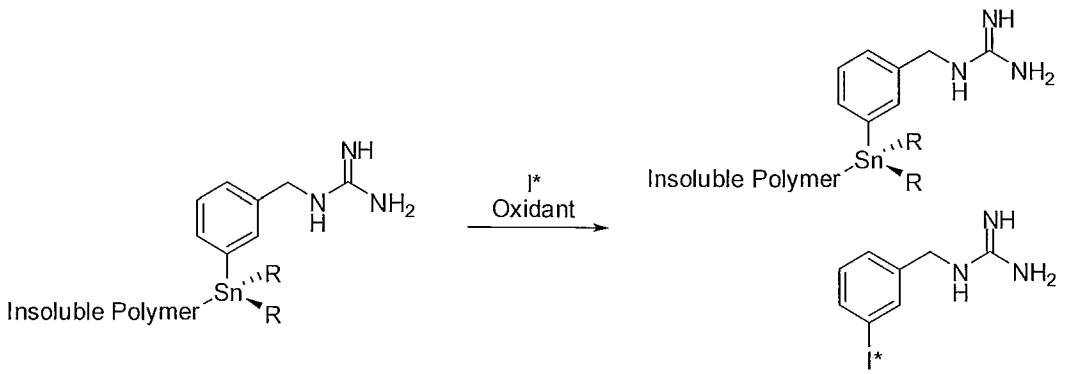

Scheme 1.4 - Polymer-supported radioiodination of MIBG

There are also examples where substrates bound to solid-supports are released following coordination to ^{99m}Tc. By attaching the thiol from the MAG3 chelator to a solid support, Dunn-Dufault *et al.* developed a method wherein the labeled compound was cleaved following coordination of Tc. This was accomplished by linking the thiol of the chelate to the resin through a maleimide group (Scheme 1.5).[44] Upon reaction with ^{99m}Tc, S donates to the metal and is cleaved from the resin. The desired product was then isolated by filtration and washing with saline. The study investigated different support and ligand combinations with varying radiochemical yields and purity (13 – 81% and 8 –

99% respectively). Another study by Mundwiler *et al.* developed a similar method for labeling with the $[^{99m}Tc(CO)_3]^+$ core by attaching a tertiary amine to a resin.[45] When the Tc is chelated, the bond between the amine group and the resin is cleaved, releasing the product into solution and from the resin. The yields ranged from 11 to 87% depending on the conditions used and the nature of the chelate.

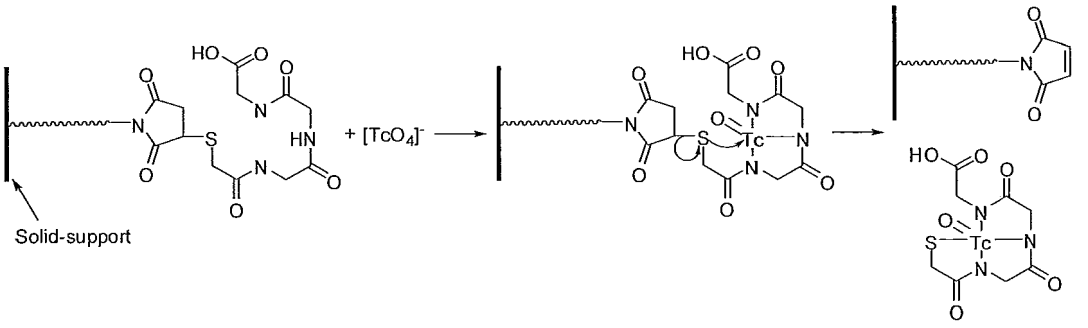

Scheme 1.5 - Solid-support radiolabeling of the MAG3 ligand with Tc [44]

Similar work has been completed by Riddoch *et al.* using a MAMA (monoamide monoamine) ligand on a Merrifield-type resin.[46] These ligand were incorporated into peptides using solid-phase peptide synthesis methods and then reacted with Re or ^{99m}Tc. Yields of 85% were obtained with Re but the highest yield for the ^{99m}Tc complex was 40%. Other than moderate yields and purity, one major issue associated with these methods is the loading of the resin prior to addition of the metal. As characterization post immobilization is very difficult, the loading must be quantitative and only bind through the desired functional group. A second issue was non-specific binding which would reduce radiochemical yield. One possible solution to improving yields and purities of metal-based probes is to chemoselectively sequester excess ligands onto solid-supports following the labeling reaction.

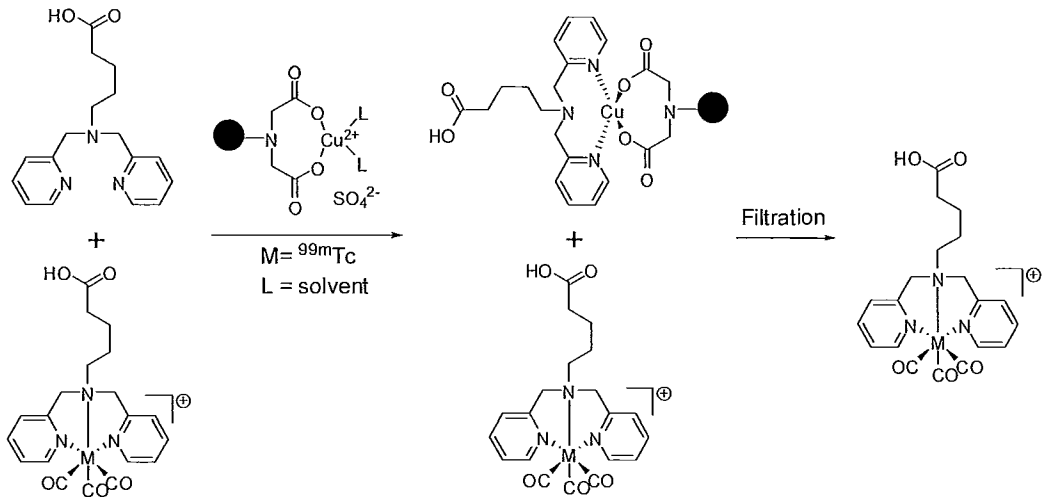

Scheme 1.6 - Solid-phase ligand capture strategy

To this end, a resin-bound copper iminodiacetic acid complex was used to capture free unlabeled ligand following radiolabeling reactions (Scheme 1.6). In recently reported work, Cu (II) was bound to a commercially available Amberlite resin through a diacetic acid moiety and this resin was packed into cartridges.[1, 47] When the radiolabeling mixture containing a dipyridyl chelator and Tc-labeled chelate was passed through the resin, >99% of the unlabeled ligand was retained by coordination of the ligand to the labile Cu binding sites. Unfortunately, there was also a significant amount of non-specific binding to the resin which caused an average loss of activity of 22%. Another limitation was the heterogeneous nature of the system which resulted in slow capture kinetics leading to longer than optimal purification times. To address this issue, it was necessary to use a large excess of the copper resin (100 mg) which likely increased the extent of non-specific binding compared to if a stoichiometric amount of resin was used. This solid-phase ligand capture strategy is an effective way to prepare high effective specific

activity targeted Tc molecular imaging probes, however, to become a general purpose approach, the issues of slow kinetics and non-specific binding must first be addressed. A potential solution to these issues is a chemoselective solution-phase ligand capture method that retains the ease of purification of a solid-phase approach.

1.7 – Fluorous Chemistry

Over the past 15 years, fluorous chemistry has been developed as an alternative synthesis and purification platform to solid-phase chemistry. The term "fluorous" refers to highly fluorinated molecules which display unique intermolecular interactions and is analogous to the term aqueous.[48] Fluorous compounds are both hydrophobic and oleophobic while displaying a high affinity for other fluorine rich compounds. Perfluoroalkyl solvents are immiscible with most organic solvents at room temperature and are extremely hydrophobic.[49] The solubility of fluorinated reagents in these solvents is dependent on the weight percentage of fluorine.

Compounds containing 60% or more fluorines by weight (heavy fluorous molecules) will preferentially partition into a fluorous solvent instead of an aqueous or organic solvent. Taking advantage of this effect, Horvath and Rabai created fluorous analogs of catalysts that were easily separated by either reversible miscibility (fluorous biphasic catalysis) or a triphasic extraction.[50, 51] At elevated temperatures, the fluorous layer (containing the fluorous catalyst) and the organic layer (containing reactants) become miscible. After cooling back to room temperature, the solvents become immiscible again and the catalyst partitions into the fluorous layer and can be recycled while the products remain in the organic layer. The triphasic extraction is another

approach where the reaction takes place in an organic media and then can be purified by extracting the separate components into aqueous, organic, and fluorous solvents.

It is not often amendable, however, for most molecules to contain greater than 60 weight % fluorine. To take advantage of the fluorous effect with less fluorine content, lighter fluorous molecules were developed. These can be separated from organic molecules using a technique similar to solid-phase extraction with C-18 silica. By modifying silica gel to contain perfluoroalkyl chains, fluorous compounds can be retained while organic molecules are selectively eluted (Figure 1.3). Reaction mixtures are loaded onto the fluorous solid-phase extraction (F-SPE) cartridge and any organic portions are eluted with a fluorophobic wash of 20% water in a polar organic solvent while the fluorous portion is retained on the silica. If the fluorous portion is desired then a fluorophilic wash of 100% polar organic solvent can be used.

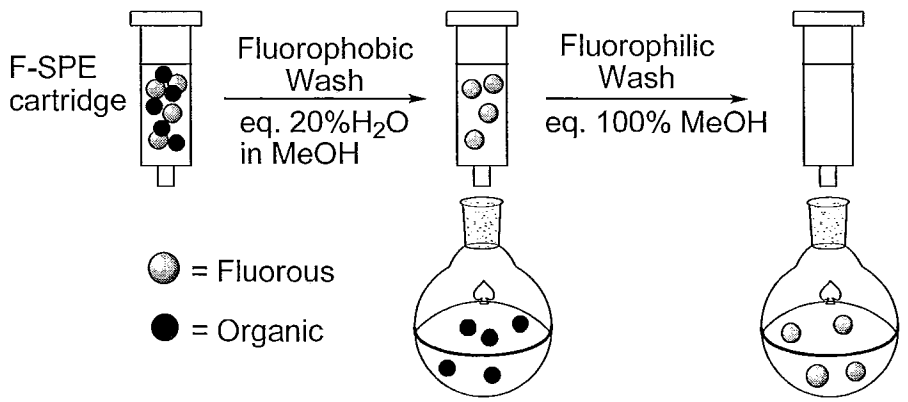

Figure 1.3 – Schematic of the fluorous solid-phase extraction (F-SPE) technique for separating light fluorous compounds

F-SPE provides purification ease on par with solid-phase separations, with several advantages. Both solid-phase and fluorous purification share facile separation protocols

and similar potential for automation, however, the fluorous chemistry offers several advantages such as adaptability of literature procedures, ease of scale up, and facile analysis of reaction products by solution-phase characterization techniques.[52] Light fluorous compounds are also soluble in most organic solvents, resulting in homogeneous reaction mixtures and eliminating the need to use fluorous solvents (expensive and persistent in the environment). When comparing the reaction rates between the two techniques, the kinetics of the fluorous reactions are faster and more alike to traditional organic chemistry.[52] Furthermore, because the fluorous silica is also "Teflon-like" with respect to binding of organic molecules, there should be a reduction in non-specific binding to this media. By taking advantage of these features of fluorous chemistry, the objective was to develop and evaluate a fluorous ligand capture strategy for the purification of radiotracers.

1.8 – Fluorous Chemistry and the Preparation of Radiopharmaceuticals

Recently, a fluorous chemistry technique analogous to a solid-support labeling has been developed to prepare iodinated radiotracers.[53] In this method, perfluoroalkyl tin groups are cleaved from an aryl group upon reaction with radioiodine in a similar fashion to the solid-support method mentioned previously (Scheme 1.7).[43] The precursor is then easily removed by F-SPE. The fluorous approach was an improvement upon the solid-phase method as there was less non-specific binding to the fluorous media (higher radiochemical yield). Reproducibility was also better as the exact composition and purity of the substrate loaded onto the fluorous-support could be determined by solution-phase characterization methods. A similar approach has also been used to prepare ^{18}F-labeled

compounds[54, 55] but fluorous chemistry has yet to be employed as a purification strategy for metal-based radiotracers.

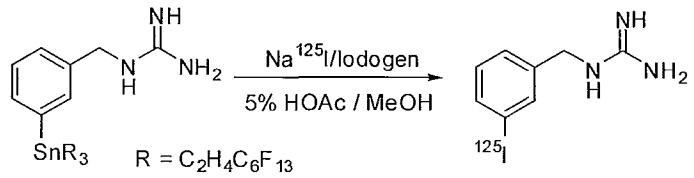

Scheme 1.7 - Fluorous labeling method (FLM) for preparing MIBG [53]

1.9 – Microfluidics

Until recently, most of the research carried out with microfluidics has focused on the engineering aspects but not their application to synthetic chemistry.[56] As with fluorous chemistry, synthetic chemists have not embraced this new technology, either due to unfamiliarity or to the cost associated with building or maintaining these instruments. However, there are many advantages to conducting syntheses using microreactors compared to the century's old method of batch chemistry. These devices are comprised of microchannels (10 – 100 μm) which are used to control small amounts of fluid and reagents.[57] The microreactors can be either fabricated from glass, silica, or from polymers, allowing for a large variety of designs. A common polymer for fabricating microreactors is poly(dimethylsiloxane) (PDMS) because the unique and integrate channels can be prepared using soft lithographic techniques and pressure-controlled valves can be incorporated to control reagents.[58-60]

A major feature of microfluidics, from which many of the advantages are derived, is the small volume within the microchannels. Small volumes lead to faster mixing times

resulting in more homogeneous heating/cooling of reagents and faster diffusion rates. Mixing can be completed in microseconds with high surface area to volume ratios, which impacts the mass and heat transfer within the reaction.[57] Thermal control can have a major impact on increasing reaction rates, yields, and selectivity.[61, 62] For example, microreactors have been use to synthesis β-peptides in quantitative yields in 20 min. compared to batch methods which produced 50% yields after 24 hr.[63, 64] To optimize reaction conditions of microreactors, only small amounts of precious compounds are needed and less waste is generated (higher efficiency reactions). Another advantage of completing reactions in a flow system is the ability to monitor the reaction progress online with UV/vis or IR detectors.

Flow of solvents within the microfluidic device can be controlled in two manners; pressure induced or electroosmotic flow.[64] With electroosmotic flow, the solution is pumped through the channels by a potential voltage applied by electrodes placed at the ends. The solvent, therefore, must be polar enough to be affected by the charge. Pressure-driven flow results in laminar fluid movement and a parabolic velocity profile.[65] In a single-solvent system, this leads to mixing by diffusion. In a system where there are two immiscible solvents mixing at a junction, micro droplets will form, creating microscopic reaction vessels. These compartments allow for completing combinatorial libraries in addressable droplets, unique diffusion characteristics, and control of reagents being added in multi-step synthesis.

Once optimized, reactions conducted using microfluidic systems are not scaled up as batch methods are, rather production is augmented by increasing the number of

microreactors running in parallel (so called "numbering up").[66] This creates safer reaction conditions as smaller volumes of toxic reagents are used and there is better control of excessively exothermic reactions because of efficient heat transfer. With all of these benefits to conducting reactions using microfluidic devices, there are still issues which must be addressed. Often the materials used to fabricate the devices have inherent incompatibilities with reagents and solvents. This can be addressed on a case-by-case basis by changing the solvents or by modifying the materials used, such as by etching or perfluorination.[67] Another concern is backpressure developed in flow, as well as removal of unwanted side products, such as the excess unlabeled precursor following a labeling reaction.

1.10 – Microfluidics and Molecular Imaging

There is much interest in applying microfluidics to radiopharmaceutical chemistry, as seen by the large number of abstracts at a recent Society of Radiopharmaceutical Science meeting.[68] Microfluidics is well suited for conducting radiolabeling reactions and radiopharmaceutical production. Requirements for such production include expedited chemical kinetics, containment of radioactivity, and use of small amounts of reagent to produce low mass quantity products in an ever expanding and diversifying catalog of probes.[69] Thus, preparation of molecular imaging agents provides a unique opportunity for extending the usage of microfluidics.

In 2005, the Quake laboratory at Stanford prepared a dose of [^{18}F]FDG to image a mouse using an integrated microreactor circuit.[70] This "lab-on-a-chip" was used to conduct all 5 steps of the labeling process. PDMS was chosen here for the inclusion of

control valves to isolate distinct regions of the chip as well as for its gas permeability, allowing for solvent exchange to dry the fluoride ion. Another feature of this microreactor was the preparation of *in situ* affinity and ion exchange columns using different valves which allowed fluids to pass but not the beads for the column. In the end, 190 μCi of [^{18}F]FDG was prepared (38% radiochemical yield, 97.6 % radiochemical purity) in 14 min. in an automated fashion. There is also one example in the literature where ^{99m}Tc perfusion agents were prepared in a microfluidic device and another manuscript in preparation wherein a bifunctional chelate has been labeled with a $[^{99m}Tc(CO)_3]^+$ core. [71, 72]

1.11 – Fluorous Chemistry in Microfluidics

There are also examples in the literature where the advantages of microfluidics and fluorous chemistry are combined. The benefits of both new technologies can be seen in the work by Mikami and co-workers where cyclic ketones were converted to the corresponding lactone *via* the Baeyer-Villiger reaction in 91% yield and 100% regioselectivity using a fluorous lanthide catalyst (Scheme 1.8).[73] The high yield can be attributed to the short diffusion distances in the microchannels and ease of removing the catalyst post reaction. This approach did not purify the reaction mixture within the microreactor itself but there are examples where fluorous purification has been incorporated inline.

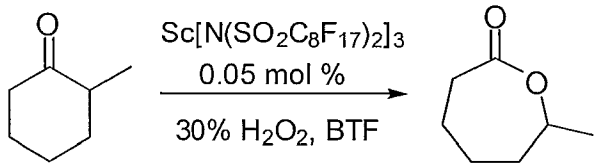

Scheme 1.8 - Baeyer-Villiger oxidation in a microfluidic device with fluorous catalyst

A fluorous polymer membrane has been used as a means to continuously separate fluorous components from reaction mixtures in a microfluidic reactor.[74] Aqueous droplets in an organic or fluorous solvent are segregated as the organic or fluorous solvent passes through the membrane, leaving aqueous soluble molecules behind. Another example of in line purification was the use wells filled with fluorous silica.[75] By filling a reservoir which was deeper than the rest of the channels with fluorous beads, fluorous-tagged amino acids could be separated within the microfluidic device (Figure 1.4). This technique could similarly be applied to radiochemistry if a fluorous ligand capture method could be developed.

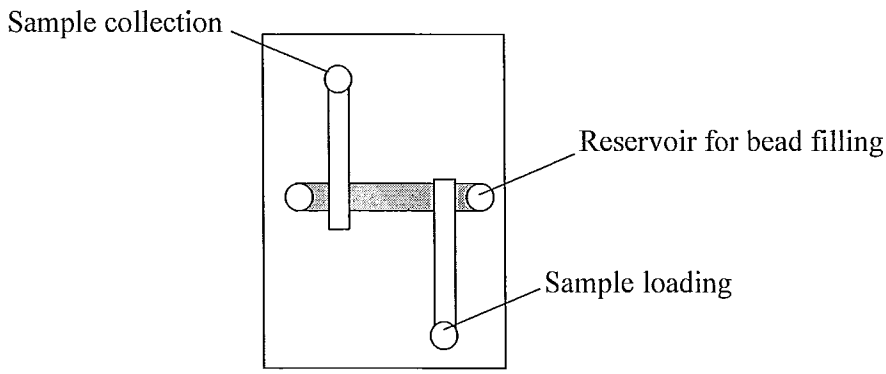

Figure 1.4 - Microfluidic F-SPE chamber [78]

1.12 – Objectives

This thesis explores the development of a fluorous ligand capture (FLC) method for purifying Tc(I) labeled compounds. The work is broken down into key steps which include: preparation of the FLC agent (Chapter 2) and evaluation of FLC using a model system and a peptide-based agent (Chapter 2). This is followed by evaluating the use of a microfluidic platform for performing FLC and the use of a unique preloading strategy (Chapter 3).

Chapter 2

2. Fluorous Ligand Capture Strategy

2.1 - Introduction

To achieve high radiochemical yields during the preparation of metallo-radiopharmaceuticals, a large excess of ligand is commonly required. For reactions involving ^{99m}Tc, a 10^6 fold excess of ligand is often used [17] and while having an excess precursor is not detrimental for obtaining an effective image of perfusion-based molecular imaging agents, the same is not true for targeted agents.[76] For specific molecular imaging agents, the precursor ligand will bind to the target whether or not the radiometal is present. Consequently, the excess non-radioactive ligand will have a greater probability of interacting with the target of interest which in the case of molecular imaging is generally expressed in low concentrations (Figure 2.1).[77] The excess ligand can therefore lower target: non-target (T:NT) ratios and lead to poor image quality, and has hindered the development of ^{99m}Tc-based molecular imaging probes.

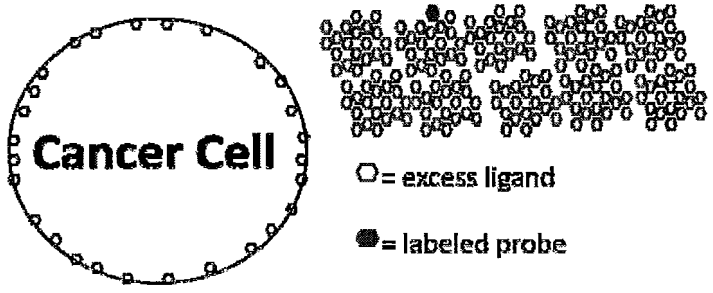

Figure 2.1 – A schematic demonstrating relationship between a molecular imaging probe with a low effective specific activity and the finite number of target sites on a cancer cell

For molecular imaging probes to be effective it will be beneficial to obtain highly pure products (i.e., no excess ligand). The T:NT ratio can be estimated by dividing the total expression of the target (B_{max}) by the equilibrium dissociation constant between the compound and the target (K_D).[38, 39] As the number of receptors is finite, the most obvious means to increase the T:NT ratio is to decrease the value of K_D (increase the binding affinity of the compound). Nonetheless, the increase in target affinity is not beneficial if a mixture of a minute amount of radiolabeled product and an excess of non-radiolabeled precursor is injected having similar K_D values. It is therefore paramount to develop methods to obtain targeted molecular imaging agents in high effective specific activity.[76]

Instant kits provide a convenient and reproducible means of preparing ^{99m}Tc-based radiopharmaceuticals and are used for the manufacturing the most widely used agents including the cardiac perfusion agent, ^{99m}Tc-Sestamibi.[19] Perfusion agents, unlike targeted compounds, do not require purification and are prepared by mixing $[^{99m}TcO_4]^-$ obtained from a ^{99}Mo/^{99m}Tc generators with a reducing agent and a coordinating ligand in prepackaged vials. The reaction mixture is then filtered to remove any particulate matter and checked by radio-TLC for radiochemical purity. The ease, reproducibility, and speed of preparation makes instant kits an attractive avenue for preparing molecular imaging agents at any radiopharmacy. In order to formulate an instant kit for targeted compounds, there would need to be a purification step integrated with the platform in order to remove excess precursor.

Currently, HPLC is used as the primary purification tool to isolate targeted agents in high effective specific activity. While highly pure products can be obtained, this method requires the use of organic solvents, which must be removed prior to injection, and are slow with respect to radioisotope decay. There is also a need to shield the operator of the instrument from the high levels of radiation emitted during routine clinical production runs.

Solid-phase labeling and scavenging strategies mentioned in Section 1.6 are methods which may be used within kit formulations to purify Tc-labeled compounds in high effective specific activity (Scheme 2.1). As stated, the solid-phase methods suffer from the drawback of conducting purification as a heterogeneous mixture. Fluorous chemistry has the benefit of simple purification using an orthogonal phase which allows the ligand sequestering step to occur in a homogeneous solution. The fluorous labeling method for radiohalogenations with multiple isotopes of iodine and ^{18}F have been established [53-55, 78] but there has been no use of fluorous purification strategies to isolate Tc-based agents in high effective specific activity.

2.2 – Objective

To purify the radiolabeled product in a kit friendly manner, the excess ligand must be removed quickly and efficiently in a reproducible manner. The solid-phase ligand capture method recently developed by Causey *et al.* satisfied both these criteria but suffered from high levels of non-specific binding (circa 22%) and poor reaction kinetics due to the heterogeneity of the purification process (Scheme 2.1).[1] As a result, our first objective was to determine if the size of the resin polymer played a role on the extent of

non-specific binding. Following these experiments, a fluorous analog to the resin-bound iminodiacetic acid Cu(II) agent was prepared in order to capture excess ligands. Once the ligand coordinates the Cu-fluorous complex, it can be removed by fluorous solid-phase extraction (F-SPE) with fluorous silica. This fluorous method offers two advantages; the capture step occurs in a homogeneous solution and the fluorous silica has minimal intermolecular interactions with both hydrophobic and hydrophilic compounds. These features will lead to faster reaction kinetics and less non-specific binding, respectively. Following the comparison of fluorous and solid-phase purification methods using a model chelate system, the fluorous ligand capture procedure was used with a peptide-chelate conjugate to further test the utility of this strategy.

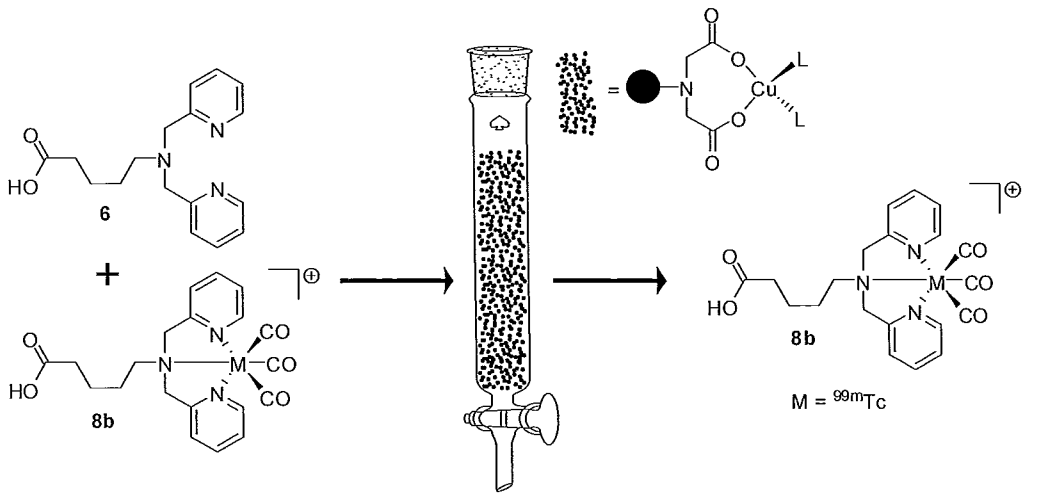

Scheme 2.1 – The proposed solid-phase ligand capture method

2.3 – Model System to Test Ligand Capture

As a proof of principle experiment to determine the utility of the copper resin and **5** as a ligand capture agents, a small molecule chelator was used as a model system.

Bispyridyl valeric acid (BPV, **6**, Figure 2.2) is a bifunctional chelator which can coordinate to the $M(CO)_3^+$ (M = ^{99m}Tc or Re) core and be incorporated into a targeting vector through the carboxylic acid moiety.[79] This compound was prepared from a literature procedure and a calibration curve was generated such that the amount of ligand removed following each procedure could be determined. Four different data points were collected in triplicate and a linear regression applied to the data to determine the equation of the curve to estimate the limit of detection (16.8 ng, Figure 2.3).

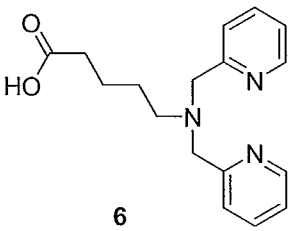

6

Figure 2.2 – Bispyridyl valeric acid, 6

In order to label **6** with a $[^{99m}Tc(CO)_3]^+$ core, $[^{99m}TcO_4]^-$ from the generator must be first converted to $[^{99m}Tc(CO)_3(OH_2)_3]^+$. For this reaction, 10 mg of potassium tartrate (used to stabilize intermediary oxidation states of Tc), 6 mg of sodium carbonate and sodium borate (buffers) along with 8 mg of potassium boranocarbonate (reducing agent which also supplies carbon monoxide) were added to a reaction vial with the pertechnetate in saline. Once the salts and activity are combined, the reaction mixture was heated to 130°C for 3 min. in the microwave prior to addition to the ligand. The BPV ligand (1 mg) was then added with $[^{99m}Tc(CO)_3(OH_2)_3]^+$ (740 MBq) in 1 mL of 20% MeCN in saline and the mixture was heated in the microwave for 2 min. at 150°C

(Scheme 2.2). It should be noted that the pH of the saline solution containing the $[^{99m}Tc(CO)_3(OH_2)_3]^+$ was approximately 11 and was not neutralized prior to the addition of the ligand.

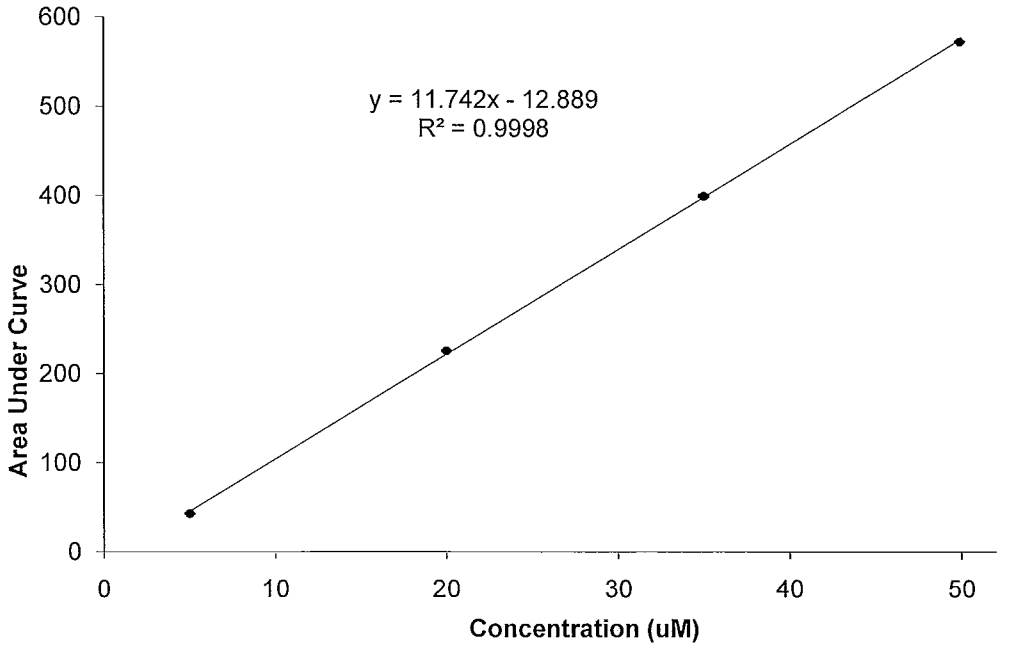

Figure 2.3 - Calibration curve of BPV

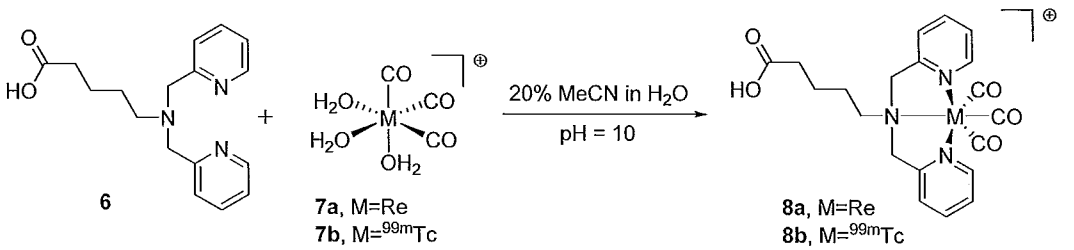

Scheme 2.2 – Coordination of 7a or 7b by 6

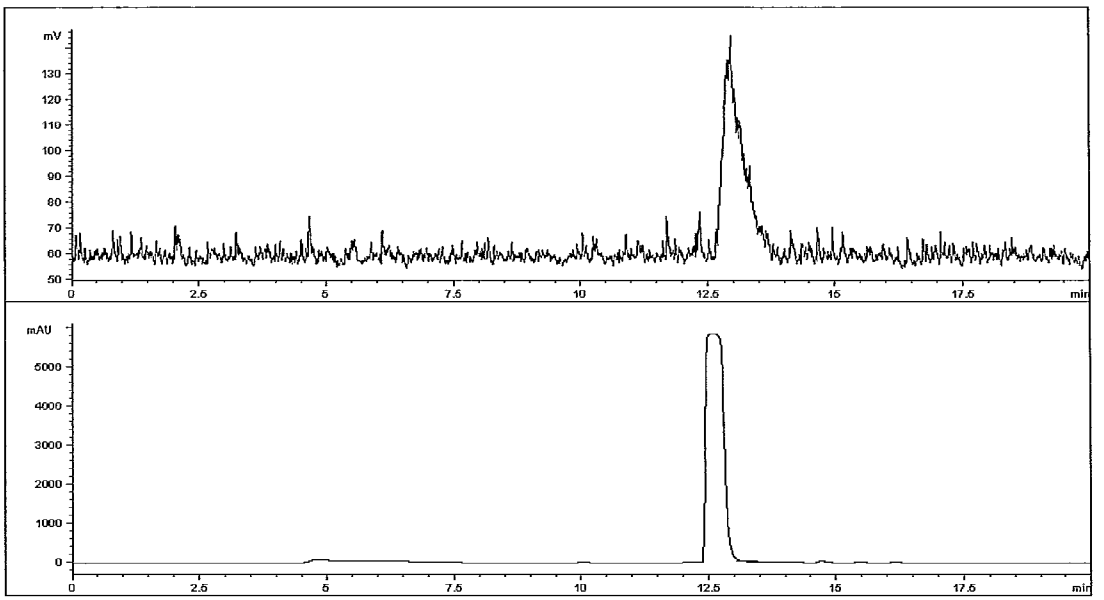

Figure 2.4 – HPLC chromatogram of a mixture of 8a and 8b. Top = γ trace showing 8b (t_R = 12.9 min.). Bottom = UV trace showing 8a (t_R = 12.6 min.). Phenomenex Gemini C18 5μm column (4.6 x 250 mm), 1 mL/min, gradient method A.

Because of the extremely low concentrations of radiolabeled product, the main method for characterizing reactions is HPLC using both UV and gamma detectors. A non-radioactive analog was prepared and fully characterized by NMR, IR and mass spectroscopy and showed the similar retention time as the Tc analog **8b**. Because there is no stable isotope of Tc, rhenium was used to make the standard as complexes with Re are isostructural with Tc compounds. Rhenium is suitable because it is found directly below Tc and the lanthanide contraction results in the two elements sharing similar physical and chemical properties.[21] The UV HPLC chromatogram in Figure 2.4 displays a peak for the Re standard (t_R = 12.6 min.) while the γ chromatogram showed one single peak (t_R = 12.9 min.) which corresponded with the Re standard. With the identity of the Tc complex **8b** confirmed and the absence of other peaks except for a small TcO_4^- peak in the γ

chromatogram, it was determined that the majority of the $[^{99m}Tc(CO)_3(OH_2)_3]^+$ had been coordinated by the ligand (91.7 ± 1.2 % radiochemical yield).

2.4 – Solid-Phase Ligand Capture Approach

Previous solid-phase extraction methods used inexpensive, commercially available resins with poorly characterized particle size. Solid-phase ligand capture experiments have therefore been repeated herein with new resins which have been separated according to particle size. Three different size resins (20 – 75, 75 – 150, and 150 – 300 micron) were combined with a saturated solution of $CuSO_4$ and shaken for 5 hours. The resin was collected by filtration and washed with water, THF, and DCM before being resuspended into a fresh saturated $CuSO_4$ solution and shaken for another 24 hours. Afterwards, the larger $CuSO_4$ crystals that had formed were removed by filtering the resin through a Hirsch funnel that did not contain filter paper. The resin was then collected by suction filtration and washed with copious amounts of water until the solution was clear and colourless. Further washing was completed using 100 mL of both DCM and THF before the resin was dried overnight under high vacuum.

Syringe cartridges were loaded with the copper resin (100 mg resin: 1 mg BPV) and were prewashed with a slightly acidic saline solution (pH = 4). For these experiments, the solution containing $[^{99m}Tc(CO)_3]^+$ was neutralized prior to the addition of **6** as basic solutions would displace Cu^{2+} ions from the resin, introducing a new contaminate and resulting in more non-specific binding with the now free acetate groups. Adjusting the pH had to be completed carefully as the dipyridyl ligand system does not label well below pH = 7.[37] After successfully completing the radiolabeling reaction, the mixture was

dripped slowly onto the resin. Approximately 1/3 of the activity was eluted during the loading process and another 40 – 50% was eluted with a 3 mL saline wash. Further washes with both saline and MeOH did not elute significant amounts of activity (< 1% of what remained on cartridge).

Even with a neutral solution, there was still some Cu eluted which was evident in that the solution had a slight blue colour. This may have resulted because of tartrate in the solution coordinating to the Cu and displacing it from the resin. By passing the solution through C18 solid-phase extraction cartridge, the blue colour could be removed. After following standard elution protocols (6 mL water elution to remove salts 6 mL EtOH to remove organics), the solution containing the radioactivity was concentrated to 1 mL and a 100 μL aliquot was added to 900 μL of water for HPLC analysis (Figure 2.5).

Table 2.1 - Results from solid-phase ligand capture

Resin	Average % Ligand Captured	Average % of Non-specific Binging
150 – 300	91.1 ± 4.8	21.2 ± 1.0
75 – 150	90.1 ± 2.8	22.4 ± 1.1
20 – 75	86.0 ± 2.2	26.7 ± 2.7

The average results for the 3 different resins can be seen in Table 2.1 (n = 3). These results compare well with those reported in the literature.[1] Based upon the observed results, the size of the resin does not appear to make a significant difference in the ligand capture ability or the non-specific binding. The 150 – 300 μm resin preformed slightly better than the 75 – 150 μm resin and the smallest resin size performed a little

worse. There was also a new peak in the UV traces introduced at the solvent front from the copper salts which eluted with the radiolabeled product.

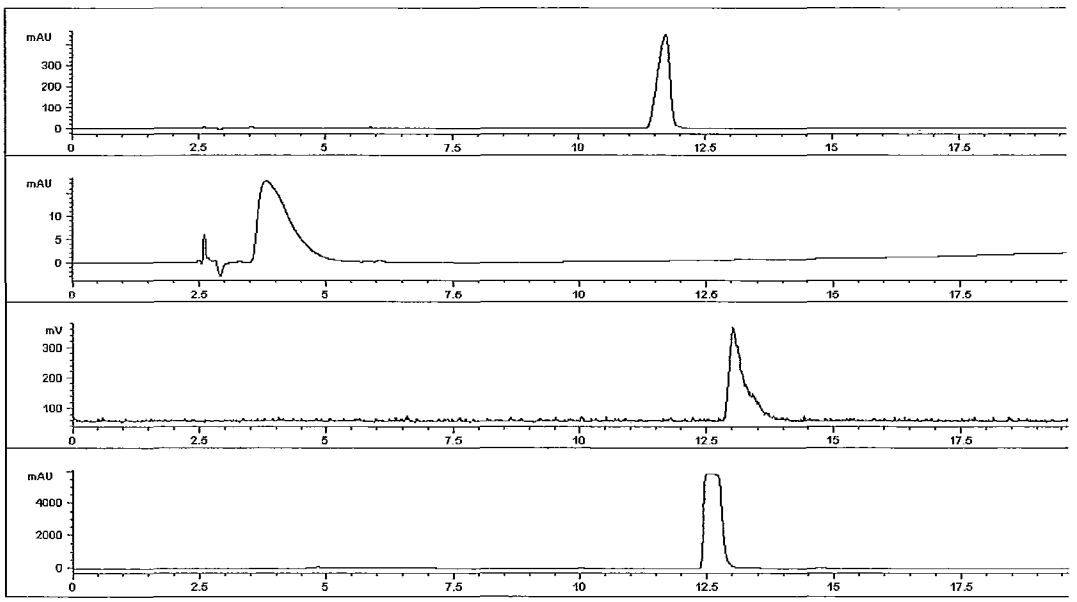

Figure 2.5 - HPLC chromatograms of results from solid-phase ligand capture of 6 with 20 - 75 μm resin. Top = UV trace showing crude labeling reaction mixture of 6 (t_R = 11.4 min.). Second = UV trace following FLC showing Cu salts (t_R = 3.6 min.) and removal of 6. Third = γ trace showing 8b (t_R = 12.9 min.). Bottom = UV trace showing 8a (t_R = 12.6 min.). Phenomenex Gemini C18 5μm column (4.6 x 250 mm), 1 mL/min, gradient method A.

2.5 – Preparation of the Fluorous Ligand Capture Agent

2.5.1 – Benzyl 2,2'-(3-perfluorooctylpropylazaenediyl)diacetate (3)

To prepare the fluorous analog, the first step involved the synthesis a fluorous iminodiacetic acid copper compound to capture dipyridyl ligands.[1, 47] Attempts were made at directly synthesizing the acid from the fluorous amine and bromoacetic acid but it was difficult to isolate the desired product. To resolve this issue, the benzyl ester of the bromoacetic acid was used (Scheme 2.3). By using the ester, the overall polarity of the compound was reduced, thereby facilitating the isolation. The benzyl group also provided

a UV active chromophore which made it more convenient to monitor the reaction by thin layer chromatography.

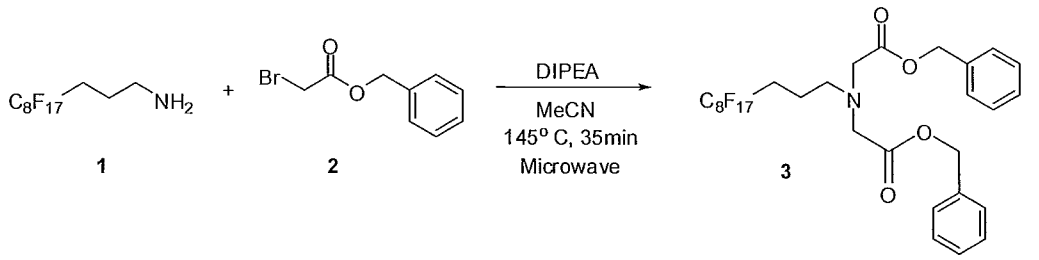

1 2 3

Scheme 2.3 - Preparation of 3

To activate the amine, two non-nucleophilic bases, K_2CO_3 and diisopropylethyl amine (DIPEA), were evaluated where the latter was chosen due to higher yield of the associated reaction. The solvent chosen was acetonitrile (MeCN) as this polar aprotic solvent would enhance the S_N2 reaction between the amine and the primary bromide. Following a literature procedure [80] for a comparable substitution reaction, a mixture of **1** and **2** was heated to reflux for 24 hours and the desired product was obtained in 62%. The reaction was also attempted using a microwave reactor to reduce the reaction time and increase yield.[81, 82]. A time and temperature course was conducted to determine the optimal yield (Table 2.2) and from these experiments, it was found that heating to 145°C for 35 min. were the ideal conditions and a yield of 98% was obtained following purification.

The first attempt to purify the compound was made using a triphasic extraction with water, dichloromethane (DCM), and perfluorohexane (FC-72), however, this was unsuccessful, most likely due to the low weight percent of fluorine in **1** (42%).

Compound **3** is referred to as a light fluorous compound [83] where F-SPE is a more suitable isolation protocol. Using an F-SPE cartridge, the product was isolated in nearly 40% yield. The low yield was most likely due to breakthrough of the fluorous compound into the fluorophobic wash. Ultimately, a much better yield of 98% was obtained using the Biotage flash chromatography system (7% ethyl acetate in hexanes to 60% ethyl acetate over 10 column volumes using a silica stationary phase). After removing the solvent, a clear, colourless oil was isolated.

Table 2.2 - Optimization of the reaction of 1 and 2 in a microwave reactor

Reaction	Time (min)	Temperature (°C)	TLC results
1	20	160	Faint product spot, 2 impurities
2	25	160	Darker product spot but darker impurities
3	35	160	Dark product spot, 3 impurities
4	30	100	Very faint product spot
5	30	115	Faint product spot, 1 impurity
6	30	130	Faint product spot, 1 impurity
7	30	145	Dark product spot, 2 impurities

To characterize compound **3**, proton and carbon-13 NMR spectra were obtained, as well as infrared and high resolution mass spectrometry data (See Appendix A). In the ^{1}H NMR spectrum, there were three singlets at 7.35, 5.09, and 3.60 ppm which represented the aromatic protons and two sets of methylene protons, respectively. The signal at 7.35 ppm integrated for 10 protons and the other integrations were consistent with those expected from the desired product. At lower field, there was a triplet at 2.81 ppm and two multiplets at 2.14 and 1.71 ppm which represent methylene protons in the

propyl group between the N and the perfluoroalkyl chain. The triplet was associated with the protons adjacent to the N as it only has two neighbouring NMR active nuclei to couple with. As for the two multiplets, these resulted from multiple coupling to other protons as well as the fluorine atoms of the fluorous chain.

The ^{13}C NMR was also consistent with the proposed structure of the product. Four of the aromatic peaks were in very similar environments around 128 ppm with only the carbon attached to the methylene spacer discernable from the others at 135.8 ppm. There was also a peak at 171.0 ppm which corresponded to the carbonyl carbon atom. As for the remaining signals, the methylene carbons were at highest field for the sp^3 carbon at 66.5 and 55.1 ppm. The carbon atoms which make up the propyl group corresponded to the peaks at 53.1 (C adjacent to N), 28.7 (triplet due to proximity to C-F groups), and 19.4 ppm (middle carbon). Because of multiple peak splitting and quaternary substitution of all the carbon atoms of the fluorous chain no signal were seen for these nuclei which is consistent with literature reports for analogous compounds [84, 85]. In the FT-IR spectrum, there was one peak of interest representing the carbonyl vibrations at 1764 cm^{-1}. The high resolution electrospray MS [M^+] peak at 774.1507 m/z was also in good agreement with the calculated value of 774.1512 m/z (0.65 ppm error).

*2.5.2 – 2,2'-(3-perfluorooctylpropylazanediyl)diacetic acid (**4**)*

Once the benzyl ester had been isolated, an optimal deprotection strategy was investigated. While there was a procedure described in the literature for deprotecting benzyl esters using alumina, it was not effective with our compound.[86] For

hydrogenation, compound **3** was dissolved into MeOH and added to a flask containing 10% (by weight) Pd/C suspended in MeOH (Scheme 2.4). The flask was evacuated with argon to remove any moisture and then further purged with hydrogen gas. The final step was to leave the reaction stirring under an atmosphere of hydrogen for two hours. Following filtration through celite to remove the catalyst, the solvent was evaporated and the diacetic acid **4** was isolated in 93% yield without requiring any further purification.

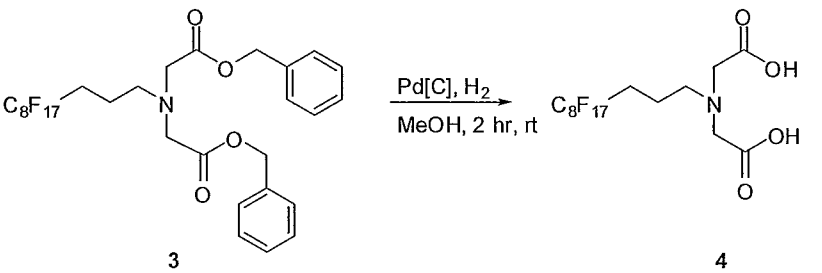

3 4

Scheme 2.4 - Preparation of *4*

The conversion of **3** to **4** could be monitored by ^{1}H NMR following the disappearance of the signals at 7.35 ppm and 5.09 ppm (aromatic and benzyl methylene protons, respectively). All other ^{1}H chemical shifts remained relatively unchanged following hydrogenation other than a slight shift in the signal associated with the four methylene protons between the amino and carbonyl groups from 3.61 ppm to 3.76 ppm. In the isolated product, the ^{13}C NMR also showed the disappearance of the 4 aromatic peaks around 128 ppm and at 135.8 ppm, as well as the methylene spacer of the benzyl group at 66.5 ppm. As with the ^{1}H NMR, all of the other carbon signals remained unchanged. The FT-IR showed a slight change in the shift of the carbonyl group from 1764 cm^{-1} to 1734 cm^{-1} which was to be expected when the ester was transformed to a

carboxylic acid. ESMS showed a [M^+] peak at 594.0580 m/z which was consistent with the calculated molecular weight of the desired product (594.0573 m/z, 1.18 ppm error).

*2.5.3 – Copper (II) 2,2'-(3-perfluorooctylpropylazanediyl)diacetate (**5**)*

With the fluorous chelate in hand, the next step was to prepare the Cu(II) complex (Scheme 2.5). In order for the ligand capture procedure to be successful, the ancillary ligands on the Cu must weakly interact with the metal as they need to be replaced by the free ligand remaining in solution following labeling with ^{99m}Tc. Copper (II) sulfate was chosen because the sulfate anion is well known as a weakly coordinating ligand.[47] Unfortunately, the salt proved to be difficult to work with in conjunction with **2** because of solvent incompatibility. Nevertheless several reactions were attempted in a variety of solvents.

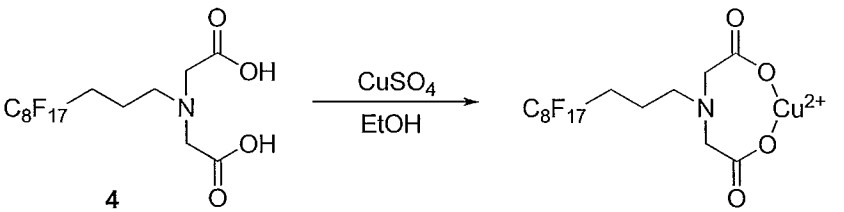

Scheme 2.5 – Reaction of 4 with $CuSO_4$

With a very lipophilic tail and a polar head group, compound **2** was not soluble in any solvents other than low molecular weight alcohols and dimethyl formamide (DMF). Ethanol was chosen as the first reaction solvent; however, the limited solubility of the copper salt prevented any reaction from occurring. A binary solvent mixture was then attempted with the excess of copper sulfate dissolved into water and the diacetic acid dissolved in ethanol. Unfortunately, there was not enough mixing of the phases to

produce any of the desired products. Next, methanol was employed as both the copper salt and ligand were soluble. The main product of the reaction, however, was formation of methyl esters as determined by ESMS (m/z = 622). Changing the pH of the EtOH solution to pH = 2 using 1 M H_2SO_4 or to pH = 12 using 1 M DIPEA also did not yield the desired product. The final attempt with $CuSO_4$ was to use a microwave reactor to improve solubility and to drive the reaction to completion.[82] Unfortunately the approach was also unsuccessful.

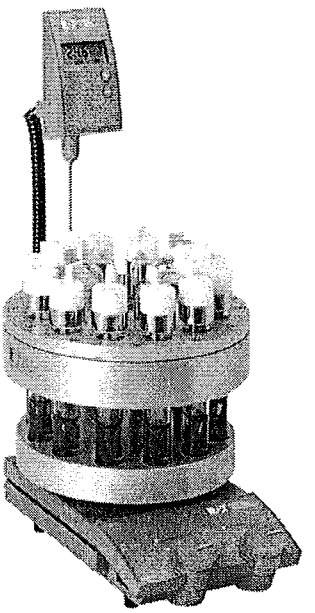

Figure 2.6 – Photograph of Radley's Carousel Classic 12 parallel synthesis apparatus. Reprinted from www.radleys.com

To overcome the solubility issues, a new series of experiments were conducted with different copper salts and solvents. As a time saving measure, these were conducted using a Radley parallel synthesis apparatus which allowed for 12 simultaneous reactions (Figure 2.6). The copper (II) salts included copper (II) bromide and copper (II) chloride as

the halogens should only weakly coordinate to the Cu complex (Scheme 2.6). Solvents were chosen on the basis of solubility of both the copper salt and fluorous ligand. Another consideration was that copper salts can catalyze the formation of methyl esters. If the diacetic acid was left in methanol overnight, no conversion takes place but once the copper was added, there was almost instantaneous, quantitative conversion to the methyl ester as seen on the ESMS (m/z = 622). Taking these issues into account methanol was not evaluated and EtOH, isopropanol (IPA), and DMF were selected as reaction solvents.

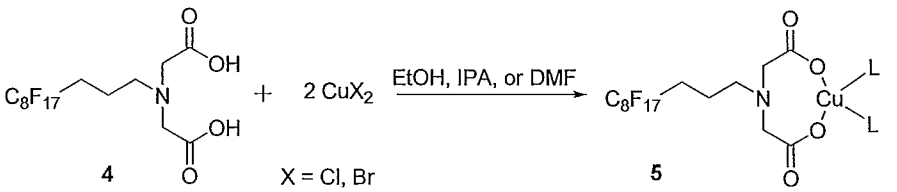

Scheme 2.6 - Preparation of the fluorous ligand capture agent, 5

By using the Radley reactor, each of the three solvents with two salt combinations could be evaluated simultaneously. In Table 2.3, the colour and transparency of each combination is presented. Reactions were initially stirred at room temperature for 3 days and attempts were then made to isolate the Cu complex. With EtOH and IPA, the solvent was removed under vacuum and the residue redissolved in DCM. The solution was filtered and sample of solid and filtrate was submitted for MS analysis. Due to the high boiling point, the reaction mixtures containing DMF were washed with water and then the residual solvent was extracted with ethyl acetate. This procedure led to formation of emulsions which were also submitted for MS analysis.

Table 2.3 - Solvent and copper salt combinations

Reaction	Solvent	CuX_2	Colour	Transparency
a	EtOH	$CuCl_2$	pale green	clear
b	IPA	$CuCl_2$	green/yellow	clear
c	DMF	$CuCl_2$	yellow	clear
d	EtOH	$CuBr_2$	yellow	opaque
e	IPA	$CuBr_2$	green	opaque
f	DMF	$CuBr_2$	green	opaque

The reaction which produced the desired copper complex was the EtOH/$CuBr_2$ combination (reaction d from Table 2.3). There was a blue precipitate that formed after three days with this combination. This precipitate was dried by vacuum filtration and washed with cold ethanol to remove any remaining salts and then DCM to remove residual alcohol. It was found that the same precipitate could be isolated by slowly dripping a concentrated solution of $CuBr_2$ in EtOH (dark yellow) into a stirring solution of containing the diacetic acid ligand, **4**, also in EtOH (clear, colourless) until the solution began to turn pale blue. (Scheme 2.7). Once the colour change stopped and the solution began to turn yellow, the blue precipitate was collected by filtration and dried under vacuum. This procedure greatly reduced the reaction time to mere minutes where the average yield was 76%.

NMR spectra of **5** could not be obtained for this complex because the copper (II) species is paramagnetic. The unpaired electrons shorten the relaxation times of the nearby

nuclei to such an extent that the peaks are too broad to obtain useful information.[87] Fourier transformed infrared spectroscopy was used to determine the shift in the carbonyl signals upon complexation of the ligand to the copper. The FT-IR signal for the carbonyl of the ligand appeared at 1734 cm^{-1} and the peak was shifted to 1594 cm^{-1} following addition of copper. With the loss of protons due to Cu coordination, there is a shift of electron density towards the metal and away from the carbonyl group. This shortens the double bond and increases the frequency of the carbonyl vibration.[88]

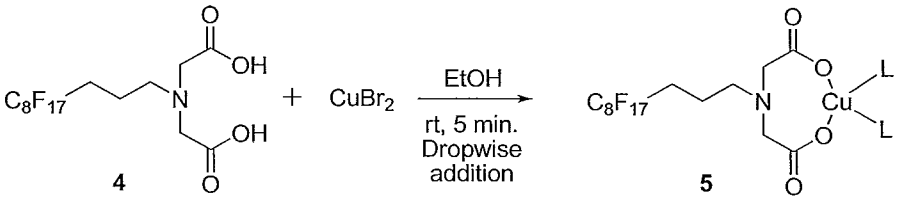

Scheme 2.7 - Expedited preparation of *5*

The other method of characterization conducted was high resolution ESMS which was obtained once **5** was fully solublized in DMF. The complex was insoluble in any other solvent and must be sonicated for it to dissolve in DMF. After stirring in DMF for a few hours, the ancillary ligands were replaced by the solvent and a high resolution mass spectrum was obtained for **5** with L = DMF and an m/z of 801.0778 correspond to the calculated m/z of 801.0768 (1.25 ppm error). With the fluorous ligand capture agent in hand the next step was to test the ability of **5** to capture unlabeled ligand.

2.6 – Fluorous Ligand Capture Methods

To test the ability of **5** to remove the excess ligand from solution using the FLC strategy, compound **5** (5 mg) was dissolved in DMF (0.5 mL) and added to a 1 mL

solution containing a mixture of **6** and **8b** (Scheme 2.8). The mixture was stirred for 5 min. and then loaded onto a F-SPE cartridge. Once loaded, a 4 mL fluorophobic wash of 20% water in MeOH was used to elute **8b** in 99% purity; however, only 60% of the overall activity was recovered. Another 4 mL wash was therefore completed leaving less than 10% of the activity on the cartridge.

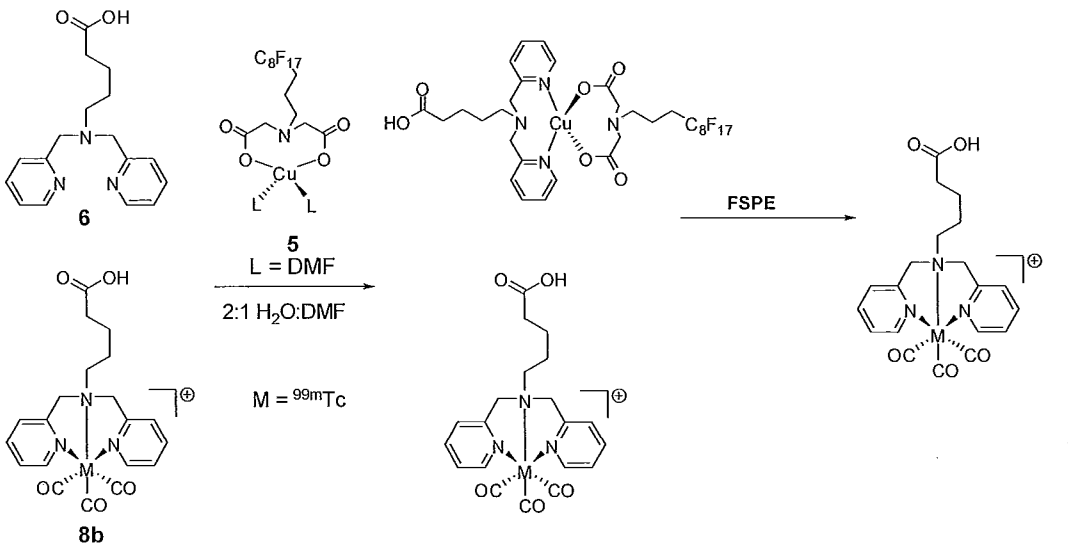

Scheme 2.8 - Fluorous ligand capture of excess *6*

HPLC was used to determine the residual concentration of unlabeled BPV. The radiochemical purity was greater than 99% with very high recovery of activity (Figure 2.7). These results have shown improvement over the solid-phase analog with much less material being used (5 mg vs. 200 mg) and less activity lost due to non-specific binding. The analysis of the UV spectrum demonstrated there was less than 1% of the original amount of ligand remaining (below the detection limit of 16.8 ng). The specific activity of the solution therefore changed from 0.740 GBq/mg prior to FLC to 33 500 GBq/mg

afterwards (based on eluting the generator every 24 hr and 60 min. synthesis and isolation time [89]).

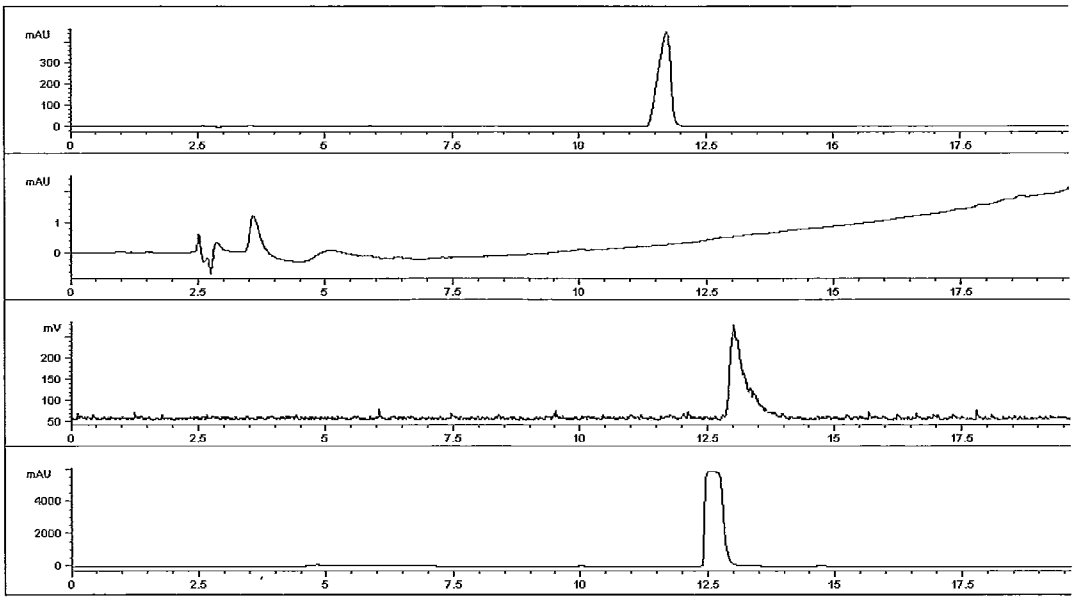

Figure 2.7 - HPLC chromatograms of results from FLC of 6. Top = UV trace showing crude 6 (t_R = 11.4 min.) prior to FLC. Second = UV trace showing removal of 6 following FLC. Third = γ trace showing 8b (t_R = 12.9 min.). Bottom = UV trace showing 8a (t_R = 12.6 min.). Phenomenex Gemini C18 5µm column (4.6 x 250 mm), 1 mL/min, gradient method A.

2.6.1 – Comparison between Solid-Phase and Fluorous Approaches

Both of the ligand extraction methods were highly efficient at capturing free ligand with the fluorous technique showing slightly better results. The best resin was the largest (150 – 300 µm) with 91.1 ± 4.8 % ligand capture while the FLC method removed greater than 99% of the ligand. Total synthesis time for the fluorous ligand capture agent **5** was shorter than the Cu resin (6 and 30 hours, respectively) and less Cu metal was wasted in the preparation of the fluorous agent. Comparing the radiochemical yields of the two methods, there was less non-specific binding to the fluorous components

compared to the polymeric resin (8.5 ± 1.6% versus 21.2 ± 1.0%) and the fluorous ligand capture did not require the need to remove any Cu salts from the solution after the chemoselective filtration. One limitation of the fluorous method is that it requires DMF, however, the residual DMF is eluted prior to isolation of the product in alcohol-water.

2.7 – Fluorous Ligand Capture of a Peptide Conjugate, dpKGGGLTVSPWY

The evaluation and optimization of FLC using a model system was an important first step, however, the ability of FLC to capture chelate derivatized molecules is a crucial test of the strategy. As a means to further evaluate this new method of purification, a peptide conjugate of the dipyridyl ligand which targets the erbB2 receptor was chosen. ErbB2 is a human epidermal growth factor that has been shown to be up-regulated in approximately 30% of breast cancers. In such cases, the prognosis is generally poor as this receptor activates Akt, a serine/threonine kinase which promote cellular survival.[90] A heptapeptide LTVSPWY was chosen as the targeting vector for erbB2 as it has been shown (through fluorescence studies with green fluorescent protein) to be rapidly internalized by erbB2 expressing breast cancer cells.[91] The peptide has been modified at the N-terminus with a triglycine linker and a single amino acid chelate (SAAC) group for coordination to the $[^{99m}Tc(CO)_3]^+$ core (Figure 2.8). Obtaining high effective specific activity of this product would increase the utility of this peptide conjugate as the B_{max} for this low expression receptor in breast cancer tissue is circa 1 million receptors per cell versus 10 000 receptors per cell in regular breast tissue.[92, 93] If there is excess ligand remaining the receptor would be easily saturated, hindering the diagnostic image quality.

Fluorous ligand capture will be employed as a means to remove this excess ligand to isolate high effective specific activity radiolabeled product.

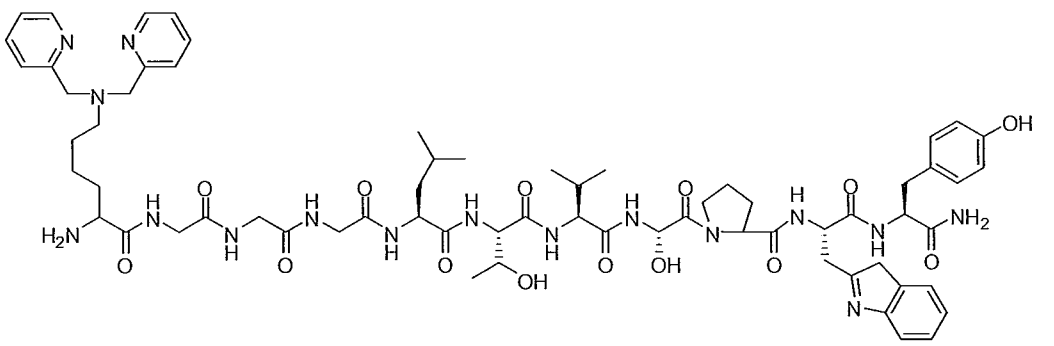

Figure 2.8 – dpKGGGLTVSPWY (9)

Compound **9** was prepared by solid-phase peptide synthesis following the method reported by Shadidi and Sioud [91] using a CEM Liberty synthesizer. Each of the amino acids were prepared in 5 mmol solutions along with coupling and deprotection agents. A 100 - 200 mesh Wang resin was used and the total synthesis time was approximately 6 hours. The peptide was then precipitated into cold diethyl ether following cleavage from the resin using a TFA, H_2O, and triisopropylsilane (98:1:1) cocktail. To isolate **9**, semipreparative HPLC was conducted on a Phenomenex Gemini NX 5 μm C18 column (10.0 x 250 mm) by gradient elution (5% MeCN + 0.1% TFA in water to 50% MeCN + 0.1% TFA in water over 23.6 minutes at 4.73 mL $min.^{-1}$) with a retention time of 18 minutes. The fractions were combined, frozen, and the peptide was lyophilized to yield 80% product. This product was characterized by LCMS and the measured $M^+ + H$ was 1345.8 m/z while the calculated value was 1345.7 m/z. Analytical HPLC was also completed to determine the purity of **9** (Figure 2.9).

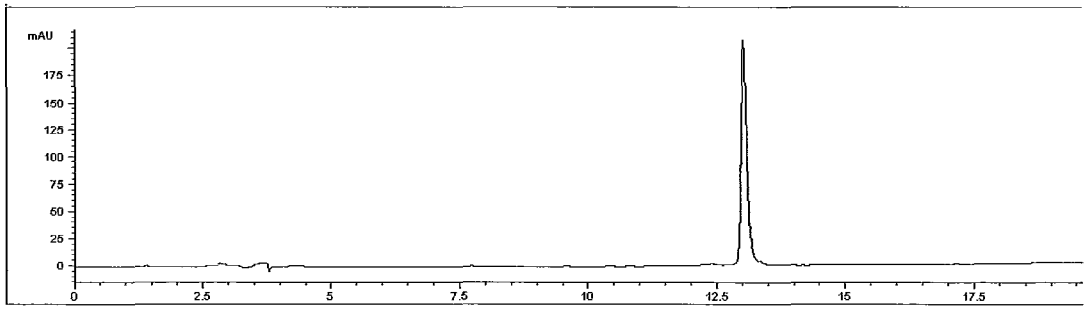

Figure 2.9 – UV HPLC chromatogram showing purified 9 (t_R = 13.0 min.). Phenomenex Gemini C18 5µm column (4.6 x 250 mm), 1 mL/min, gradient method B.

Approximately 1 mg of peptide **9** (in 0.2 mL MeCN) was labeled with $[^{99m}Tc(CO)_3(OH_2)_3]^+$ solution (370 GBq in 0.8 mL, pH = 7.0 – 7.4, Scheme 2.9). The pH of solution was neutralized to avoid degradation of the peptide. The reaction was heated to 75°C for 10 min. in the microwave and upon completion; a 100 µL aliquot was removed and added to 900 µL of water for crude HPLC analysis (Figure 2.11). There was one peak in the UV chromatogram at 13.0 min. representing the unlabeled ligand. In the gamma chromatogram, there was only one peak at 15.6 min. which corresponds to the Re standard (t_R = 15.2 min.) which was added separately after the purification described below.

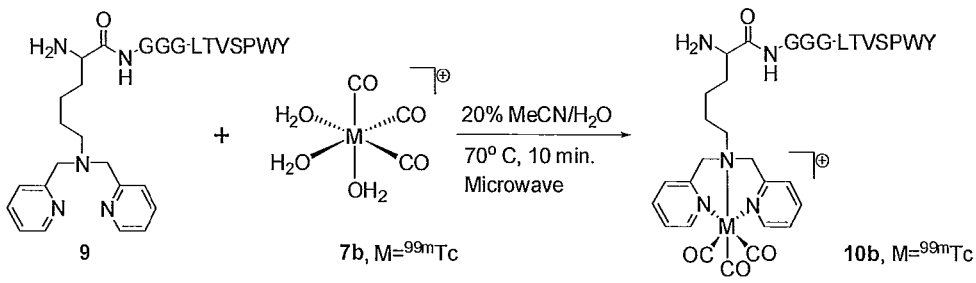

Scheme 2.9 - Radiolabeling of peptide 9

A calibration curve for the peptide conjugate was completed in order to determine the limit of detection and to determine the amount of excess ligand remaining in solution. Five solutions containing various concentrations of peptide **9** (0, 45, 225, 450, and 670 nM) were prepared and injected in triplicate (50 μL each). The pooled results were used to estimate the limit of detection by linear regression of the data and the value was 1.35 nM (Figure 2.10).

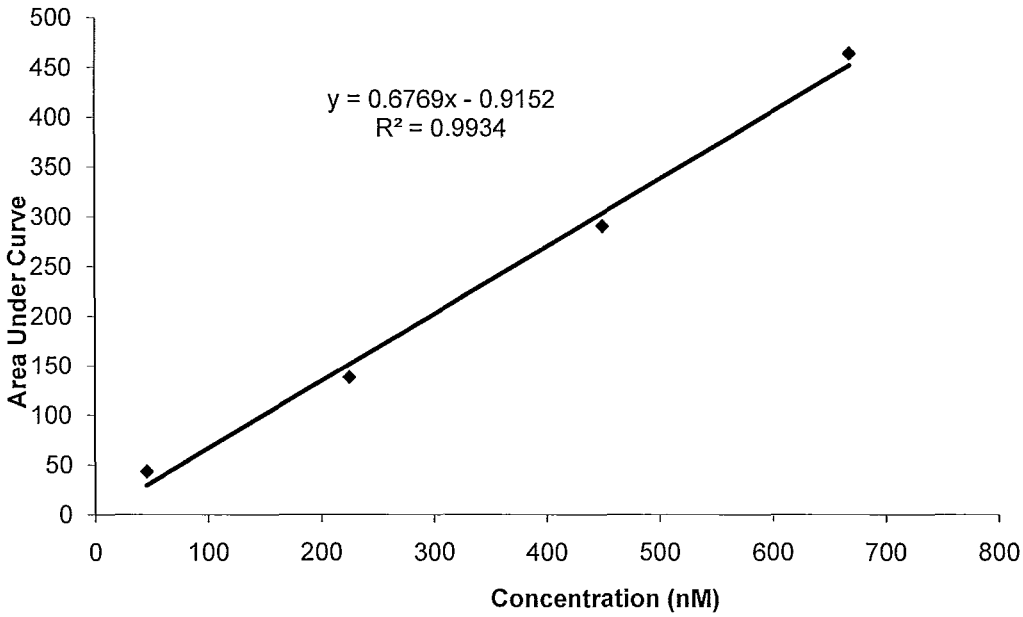

Figure 2.10 – Calibration curve of peptide 9

To test the ability of the FLC method to remove residual ligand, more FLC agent had to be used due to the increased sterics caused by the peptide conjugated to the chelate. This increase in mass of **5**, however, required more DMF to solvate and this can lead to breakthrough on the F-SPE cartridge. Thus, the mixture of **5**, **9**, and **10b** was sonicated for 5 min. to increase the solubility of all reagents. After sonicating for 5 min.,

the mixture was loaded onto a 2g F-SPE cartridge and eluted with a fluorophobic wash consisting of 20% H_2O in MeCN (8 mL). The solvent in the fractions was removed by a Biotage V10 rapid evaporation system and the residue was then dissolved into 1 mL of water. A 100 μL aliquot was added to 900 μL water for HPLC analysis with the Re standard added (Figure 2.11).

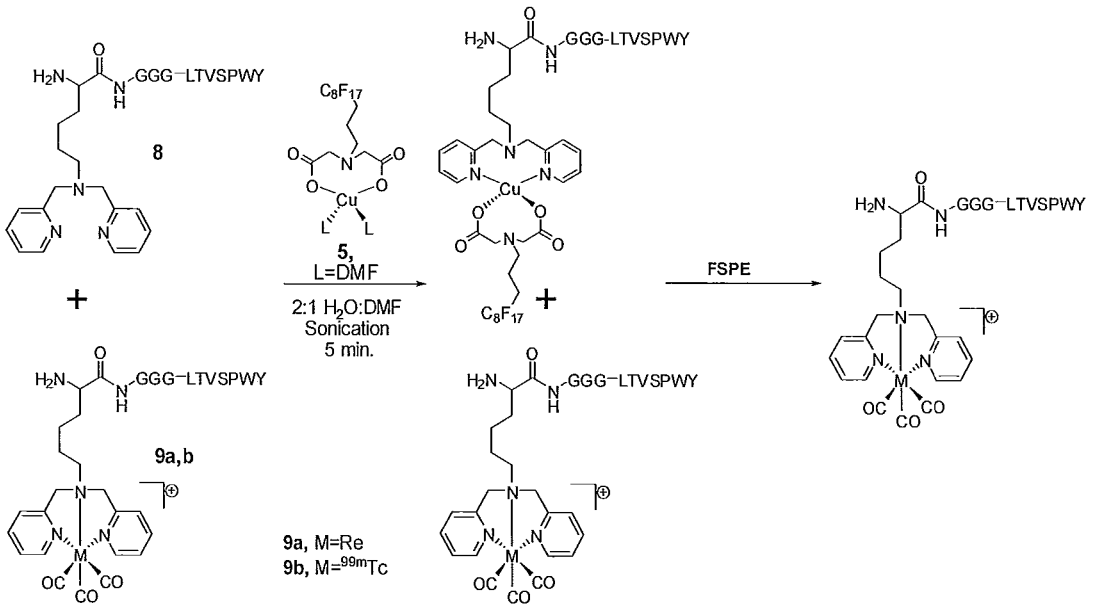

Scheme 2.10 - Fluorous ligand capture of erbB2 targeting peptide

Similar results were obtained for the effectiveness of ligand removal (approximately 99% of **9** was removed) but there was increased loss of activity due to non-specific binding to the cartridge (circa 40%). In order to determine where the radioactivity was binding, the cartridge was taken apart and the different components were placed into the well counter. The result was all of the activity which remained on the cartridge was on the fluorous silica. Because of the weak intermolecular forces between

organic molecules and fluorous groups and based on the experience with the non-conjugated ligand, there should have been minimal retention of the radiolabeled product on the fluorous silica. One explanation for the high non-specific binding could be the presence of uncapped Si-OH groups interacting with amino acid residues. With reactions conducted on the macro scale, small amounts of free Si-O and Si-OH would not pose a problem but when the reaction is on the tracer level, a small percentage of fluorous silica within a 2 g cartridge represents a large excess compared with the radiolabeled product.

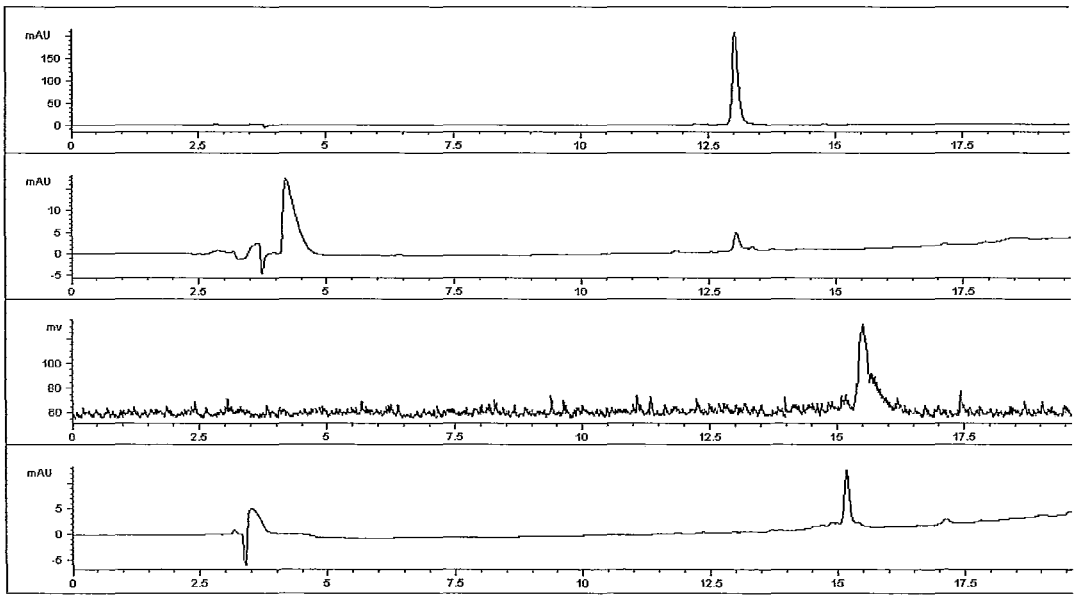

Figure 2.11 - HPLC chromatogram results from FLC of *9*. Top =UV trace showing crude 9 (t_R = 13.0 min.). Second = UV trace showing removal of 9. Third = γ trace showing 10b (t_R = 15.6 min.). Bottom = UV trace of 10a (t_R = 15.2 min. Phenomenex C18 5μm column (4.6 x 250 mm), 1 mL/min, gradient method B.

One additional difference between these two FLC procedures was the pH of the solutions being loaded onto the cartridges. With the model chelate system, the radioactive solution of **7b** was not neutralized (pH ~ 11) but to avoid degrading the peptide, the same solution had to be neutralized when labeling **9**. In subsequent attempts, prior to loading

the reaction mixture, the F-SPE cartridges were washed with a basic solution of DIPEA in DMF. Following the treatment, non-specific binding was decreased from circa 40 % to 13% as a result of creating a consistent pH throughout the cartridge. With a high level of ligand removal (95.1 ± 0.8%, Figure 2.11) and small mass losses (12.1 ± 1.2%), the fluorous ligand capture strategy appears to be a viable approach to purifying peptides as well as small molecules.

2.8 – Conclusions

Investigations into purification methods which are designed to remove unlabeled ligand in a kit friendly manner have led to the development of the fluorous ligand capture methodology. This new method showed improved efficiency over a solid-phase approach (Table 2.4). Compound **5** was used to removed excess precursor after radiolabeling a simple ligand (**6**) and a larger peptide (**9**) with $[^{99m}Tc(CO)_3]^+$ core (> 99% and 95% ligand removed, respectively) while minimizing the amount of desired product which is lost due to non-specific binding. Fluorous ligand capture also required less material in terms of capture agents because the sequestering step occurs in a homogenous solution so the kinetics of capturing the precursor occurs more quickly. Further experiments must now be undertaken to explore the non-specific binding of different charged amino acid side chains to the fluorous silica prior to any definitive conclusions can be made with regard to the effectiveness of FLC of peptides. Once optimized for peptides, this new technique will enable targeted ^{99m}Tc-based radiopharmaceuticals to be prepared using instant kits.

Table 2.4 – Summary of ligand capture results

Method	Ligand Removed	Non-Specific Binding
Solid-phase (20 – 75 μm)	86.0 ± 2.2%	26.7 ± 2.7%
Solid-phase (75 – 150 μm)	90.1 ± 2.8%	22.4 ± 1.1%
Solid-phase (150 – 300 μm)	91.1 ± 4.8%	21.1 ± 1.0%
FLC (6)	> 99%	8.5 ± 1.6%
FLC (9)	95.1 ± 0.8%	12.1 ± 1.2 %

2.9 – Experimental Procedures

Reagents were purchased from Sigma-Aldrich and Fluorous Technologies and were used without further purification. Fluorous solid-phase extractions were conducted using Fluorous Technologies Inc. FluoroFlash® 2 g SPE cartridges. $[Re(CO)_3(OH_2)_3]Br$ (**7a**), bispyridyl valeric acid (**6**), and dpK-GGG-LTVSPWY peptide (**9**) were prepared according to literature procedures.[17, 36, 91, 94] ^1H and ^{13}C NMR spectra were recorded on Bruker AV600 spectrometers. ^1H NMR chemical shifts are reported in ppm relative to the residual proton signal of the deuterated solvents. Coupling constants (*J*) are reported in Hertz (Hz). ^{13}C chemical shifts are reported in ppm relative to the carbon signal of the solvent. Low resolution electrospray ionization mass spectroscopy experiments were performed on a Waters/Micromass Quattro Ultima instrument. High resolution mass spectra were obtained on a Waters/Micromass Global Q-ToF spectrometer. Infrared spectra were obtained on a Bio-Rad FTS-40 Fourier transform IR spectrometer. Non-

radioactive products requiring column chromatography were isolated on a Biotage SP1 normal phase automated purification system.

Analytical HPLC was conducted using an Agilent 1100 series HPLC and C-18 Phenomenex column (4.6 x 250 mm). The elution protocols were: Method A: Solvent A = water (with 10mM ammonium formate), Solvent B = methanol: Gradient elution 0 min., 20% B; 20 min., 90% B. Method B: Solvent A = water (with 0.1% TFA), Solvent B = acetonitrile (0.1% TFA): Gradient elution 0 min., 5% B; 20 min., 60% B. Method C: Solvent A = water (with 0.1% TFA), Solvent B = acetonitrile (0.1% TFA): Gradient elution 0 min., 5% B; 23.6 min., 50% B. For method A and B, the flow rate was 1.0 mL $min.^{-1}$ and for method C the flow rate was 4.3 mL $min.^{-1}$. For all experiments, UV monitoring was performed at 254 nm.

*2.9.1 – Peptide Synthesis dpKGGGLTVSPWY (**9**)*

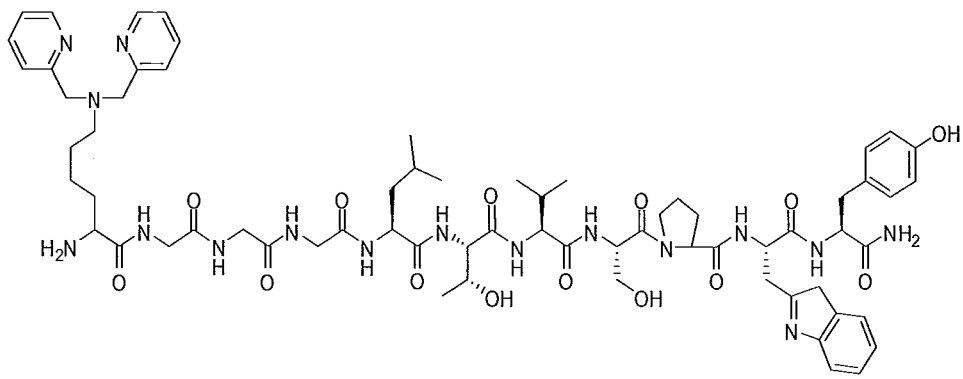

Peptide **9** was prepared on a CEM Liberty solid-phase synthesis system. Rink amide resin was suspended into DMF and then added to the microwave reactor of the system. The resin was washed with DMF and DCM prior to the addition of the first Fmoc protected amino acid as a 0.1 M solution in DMF. Following coupling using HATU, the

Fmoc group was removed using a 20% piperidine in DMF solution. This process was repeated for each amino acid in the sequence. Once the coupling reactions were complete, the resin was filtered and washed with cold DMF followed by cleaving the peptide from the resin (cleavage cocktail = TFA (3.8 mL), triisopropyl silane (0.1 mL), and water (0.1 mL)). The resin was shaken in the cleavage cocktail for 4 hours at room temperature and 350 rpm before filtering the suspension through glass wool into cold diethyl ether (40 mL). The resulting heterogeneous solution was centifuged at 3000 rpm for 10 min. at 4°C, forming a white pellet. After decanting the diethyl ether, the process was repeated twice more. Once completed, the white solid was dissolved into 10% CH_3CN in water and lyophilized, yielding a white solid. The peptide **9** was then purified using semipreparative HPLC using a Phenomenex Gemini-NX C-18 column (250 x 10 mm) and Method C: t_R = 18.0 min.

2.9.2 – Calibration Curves

Calibration curves for compounds **6** (t_R = 11.7 min.) and **9** (t_R = 13.0 min.) were prepared using an Agilent 1100 series UV-HPLC employing elution methods A and B respectively using a Phenomenex Gemini NX 5 μm C18 column (4.6 x 100 mm). The actual concentrations of **6** were 0, 5, 20, 35, and 50 μM and 50 μL of each sample were injected. The limit of detection was determined by linear regression of the average of triplicate calibration curves to be 1.12 μM. Both the graph and regression data can be found in Figure 2.3. The actual concentrations of **9** were 0, 45, 225, 450, and 670 nM and 50 μL was injected for each. The limit of detection was determined by linear regression of

the average of triplicate calibration curves to be 1.35 nM. Both the graph and regression data can be found in Figure 2.10.

2.9.3 – Preparation of Cu Resin

Commercially available Amberlite IRC-748 resin (three sizes, 20 – 75, 75 – 150, and 150 – 300 μm, 2 g of each) was washed with water then suspended in a saturated aqueous solution of $CuSO_4$. This suspension was stirred for 5 hours. The blue resins were then washed with 100 mL of water, THF, and DCM prior to resuspending in a fresh $CuSO_4$ saturated solution. Following 24 hr of shaking, large crystals of $CuSO_4$ had formed and these were manually separated from the resin or by collecting them into a Hirsh funnel that did not contain filter paper. The resin, which passed through the funnel, was then collected by suction filtration and wash with 500 mL of water and 100 mL of THF and DCM. The residue was then dried under vacuum overnight and used without any other modification or characterization.

*2.9.3 – Preparation of $C_{29}H_{24}F_{17}NO_4$ (**3**)*

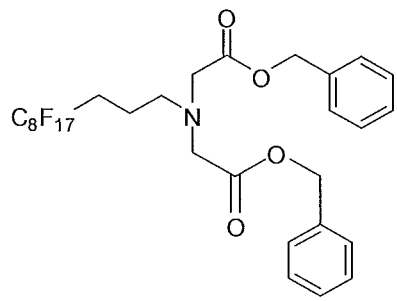

3-(Perfluorooctyl)propyl amine (**1**, 950 mg, 2.0 mmol) was added to a 20 mL microwave vial, followed by acetonitrile (14 mL) and diisopropylethyl amine (2.8 mL, 16 mmol). To the stirring solution, benzyl bromoacetate (**2**, 1.3 mL, 8.0 mmol) was added

dropwise. The vial was sealed and heated to 145°C for 35 min. with stirring in a Biotage Initiator 60 microwave reactor. After cooling to room temperature, the solvent was removed by rotary evaporation and the residual orange solid was dissolved in a small volume (1.0 – 2.0 mL) of $CHCl_3$. The desired product was isolated by silica gel chromatography using a Biotage SP1 automated purification system (Solvent A = hexane, solvent B = ethyl acetate.7% B, 0 to 4 min., up to 60% B, 4 to 40 min., hold to 47 min.) as a clear, colourless, viscous oil. (1.52 g, 98%). FTIR NaCl disc (cm^{-1}) 3036, 2957, 1746, 1242, 1212, 737, 699. ^1H NMR (200 MHz, $CDCl_3$) δ 7.35 (s, 10H), 5.09 (s, 4H), 3.60 (s, 4H), 2.81 (t, J= 6.8, 2H), 2.14 (m, 2H), 1.72 (m, 2H). ^{13}C NMR (50 MHz, $CDCl_3$) δ 171.0, 135.7, 128.7, 128.5, 66.5, 55.1, 53.1, 28.4 (t, $^3J_{C\text{-}F}$= 22.3 Hz), 18.9. TLC (30% ethyl acetate in hexane) R_f = 0.52. HRMS-ESI (*m/z*) for [$C_{29}H_{24}F_{17}NO_4$] calcd. 774.1512, found 774.1507.

2.9.4 – Preparation of $C_{15}H_{12}F_{17}NO_4$ (4)

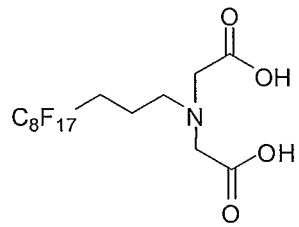

Compound **3** (440 mg, 0.60 mmol) was added to a 25 mL round bottom flask and dissolved in methanol (5 mL). To this solution, a suspension of 10% Pd/C (44 mg) in ethanol (5 mL) was added. The flask was sealed and flushed with Ar for 10 minutes, then two 5 minute flushes with H_2 after which the reaction was left stirring for 2 hours. The solution was then filtered through a celite plug and washed with methanol (3 x 5 mL).

The filtrate was concentrated by rotary evaporation leaving a white powder (404 mg, 92%). m.p. = 161°C decomp. FTIR KBr (cm^{-1}) 3438, 1734, 1636, 1240, 1149. ^1H NMR (200 MHz, CD_3OD) δ 3.76 (s, 4H), 3.12 (t, *J*= 7.4, 2H), 2.26 (m, 2H), 1.90 (m, 2H). ^{13}C NMR (50 MHz, DMSO, d_6) δ 172.7, 54.7, 52.5, 27.4, 18.4. HRMS-ESI (*m/z*) for $[C_{15}H_{12}F_{17}NO_4]$ calcd 594.0573 , found 594.0580.

*2.9.5 – Preparation of $C_{15}H_{10}F_{17}NO_4Cu(II)$ (**5**)*

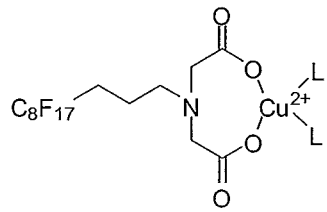

Compound **4** (100 mg, 169 mmol) was added to a 50 mL round bottom flask and dissolved into ethanol (20 mL). To this stirring solution, copper(II) bromide was added (75.3 mg, 337 mmol) and the clear green solution stirred for 3 days at room temperature. After this time, a pale blue powder was collected by suction filtration from the dark orange solution. After washing with cold DCM and ethanol (3 x 10 mL each), the solution was dried under high vacuum. Upon stirring in DMF for 6 hours, the mixture of ancilliary ligands were all exchanged for DMF and no colour change was observed. Removal of the DMF solution resulted in a pale blue solid (348 mg, 78%). m.p. = 254 - 255°C. FTIR KBr (cm^{-1}) 3250, 1637, 1594, 1203, 1152. HRMS-ESI (*m/z*) calcd 801.0768, found 801.0778 (L = DMF).

*2.9.6 – Preparation of $[^{99m}Tc(CO)_3(OH_2)_3]^+$ (**7b**)*

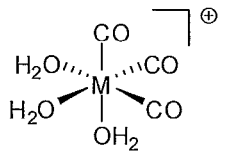

$^{99m}TcO_4^-$ was eluted, with 0.9 % saline, from a commercially available ^{99}Mo generator (2960 MBq, 5.0 mL). This eluent was added to a crimp sealed vial (which had been purged with argon) containing potassium sodium tartrate (16.0 mg), sodium tetraborate (6.5 mg), sodium carbonate (6.0 mg), and potassium boranocarbonate (10.0 mg). This reaction mixture was heated in the microwave to 120°C for 3 min. with stirring. γ HPLC method A: $R_T = 2.4$ min.; method B: $R_T = 9.1$ min. Yield: 2660 MBq, 98%.

*2.9.7 – Preparation of $[C_{17}H_{21}N_3O_2{}^{99m}Tc(CO)_3]^+$ (**8b**)*

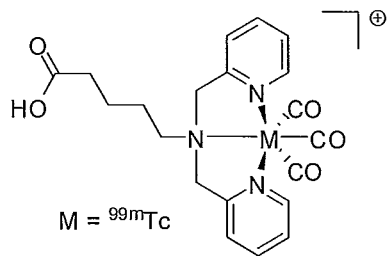

Compound **6** (0.2 mL, 5 mg/mL in CH_3CN) was added to a crimp sealed microwave vial and purged with argon for 15 min. To this, compound **7b** was added (740 MBq, 0.8 mL) and then heated to 150°C for 2 min. with stirring. Compound **8b** was purified by two separate ligand capture experiments. The first approach was a solid-phase method developed by Causey *et al.*[1] The resin was prepared following the above method and 100 – 150 mg of each resin (20 – 75 ,75 – 150, and 150 – 300 μm) was

loaded into 1 mL syringe cartridges. The reaction mixture was neutralized and loaded onto resin followed by eluting with 3 mL of saline. The solvent was removed using the Biotage V10 rapid evaporation system and the residue was redissolved into 1 mL of water. A 100 μL aliquot was removed and added to 900 μL of water. This solution was used to measure the amount of ligand removed by analytical HPLC Method A: t_R = 12.9 min.; Yield: 573 MBq, 77.4 ± 1.6 %.

The second approach was the FLC method wherein **5** was dissolved in DMF (5 mg, 0.5 mL) as a pale blue solution and then added to the reaction mixture. This solution was stirred for 5 min. and then loaded onto a 2 g Fluoro Flash SPE cartridge, which had been prewashed with 4 mL DMF and 8 mL of a fluorophobic solution (20% water in methanol). After loading the sample onto the cartridge, another 8 mL fluorophobic wash was conducted to elute the radiolabeled complex. The solvent was removed using the Biotage V10 rapid evaporation system and the residue was redissolved into 1 mL of water. A 100 μL aliquot was removed and added to 900 μL of water. This solution was used to measure the amount of ligand removed by analytical HPLC Method A: t_R = 12.9 min.; Yield: 677 MBq, 91.5 ± 1.6 %.

*2.9.8 – Preparation of [^{99m}Tc(CO)$_3$-dpKGGGLTVSPWY]$^+$ (**10b**)*

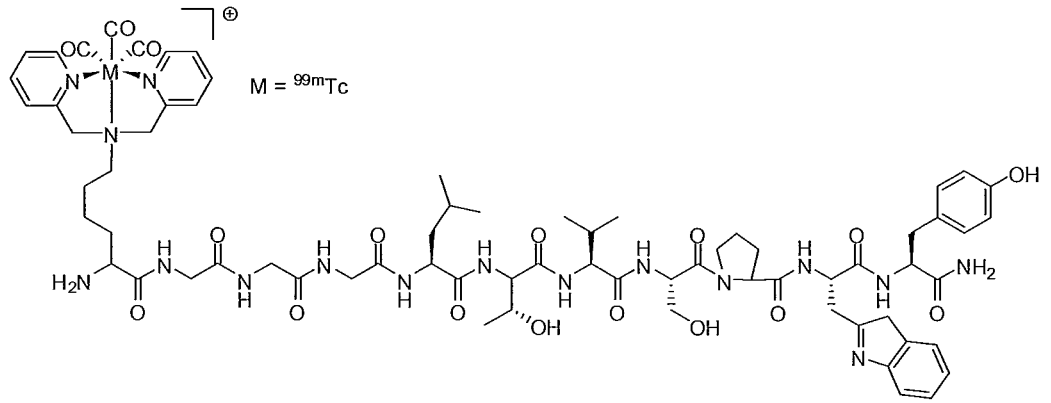

Compound **9** (0.2 mL, 5 mg/mL in 1:1 CH_3CN in water) was added to a crimp sealed microwave vial and purged with Ar for 15 min. To this, compound **7b** was added (370 MBq, 0.8 mL) and then heated to 60°C for 10 min. in a Biotage microwave reactor with stirring. Compound **5** was dissolved in DMF (20 mg, 0.4 mL) as a pale blue solution and then added to the reaction mixture. This solution was stirred for 10 min. and then loaded onto a 2 g Fluoro Flash SPE cartridge, which had been prewashed with 4 mL DMF and 8 mL of a fluorophobic solution (20% water in CH_3CN). After loading the sample onto the cartridge, another 8 mL fluorophobic wash was conducted to elute the radiolabeled complex. The amount of ligand removal was measured by analytical HPLC Method A: t_R = 15.6 min.; Yield: 330 MBq, 87.1 ± 1.2%.

Chapter 3

3. Fluorous Ligand Capture in a Microfluidic Device

3.1 – Introduction

As demonstrated in the previous chapter, the newly developed fluorous ligand capture (FLC) method (Scheme 3.1) has been shown to be an effective chemoselective filtration strategy for sequestering excess precursor from radiolabeling reactions involving Tc(I) and dipyridyl ligands. This new method improved upon a solid-phase approach described in the literature. [1] While both techniques removed > 90% of the excess ligand, the fluorous approach exhibited a notable reduction in the amount of radiolabeled product being lost due to less non-specific binding interactions. This was attributed to the Teflon nature of the fluorous silica which should bind non-fluorous compounds to a much lesser extent than an organic polymer backbone. To advance the utility of the FLC strategy for the preparation of targeted radiopharmaceuticals, an attempt was made to automate the methodology using a microfluidic device.

Currently, most molecular imaging agents are prepared within a radiopharmacy either by an instant kit or an automated synthesis module (ASM).[95] The drawbacks to instant kits have been described in the previous chapter. While ASM's are routinely used for PET probes such as 2-deoxy-2-[^{18}F]fluoro-D-glucose ([^{18}F]FDG), they do suffer from some limitations. First, there is a need to dilute the samples into moderate volumes of solvent for solution handling, resulting in reduced reaction rates. Secondly, ASMs are often dedicated for use with a limited scope of reactions (e.g., substitution with F^-) and

are not sufficiently versatile for producing a wide variety of tracers. They are also costly and not easily shielded, often requiring a dedicated hot cell or mini-cell.

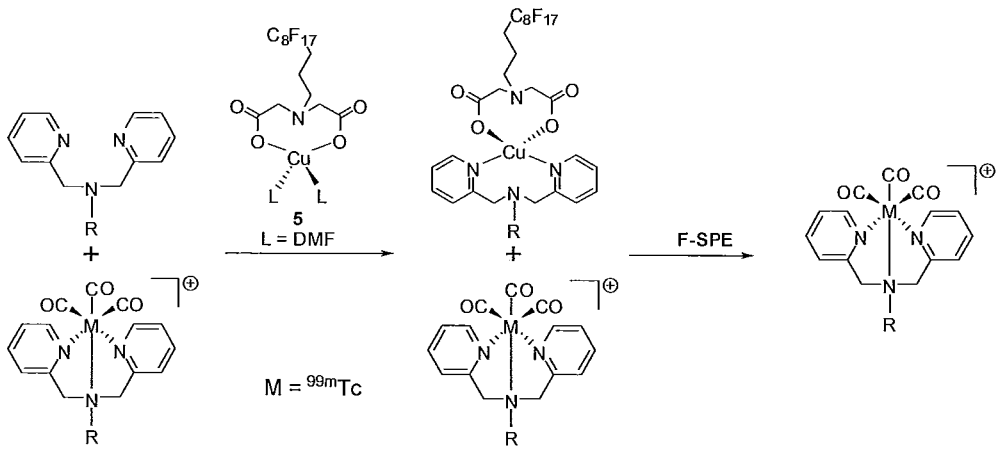

Scheme 3.1 - Fluorous ligand capture (FLC) method

Microfluidic devices consist of micro channels measuring between 10 and 100 μm in diameter. These small channels which have a large surface area to volume ratio, which leads to better heat and energy transfer and consequently enhanced reaction rates, increased reaction yields, and better reaction selectivity.[57] As an example, Wiles *et al.* demonstrated reduced reaction times with equivalent yields for an aldol reaction with silyl enol ethers (Scheme 3.2).[96] As a macroscale batch process, quantitative yields could be obtained after 24 hours but when the reaction was repeated in a microreactor, the comparable yield was achieved after only 20 minutes.

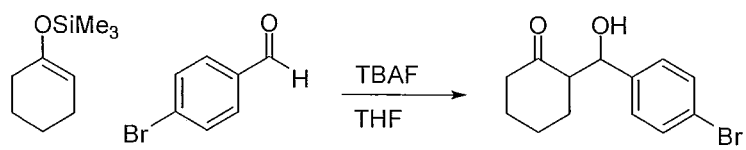

Scheme 3.2 - Aldol reaction conducted in microreactor from [96]

Along with improved reaction performance in terms of rate and yield, the atom economy is also increased due to the small channel size where less material is needed to achieve quantitative reactions. This is advantageous when preparing targeted molecular imaging probes as the mass of radionuclide is typically on the picogram or nanogram scale. In many cases, targeting vectors such as an antibody, protein, or peptide are used to direct the radionuclide to the target of interest[97-99] and these can be costly so reducing the amount of targeting vector needed also has a practical benefit.[100] Another major advantage to performing radiochemical reaction in a microfluidic system, which is often compact, is the ease with which the apparatus can be shielded.

Most of the radiolabeling experiments using microreactors that have been reported have focused on PET isotopes due to the need for quick and highly efficient reaction when working with short half-life isotopes.[69, 101-104] There is to our knowledge, however, only one published paper wherein a microfluidic device was used to radiolabel a precursor with ^{99m}Tc.[71] The goal of this study was to prepare a microreactor to label a variety of large and small molecules. Hydroxyl diphosphinate (HDP) oxidronate and macro-aggregated albumin (MAA) were chosen as the first test cases because conventional labeling methods do not require difficult purification steps as the ^{99m}Tc is complexed by mixing with precursor and obtaining near 100% radiochemical purity. Yields obtained in the microreactors were comparable to those achieved completing the labeling by the "shake and bake" batch method.

There is also a manuscript in preparation discussing the labeling of bifunctional chelates with ^{99m}Tc that can later be conjugated to a targeting vector. The investigation

was conducted by Simms *et al.* at the Centre for Probe Development and Commercialization in Hamilton, Ontario, Canada and therein a bifunctional chelate dithiazole valeric acid (DTV) was labeled with the Tc tricarbonyl core, $[^{99m}Tc(CO)_3(OH_2)_3]^+$ (Scheme 3.3).[72] As a proof of concept, they compared the results from the microfluidic experiments to conventional and microwave preparations.

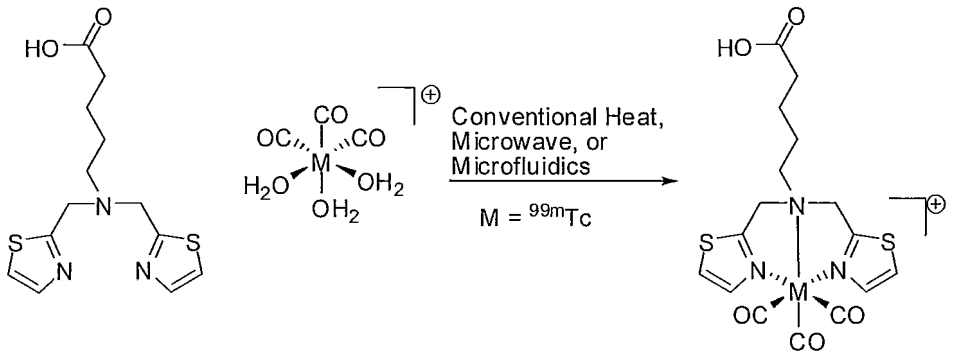

Scheme 3.3 - Radiolabeling of dithiazole valeric acid (DTV) with $[^{99m}Tc(CO)_3]^+$ core

When conventional heating was used to label a 1 mg/mL solution of DTV, it took 25 min. at 80° C to obtain 85% conversion. By diluting this solution 10-fold, only 35% yield could be obtained after 25 min. In the microfluidic reactor (100 μm channels with 4m total length), it took 7.85 min. at 80° C to achieve 94% yield at 0.10 mg/mL concentration of DTV compared to the 23% yield at the same temperature and time with conventional heating. Further dilution of the ligand solution to 0.01 mg/mL resulted in no conversion when conventional heating was used but the microfluidic and microwave conditions were able to obtain 85% and 25% yields, respectively, at 100°C. Completing reactions in microwave has been shown to also greatly increase yields and reduce reaction times. This is presumed to be due to the more even heating of the reaction vessel and the

selective absorption of microwaves by polar bonds.[81, 82, 105] While the microwave was faster at reaching maximum yield (1.57 min.), the yield did not increase with time.

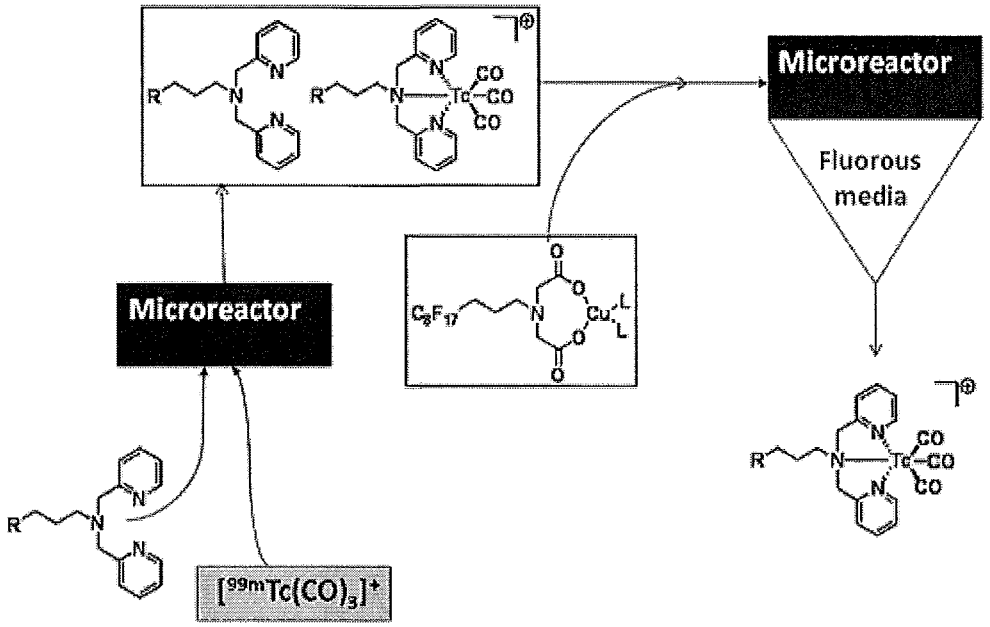

Figure 3.1 - Schematic of integrated microfluidic device for labeling and purification of ^{99m}Tc(I) agents.

Interestingly, the microfluidic approach was able to produce radiolabeled product at lower concentration than previously seen with similar ligand systems.[37] A 27% yield was obtained at 120° C after 7.85 min. with a DTV concentration of only 0.001 mg/mL. Although 1.0 μg/mL is a small mass, it is still in great excess compared to the pg amount of ^{99m}Tc used. As mentioned in previous chapters, it is imperative that this excess of ligand must be removed. Now that it has been shown that a microfluidic device can be used to synthesize ^{99m}Tc-labeled compound; the next step is to create an integrated method to purify these products by removing the excess chelator and achieve high effective specific activity (Figure 3.1). Furthermore, if the purification step could be

conducted in line, the potential for translation and minimizing radiation exposure would be greatly enhanced. It would also create an atom efficient labeling method which is growing in importance with the shortage of ^{99m}Tc.

An integrated microfluidic device for the preparation of targeted radiopharmaceuticals could be used to complete all the necessary steps for producing the radiolabeling product as well as the removal of any precursor to achieve high effective specific activity Tc-labeled agents. An excellent example of an integrated device can be seen in the work by Quake *et al.* wherein a microfluidic system was used to prepare a dose of [^{18}F]FDG.[106] All five steps needed to complete the labeling reaction were conducted on the device (concentration of fluoride, solvent exchange from water to MeCN, fluorination, solvent exchange back to water, and hydrolysis). As a means to concentrate the fluoride ion to radiolabel FDG with ^{18}F, Quake *et al.* used valves which trapped anion exchange beads but allowed solvent to pass through.[106] This created *in situ* anion exchange columns. Unlike target-specific agents, FDG does not require any purification to remove excess cold precursor and, therefore, a truly integrated approach to preparing targeted molecular imaging agents requires a purification step like the FLC method.

There are several examples of integrated purification strategies in the literature for microfluidic devices. To purify compound by chromatography, Ramsey and co-workers functionalized walls of micro channels with C18 groups. [107] They were able concentrate samples for mass spectrometry analysis with these modified components but open-channel designs such as this have limited stationary-phase capacity even at the high

surface area to volume ratio of micro channels. As a means to increase that capacity, Harrison *et al.* developed a double weir method of trapping bead-based reagent into chambers to conduct solid-phase extraction in microfluidic systems (Figure 3.2).[108] The separation between the cover plate and weir is too small for the beads to pass but the solvent can still flow through. Using a chamber packed with reverse phase chromatography beads, BODIPY was successfully concentrated onto the beads and then completely eluted when the solvent was changed from an aqueous to an organic medium.

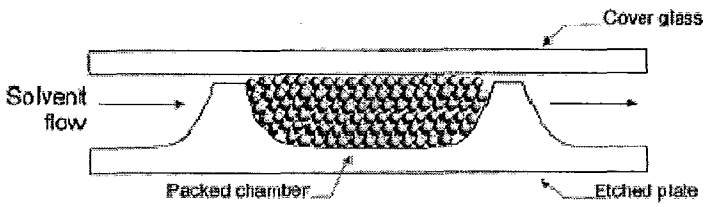

Figure 3.2 - Double weir chamber to trap bead-based reagent in microfluidic systems. Reprinted from [108].

In a similar manner, Hu *et al.* developed a fluorous solid-phase extraction (F-SPE) component for microfluidic devices to isolate fluorous-tagged amino acids for MS analysis.[75] One plate was etched with a horizontal 40 μm thick channel and another with two vertical channels 10 μm in diameter which coincided with the entrance and exit of the larger, perpendicular channel (Figure 3.3). Once the channels are fused together, the 40 μm portion is filled with fluorous silica through the R1 reservoir as a slurry. The solvent containing the analytes would then pass through the beads and fluorous components retained. As was the case with the double weir method, the beads are too large to leave the packed chamber. The method for preparing anion exchange columns for

[^{18}F]FDG synthesis could also be adapted to create *in situ* fluorous columns. It should therefore be feasible to apply the FLC method with a microfluidic device such as this.

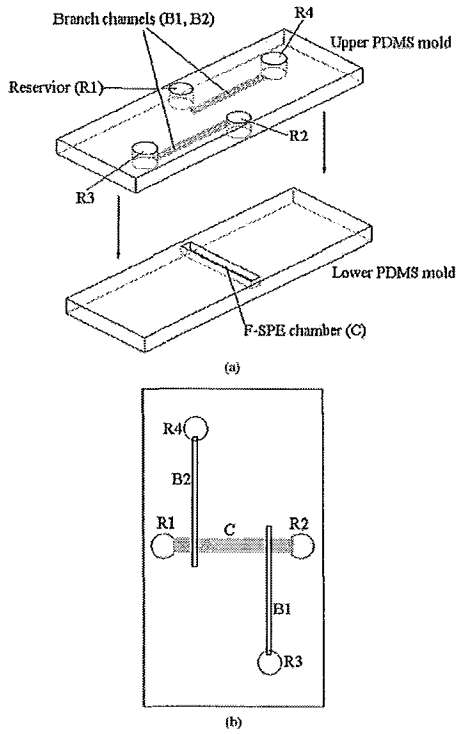

Figure 3.3 - Microfluidic fluorous solid-phase extraction component. Reprinted from [75].

3.2 – Objective

The objective was to evaluate the feasibility of performing the fluorous ligand capture method in a microfluidic device and to assess key parameters needed to achieve high radiochemical yield and effective specific activity. Once developed and optimized, a new generation of instant kits with inline purification capabilities could be developed. A parallel and complimentary objective was to determine if the FLC could be performed using cartridges preloaded with **5** versus performing the reaction in solution. The FLC

method could then by conducted by simply passing the radiolabeling mixture through the cartridge. In this manner, an *in situ* FLC column prepared with fluorous silica preloaded with **5** could be incorporated within a traditional kit or in a microfluidic device.

3.3 – Constructing the Microfluidic Apparatus

While there are commercial microfluidic components available, they are expensive and lack versatility which is needed during the research phase. Furthermore, uncertainty with regard to the solubility the compounds involved with the FLC led to the decision to construct a homemade device consisting of a syringe pump and capillary tubing (Figure 3.4). To minimize the exposure of radiation, a remote controlled syringe pump was used which consisted of the mechanical pumping mechanism attached to a cord leading to a control panel located external to the Pb shielding (Figure 3.5). For the small diameter tubing, two 30 cm length tubes and one 10 cm length tube of 100 μm wide glass capillary tubing was used. To connect the three tubes at a Y-junction, a union was used consisting of two HPLC fittings and a rubber tube insert to hold the capillary tubes when tightened into the union. At one end, the rubber fitting had two holes to receive the tubes from the reaction mixture and fluorous agent while at the other end only one tube exits. Mixing time for the two components could be control by changing the length of the 10 cm section or by changing the flow rate. Similar plastic fittings and HPLC connector were used with a Luer-lock adapter to attach the capillary tubes to their respective syringes. Once the system was put together, it was flushed with IPA and DMF to clean out the lines.

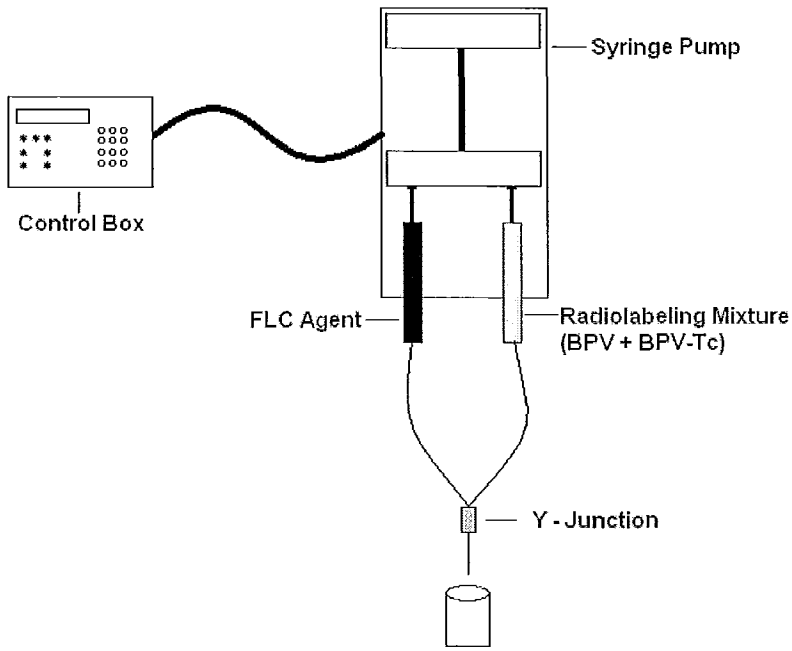

Figure 3.4 – Schematic representation of a homemade microfluidic device

3.4 – Initial Flow Tests

As the objective of this work was to show that the FLC method can remove the excess BPV from the product post labeling, assurances were needed that removal of the precursor ligand was due to the FLC agent and not non-specific adhesion to the capillary channels. An experiment was conducted where 1.0 mL of a 1 mg/mL BPV solution was flushed through the lines and collected in a vial. HPLC was then used to determine how much of the ligand was lost during this process. A 2 mL solution containing 2 mg of BPV was prepared with one half used in the microfluidic experiment and the other used as an HPLC reference standard. From the HPLC analysis there was insignificant loss of BPV during the elution through the capillary tubes. Different flow rates (10, 25, and 50 μL/min.) did not have an effect on the experimental results.

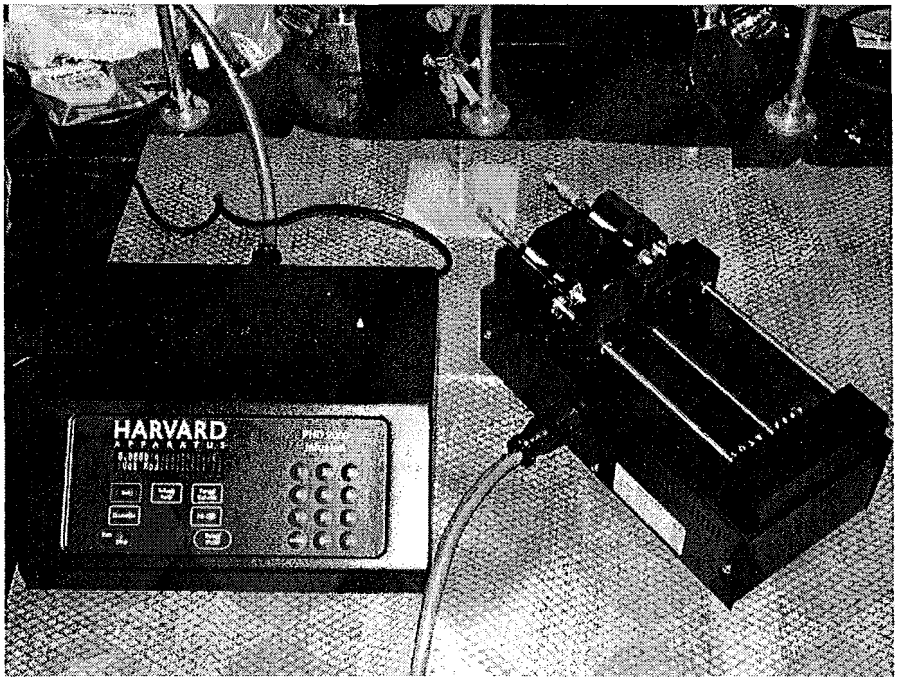

Figure 3.5 – Photograph of homemade microfluidic apparatus

Whenever dealing with radioactivity, non-specific binding can lead to a significant decrease in radiochemical yield. Thus, it was important to test for significant loss of product during the microfluidic process. One milliliter of an 81 MBq/mL solution of BPV-Tc was loaded into a 1 mL syringe and flushed through the lines. When the 1 mL was eluted, an extra wash of 30 μL was used to clear the lines. This volume was chosen because it is 10 times the volume of the micro channels. Over 95% of the radioactivity was recovered in this manner (78 MBq in 1.03 mL). FLC experiments could now be attempted knowing that there is minimum loss of product and the ligand capture should only be the result of the FLC process.

3.5 – Initial Experiments

The first hurdle to overcome was whether or not the FLC compound would precipitate upon mixing of the two liquid streams, clogging the lines and preventing the solution from exiting the system. For the radiolabeling reaction, 0.2 mL of a 5 mg/mL solution of BPV in MeCN was added to a 0.8 mL basic solution of saline containing the $[^{99m}Tc(CO)_3(OH_2)_3]^+$ (pH = 11) in a 2 mL microwave vial. This was sealed and heated to 150° C for 2 min. in the microwave. A 1 mL syringe was then loaded with the radiolabeling mixture and another was filled with a 5 mg/mL solution of **5** dissolved into DMF. After placing the two syringes into the pump, they were flushed at 50 μL/min. but there was too much backpressure and the syringe plunger bent. The 1 mL syringes were exchanged for the larger, sturdier 3 mL syringes and there was no bending of the plunger. There was, however, back flow of the radioactive material into the other syringe.

As a means to avoid these problems, the flow rate was slowed to 10 μL/min. This extends the time it takes to elute the 1 mL solution from 20 min. to 100 min. but the pressure should be lowered. Unfortunately, there was still mixing of the solutions in the syringes. It was therefore decided that a clog was forming at the Y-junction. To prevent further clogging, the concentration of **5** was lowered to 3 mg/mL and then 1 mg/mL but there was still too much backpressure and clogging for this method to be successful.

3.6 – Solubility of *5* in Microfluidic Device

As was the case with attempting to purify the erbB2 targeting peptide, the limiting factor appears to be the insolubility of **5** in any solvent. To solve this problem, the Y-junction could be placed into a heated sonicator bath as this has been shown to increase

the solubility of **5**. Prior to adopting this approach, a more simplistic option of finding a new solution to solvate **5** was completed. The first attempt was to change the pH of the DMF solution. Six solutions were prepared with various additions of acid (1N HCl) and base (DIPEA). In an acidic media, the colour changed from blue to yellow where the acid was thought to be causing the displacement of the Cu. To detect this, MS and IR spectra were obtained. The molecular ion peak at 800 m/z for **5** was still present and the IR signals for the carbonyl groups were still consistent with those of a coordination complex. Another indication that the copper remained coordinated to the fluorous group was the retention of the blue colour onto a test F-SPE cartridge. When water and fluorophobic elution were conducted, the blue colour remained on the silica, therefore, it must still have a fluorous component.

Assured that the Cu remained coordinated to the fluorous ligand, another microfluidic experiment was completed with the acidic DMF. Yet again, the lines clogged and nothing was collected. The next variable which was investigated was removing the salts from the labeling mixture. It was thought that at lower ionic strength, **5** should remain in solution. To promote better mixing, the radiolabeling solvent was also exchanged to DMF by loading the mostly aqueous labeling solution onto a C18 solid-phase extraction cartridge. The salts were first removed with water and then the BPV-Tc and BPV were eluted with DMF. Now all solutes are in DMF but again, following mixing in the microfluidic device, nothing could be collected. The last attempt to rectify this problem was to dilute the amount of viscous DMF with another solvent. MeCN was

chosen because when it was added to the acidic DMF solution there was no precipitation of **5** and the testing of the micro-FLC could be conducted.

First, a clear, salt-free DMF solution containing the radioactivity was loaded into one syringe and a clear yellow solution containing **5** was loaded into the other. After mixing the two solutions in the microfluidic device, a clear blue solution was collected and loaded onto a F-SPE cartridge. Following the standard F-SPE elution protocol, BPV-Tc was eluted with 96% ligand removal and 9% non-specific binding. At the solvent front, however, there was a large peak which had not appeared before (Figure 3.6). To investigate this, a solution containing BPV and **5** was injected into the HPLC without any activity and the only peak on the chromatogram was seen at the solvent front.

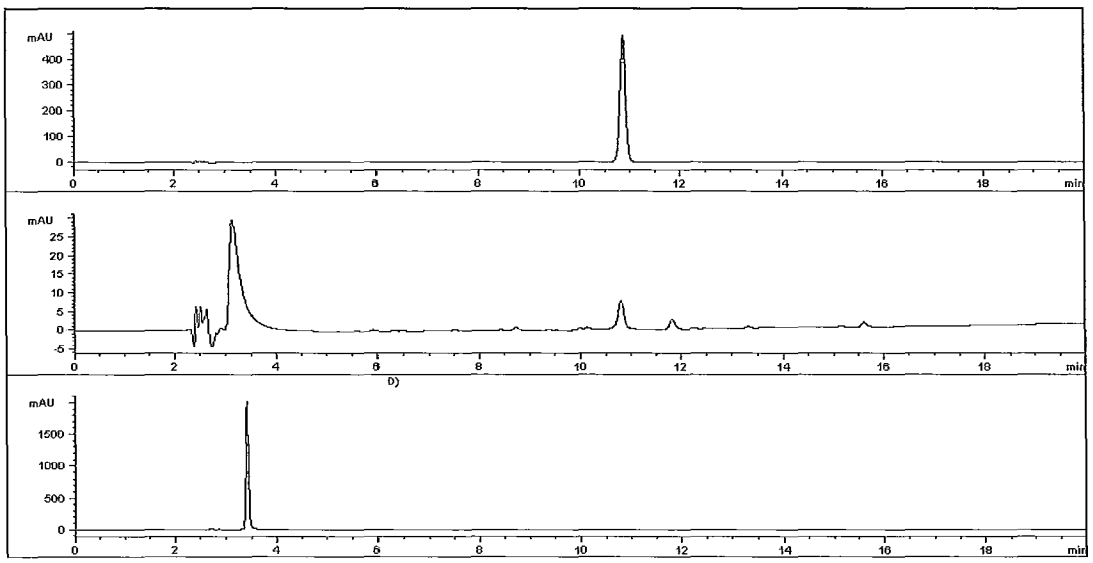

Figure 3.6 - HPLC chromatograms of first successful microfluidic FLC. Top = crude UV trace showing 6 (t_R = 10.4 min.). Middle = UV trace showing unknown peak (t_R = 3.4 min.) and 6 remaining following FLC. Bottom = UV trace showing solution of 5 and 6 (t_R = 3.4 min). Phenomenex Gemini C18 5μm column (4.6 x 250 mm), 1 mL/min, gradient method A.

When the experiment was repeated next, the BPV solution was used directly after labeling without removing the salts or changing the solvent. This did not prove to be a problem as long as the concentration of **5** was kept to below 3 mg/mL. At a flow rate of 50 μL/min. it takes 20 min. to obtain 2 mL of clear blue solution containing the BPV-Tc product and the FLC-ligand complex. As a means to remove the large peak at the solvent front, the F-SPE cartridge was eluted with 4 mL of water prior to a fluorophobic wash. The blue colour was entirely removed between the second and third fraction (4 x 1mL) and only 0.2 ± 0.01% of the activity was eluted in this wash. From the HPLC analysis, this activity was from $[^{99m}TcO_4]^-$ salts. To reduce the non-specific binding that had increased after the water wash, 4 drops of 1N HCl was added to the fluorophobic wash.

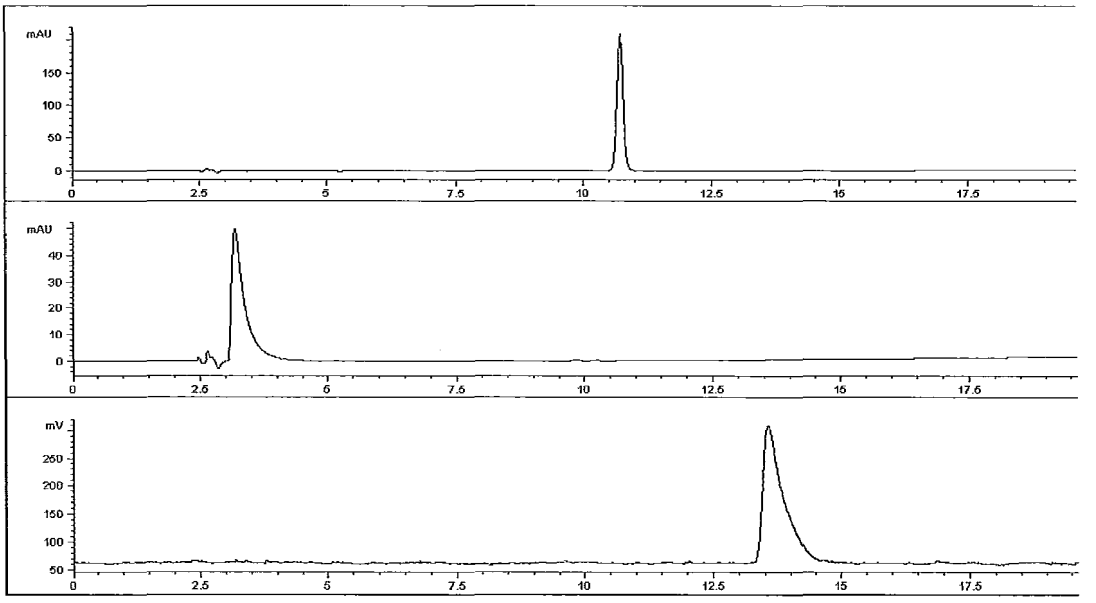

Figure 3.7 - HPLC chromatograms from microFLC experiments. Top = UV trace showing 6 (t_R = 11.4 min.) from crude reaction mixture. Middle = UV trace showing remaining 6 following microFLC. Bottom = γ trace showing 8b (t_R = 12.9 min.). Phenomenex Gemini C18 5μm column (4.6 x 250 mm), 1 mL/min, gradient method A.

Final results from triplicate trials of the microfluidic FLC were 99.74 ± 0.04 % of the free ligand was removed with 4.15 ± 1.0 % of the activity lost to non-specific binding. An HPLC chromatogram of one of the trials is shown in Figure 3.7. At a lower concentration of the FLC agent, **5**, the microfluidic approach had equivalent ligand removal (99.74 *vs.* >99.99%) and less non-specific binding compared to the batch approach (4.15 ± 1.0 % *vs.* 8.5 ± 1.6 %). Now that the FLC method has been demonstrated to efficiently remove excess ligand in a microfluidic apparatus, the next step was to begin investigating methods for integrating the F-SPE into the system.

3.7 – Development of an Integrated Microfluidic FLC Method

Integrated microreactors eliminate handling chemicals for the complete preparation of radiopharmaceuticals by conducting the synthesis and purification within one device. There are a few examples of microreactors which use beads for purification and separation.[75, 106-108] These could be adapted for trapping fluorous compounds onto fluorous silica or by preloading the FLC agent onto the fluorous silica and capturing the excess unlabeled ligand as it passes through the bead chamber. Focusing on the latter process, experiments were completed to test the hypothesis of efficiently removing excess ligand by preloading the F-SPE cartridge with **5** (Scheme 3.4). By doing so, the ligand capture step would again be conducted in a heterogeneous environment (as in the solid-phase method); however, the Teflon-like solid-phase should minimize non-specific binding.

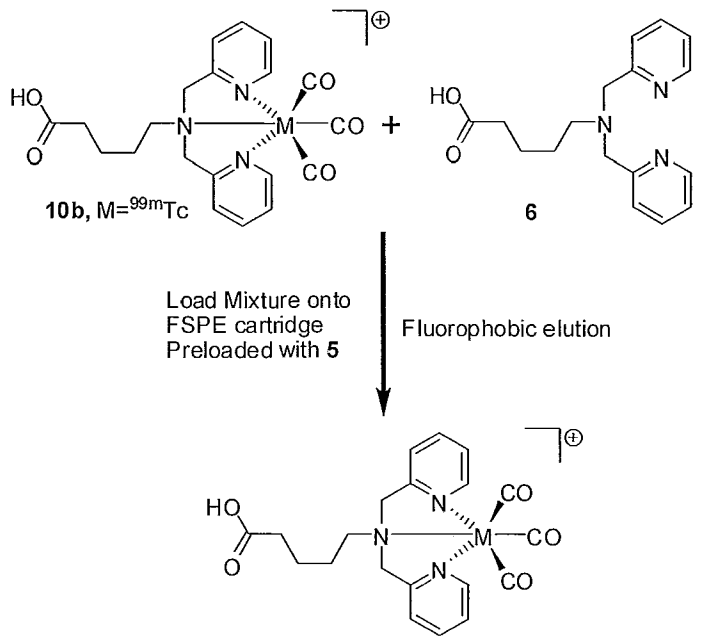

Scheme 3.4 - Purification of BPV-Tc using an F-SPE cartridge preloaded with *5*

An initial trial was conducted preloading 15 mg of **5** onto a 2g F-SPE cartridge and purifying a labeled mixture manually. The yellow solution containing **5** (1 mL 50% MeCN/DMF with 4 drops of 1N HCl) was loaded onto the cartridge under positive pressure. As the solution was loaded onto the cartridge, the yellow colour began to change to blue at the top of the silica but some **5** was not retained and came off the cartridge as a yellow solution. Next, the radiolabeling mixture containing 1.28 GBq of activity and 1 mg of BPV was loaded under positive pressure (1 mL total, 20% MeCN/H_2O). A 4 mL water wash was conducted to elute any salts which may have been present, including copper salts. No product or ligand could be seen in this fraction following HPLC analysis of this sample; however, there was some pertechnetate which appeared at t_R = 3.7 min. Three 4 mL fluorophobic washes (20% H_2O in MeOH) were

then completed to determine if the product could be isolated free from any unlabeled ligand. The resulting washes contained highly pure product with > 99% of the ligand removed with minimal loss from non-specific binding (<1%) but there was a large peak at the solvent front (Figure 3.8), mostly likely indicating the presence of salts containing copper (solutions were blue). Solutions of BPV were combined with both $CuSO_4$ and **5** and there was a peak in both chromatograms near the 3.15 min. where this new peak appeared (bottom trace in Figure 3.6).

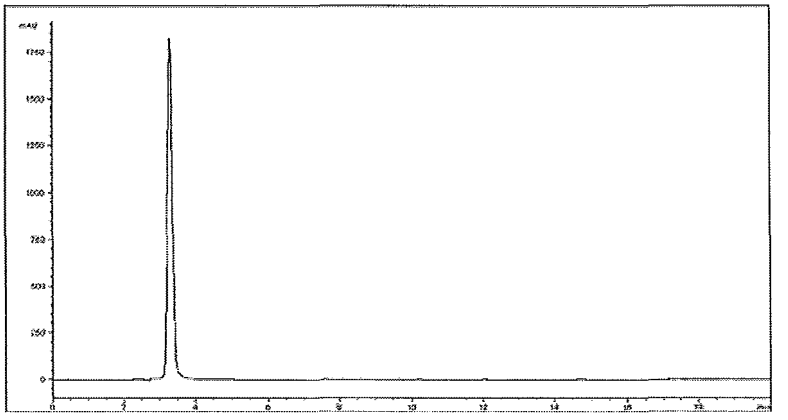

Figure 3.8 – UV HPLC chromatogram of new unknown peak (t_R = 3.4 min.) following preloaded FLC experiments. Phenomenex Gemini C18 5µm column (4.6 x 250 mm), 1 mL/min, gradient method A.

The first attempt at minimizing this new peak was to decrease the amount of **5** to 10 mg. This time, 1.12 GBq was added to the preloaded F-SPE cartridge. After washing with 8 mL of water and another 8 mL of water at pH = 4 (HCl) the blue colour remained on the silica and the peak at 3.4 min. did not appear in the HPLC chromatograms. When the fluorophobic washes were completed (3 x 4 mL, 20% H_2O in MeOH), there was similar performance with respect to non-specific binding however there was no retention

of the free ligand or a reduction in size of the salt peak (Figure 3.9). In fact, most of the ligand was actually eluted in the first 4 mL.

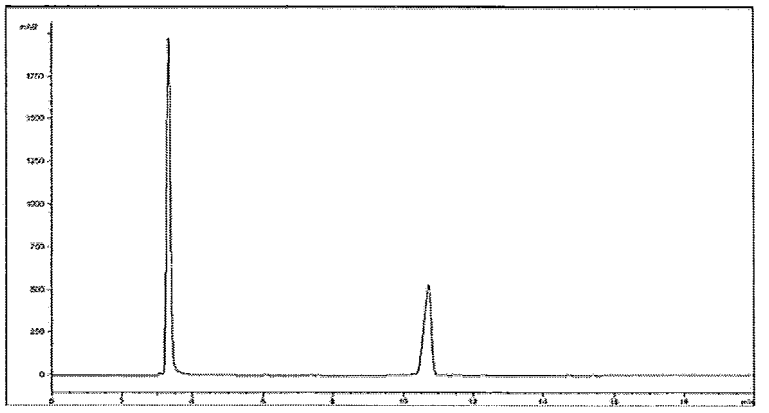

Figure 3.9 – UV HPLC chromatogram showing Cu salts (t_R = 3.4 min.) and 6 (t_R = 10.6 min.) from FLC experiments with 10 mg of 5 preloaded onto F-SPE cartridge. Phenomenex Gemini C18 5µm column (4.6 x 250 mm), 1 mL/min, gradient method A.

To improve the system and selectively elute only the radiolabeled product, a gradient elution was conducted using an F-SPE cartridge preloaded with 20 mg of **5**. Following the loading of the radioactive solution and initial 4 mL water wash, a gradient elution of 4 mL of fluorophobic solution starting at 90% water in MeOH going to 20% water in MeOH in 10% steps was applied. There was a large peak at the solvent front on the HPLC UV chromatograms from the fractions from the water wash as well as a large peak in the γ chromatogram at 3.8 min. (the retention time for $[^{99m}TcO_4]^-$). Both of these solutions were yellow and most likely contained some of the fluorous copper agent or copper salts that did not bind to the F-SPE cartridge. These salts caused the peak at the solvent front of the UV trace and pertechnetate was the species producing the peak in the γ trace.

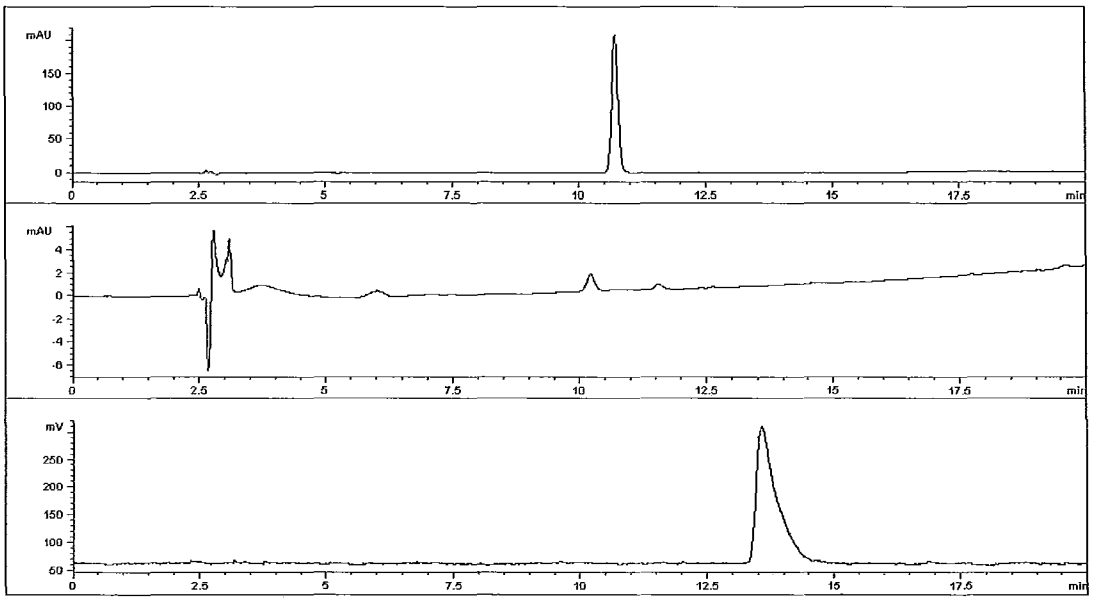

Figure 3.10 - HPLC chromatogram of successful preloaded FLC experiment. Top = UV trace showing 6 (t_R = 11.4 min.) from crude reaction mixture. Middle = UV trace showing 6 remaining following FLC. Bottom = γ trace showing 8b (t_R = 12.9 min.) following FLC.. Phenomenex Gemini C18 5μm column (4.6 x 250 mm), 1 mL/min, gradient method A.

For the first 3 steps of the gradient, there was no peak of significant size in either HPLC chromatograms until a 40% MeOH wash was completed. With this elution, there was another small $[^{99m}TcO_4]^-$ peak along with two other unknown small peaks in the γ trace. One of the two was most likely due to the presence of unreacted $[^{99m}Tc(CO)_3(OH_2)_3]^+$ but there was no peak at 13.6 min. for BPV-Tc. In this wash and the subsequent wash, there was also a small amount of unlabeled BPV present. This was the only observation of any unlabeled ligand in all of the fractions. At this point in the gradient, the product also began to elute with approximately half of the radiolabeled BPV-Tc being eluted from the F-SPE cartridge between 50% and the first 80% MeOH wash. The remaining BPV-Tc product was eluted in another 32 mL of 80% MeOH

without any appearance of BPV or large peaks at the solvent front in the UV chromatograms (Figure 3.10). After repeating the gradient experiment twice more, the average free ligand removed was found to be 99.85 ± 0.02 % and the non-specific binding was found to be 2.25 ± 0.55 %.

To remove the blue colour from the F-SPE, an 8 mL wash of acidic 80% MeOH was used. The colour was entirely removed and the HPLC analysis showed a large peak at the solvent front of the UV-trace. Eluting the preloaded F-SPE cartridge with a gradient fluorophobic was successfully removal of unlabeled ligand to achieve high effective specific activity product. Future work could be conducted to decrease the amount of fluorous silica used, lowering the necessary amount of solvent needed to conduct the fluorophobic elutions.

Using the model chelate system was a crucial first test of the preloaded FLC method, although the true utility of this method will be to purify chelate derivatized biological ligands, such as the erbB2 targeting peptide discussed in section 2.7. Compound **5** was preloaded onto the F-SPE cartridge as described above and then the cartridge was washed with 2 x 4 mL of water to remove any copper salts. The mixture of **9** and **10b** was then loaded as a 1 mL solution containing approximately 1 mg of **9**. To selectively remove the labeled product **10b** a fluorophobic wash of 16 mL (4 x 4mL fractions) of 20% water in MeCN was completed. While preliminary results showed good ligand removal (>99 %, n = 1), non-specific binding resulted in over 60% of the product remaining on the silica.

To decrease this loss, a basic prewash of the F-SPE cartridge was conducted. This was successful at reducing the non-specific binding to 33.3 ± 3.2 % but reduced the ligand removed to 95.2 ± 1.4% (Figure 3.11). While the non-specific binding is larger than desired, this proof of principle experiment has shown that it is possible to effectively remove excess precursor from a radiolabeling reaction mixture using a preloaded F-SPE cartridge. It may be possible to reduce the non-specific binding by optimizing the amount of fluorous silica used, as will be discussed in section 3.10.1, or by conducting experiments with difference solvent combinations.

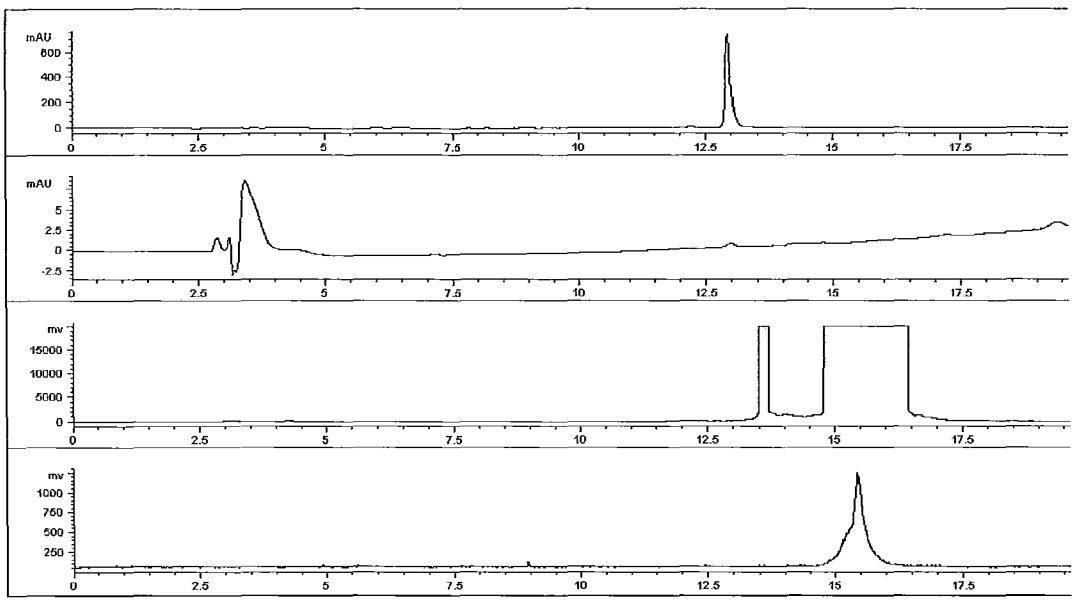

Figure 3.11 – HPLC chromatograms of FLC of 9 using F-SPE cartridges preloaded with 5. Top = UV trace showing 9 (t_R = 13.0 min.) from crude labeling mixture. Second = UV trace showing remaining 9 following FLC. Third = γ trace showing 7b (t_R = 13.6 min.) and 10b (t_R = 15.6 min.) from crude labeling reaction. Bottom = γ trace showing 10b following FLC. Phenomenex Gemini C18 5μm column (4.6 x 250 mm), 1 mL/min, gradient method B.

3.8 – Conclusion

It has been shown by the experiments above that the FLC method can be adapted to a microfluidic device without any detrimental effect on the efficiency of ligand removal. By using a microfluidic apparatus, the handling of radioactivity can be reduced and more easily shielded. The small volumes of the channels also permit using less of the ligand capture agent to remove the excess unlabeled ligand. Solubility problems caused clogging of the capillary tubes and led to the discovery of a better solution for solvating **5**.

Combining the radiolabeling mixture and **5** in the microfluidic device was a success but the true advantage to microfluidics would be to integrate the purification within the device itself instead of handling the activity onto an F-SPE cartridge. To this end, it has been shown that fluorous silica can be preloaded with **5** and the radiolabeling mixture can be purified by chemoselective solid-phase extraction to remove the ligand. A gradient wash was required but a sophisticated microfluidic apparatus should be able to repeat such elutions in an automated fashion.

To further test this approach, a chelate conjugated peptide was also purified using F-SPE cartridges preloaded with **5**. Although the product yields were not as high as the model chelate system, further optimization of this proof of concept experiment should improve the yields. It should now be possible to prepare a microreactor similar to those mentioned in section 3.1 containing beads of functionalized fluorous material. The beads used here would be preloaded fluorous silica particles which can complete the FLC after the ligand has been labeled with ^{99m}Tc. This would create a "lab-on-a-chip" for the

radiolabeling of ligands with ^{99m}Tc and could enable the rapid production of a variety of potential molecular imaging agents for biological screening.

3.9 – Future Work

3.9.1 – Improvements to the FLC Method

The success of the FLC method in obtaining targeted molecular imaging agents of high effective specific activity has demonstrated its potential for inclusion into kit formulations. In order for this process to become part of routine kit preparations in a clinical setting, the amount of toxic organic solvents used in the process must be minimized. While a C18 SPE cartridge can be used to reconstitute products into a more suitable injection solvent, traces of organic solvents need to be at minimal regulatory levels.

To optimize the preloaded fluorous silica application, a study needs to be undertaken wherein both the quantity of the silica and optimal solvent combinations are examined. The manufacturer's recommendation for maximum loading capacity of the silica is 10% by weight. Currently the smallest commercially available cartridges contain 2 g of silica which allows for loading 200 mg of total mass. At the scale at which radiolabeling reactions are conducted, this is a gross excess that can be minimized at least 10–fold. Minimizing the amount of fluorous silica required will reduce interactions with any uncapped Si-OH groups and reduce the non-specific binding of peptides to the F-SPE cartridge. Another option for improving the silica may be to silylate these groups to eliminate hydrogen bonding and ionic interactions.

Once optimized these preloaded silica beads could be incorporated into a microfluidic reactor. These devices could be fabricated as outlined in Section 3.1. Combining this work with that of Dr. Simms (see Section 3.1), a microfluidic apparatus could be conceived to label low concentrations of ligands (lower than conventional batch methods) with ^{99m}Tc and then capture any remaining precursor ligands onto an *in situ* FLC column.

Furthermore, development of FLC methods for other chelating systems would be of interest. Macrocyclic chelators are commonly used to coordinate radiometals other than ^{99m}Tc (i.e., ^{64}Cu, ^{111}In, ^{67}Ga, or ^{90}Y) to bioconjugates such as peptides or antibodies.[33] Due to the high affinity for these ligands for Cu the current compound will not suffice as a FLC agent because the Cu will be removed. A fluorous chelator with equal affinity for Cu (or another metal with open coordination sites) will need to be developed in order to expand this approach to other model chelators.

3.9.2 – Fluorous Technology for Discovering New Radiotracers

With an increase in demand for new targeted compounds, efficient screening will assist in the discovery of compounds with good binding affinities for targets of interest.[109] Current methods for high-throughput screening (*e.g.*, microplate assays[110]) are effective at determining binding affinities of ligands for receptors but as the number of systems that are being screened increases, so does the amount of reagents and time needed to complete the studies. One technique which can screen a large number of compounds for affinity for a single target with only one incubation is microarray

screening.[111] This technique involves spotting small amounts of compounds onto a substrate-coated glass slide which is followed by wash of fluorescently labeled targets. Because the target does not have to be added to each well, less material is needed and less time is required to add the target to the ligands under investigation. For example, a library of small molecules has been screened in this manner by Schreiber *et al.* to detect protein ligand interactions.[112] This technique can also be used to extrapolate binding constants (K_D) by spotting a variety of concentrations.

Traditional microarray spotting is completed by covalently immobilizing the ligands to the substrate on the slide.[113, 114] This can be disadvantageous as alternative functional groups available on the ligand may also react. For instance, if the slide is modified with aldehyde functionalities, amines on the ligand will have to be protected or a variety of orientations onto the slide will occur. Unintentional interactions between the target and the substrate coating on the slides may also occur, resulting in non-specific binding. As the target often contains the fluorescent tag used to visualize the target ligand interaction, high background signals and poor signal to noise ratios may result. To avoid these limitations, a non-covalent fluorous interaction can be used.

By coating a glass slide with a perfluoroalkylsilane-derivative, fluorous molecules can be non-covalently attached. With the surface now akin to Teflon, there should also be limited non-specific binding of the target once it is washed over the printed slides. Fluorous microarrays have recently been employed to probe the interaction between mannose derivatives and FITC-labeled concanavalin A.[115] Microarray screening using non-covalent fluorous anchors could be a convenient platform for identifying new

molecular imaging agents. Compounds could be prepared with a fluorous tag such that they can be anchored to a fluorous coated slide. To explore the utility of this technology towards screening potential ^{99m}Tc-based radiotracers, the Re chelate would need to be prepared and screened versus the target of interest (Scheme 3.5).

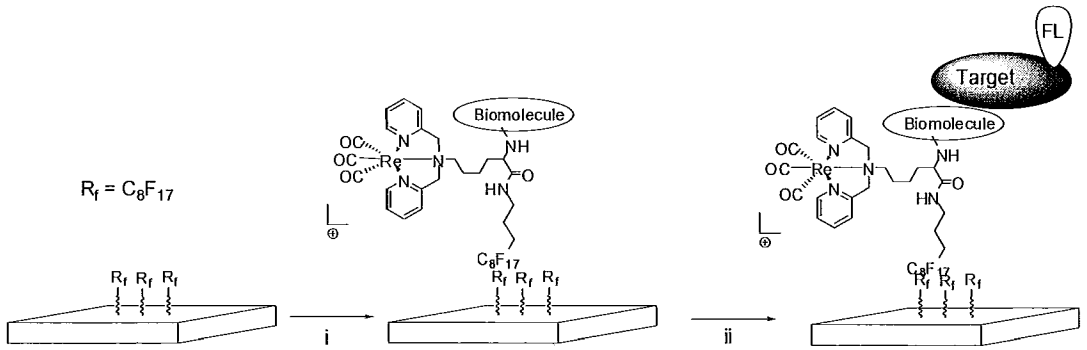

Scheme 3.5 – Fluorous microarray strategy for screening potential radiopharmaceuticals. i, print compounds onto slides, ii, incubate with fluorescently labeled targets

If SAAC conjugated peptides were the targeting vectors of choice, then the first step towards the development of a fluorous microarray screening method would be to prepare a fluorous tagged SAAC-Re chelate (Figure 3.12). This will show whether large positively charged organometallic chelates can be retained on the slides. Preliminary experiments have been conducted using a fluorous conjugated organic fluorescent dye, TAMRA. Initial printing of this molecule onto fluorous microarray slides produced good spot morphology but upon washing the slides with water there was a significant amount of streaking. The cause of this may have been the high humidity inside the chamber at the time of spotting. In the literature, the humidity is commonly set to 60% or less [115] which was not the case in the experiment conducted here(90% or greater). Further

experiments at lower humidity are needed to conclude if the metal chelates can be immobilized by fluorous-fluorous interactions. Furthermore, a spacer may need to be added to increase the distance between the fluorous tag and the metal chelate in order for printing to be successful. Once a printing protocol has been established, the fluorous microarray screening technology can be expanded to screen a potential target for radioimaging.

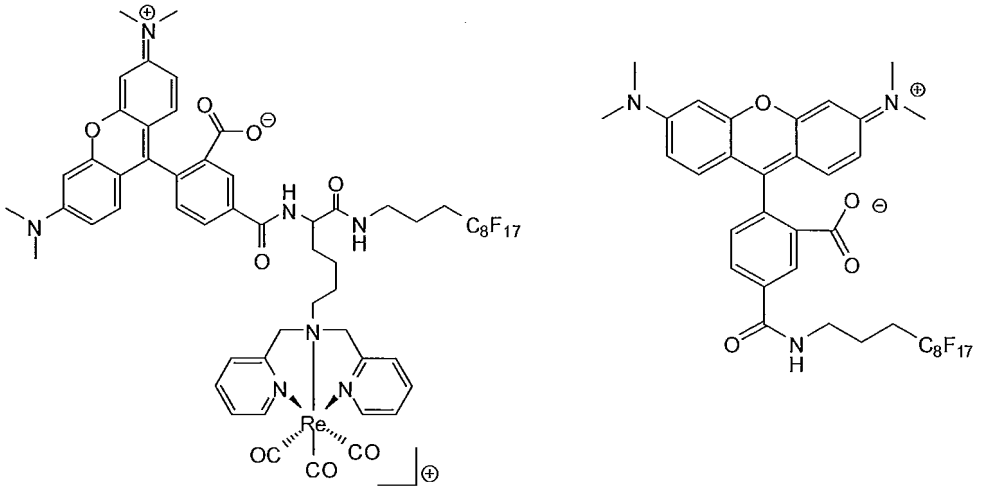

Figure 3.12 – Fluorous-tagged fluorescent SAAC-Re and fluorous TAMRA dye

After screening cold compounds on the microarrays, the radioactive analog can be prepared and then tested *in vitro* and *in vivo*. As the molecules that are non-covalently attached to the microarray slide contain a fluorous group, the question arises as to whether a lead compound, once identified, should be synthesized with or without the fluorous tag. Ideally, the compounds chosen for further screening should be as similar in structure to the one identified on the microarray as possible. To this end, the impact of the fluorous pendant group on the distribution of ^{99m}Tc-dipyridyl chelates was investigated as

there is no literature precedence for the effect of such a group on pharmacokinetics and/or binding of a radiopharmaceutical. Fluorous molecules are chemically and biologically inert due to their low intermolecular forces, resulting in both hydrophobic and lipophobic behaviour.[116] Because there are also no known enzymatic or bacterial systems which can metabolize these molecules, fluorous compounds have been used in a variety of fields from medical equipment to cooking utensils. With Teflon-like physical properties, incorporating a fluorous functionality into a radioimaging agent may in fact be beneficial and reduce non-specific binding.

A dipyridyl system similar to that used in the SAAC and BPV ligands was synthesized with an N-substituted C_8F_{17} fluorous group (Figure 3.13). To determine if the addition of a fluorous moiety would change the *in vivo* behavior of the ^{99m}Tc chelate, binding to albumin was selected as a protein target (most abundant blood serum protein, associated with increased liver uptake [117]). Partitioning coefficients (log P) were also determined and a biodistribution study was completed in C57 mice. Results from the biodistribution and log P experiments were interesting but no information could be gained from the albumin binding experiments.

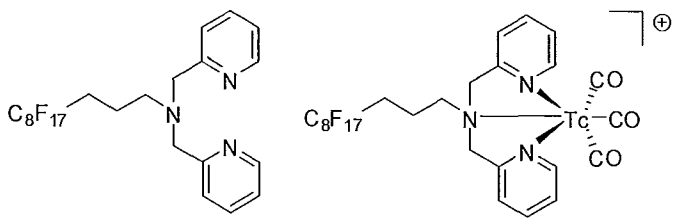

Figure 3.13 – Fluorous dipyridyl ligand and ^{99m}Tc labeled chelate

The biodistribution study showed a large accumulation of activity in the intestinal tract, which is common for this ligand system [37], but there was still a large amount of liver uptake (Figure 3.14). It can be concluded that at this percentage of fluorine (38%), the fluorous group was not having an effect on biodistribution. This was in agreement with the log P values (Table 3.1) as the fluorous ^{99m}Tc chelate was more soluble in water than fluorous solvents (log P_{WF} = -1.46). With a higher partitioning into water, it appears the positively charged chelate was having more of an influence on the physical properties of the molecule than the fluorous portion. The affect of the fluorous group will need to be evaluated for each lead compound but from these results; a small fluorous tag may not have an effect on the biodistribution of the compound to which they are attached.

Table 3.1 – Log P values of fluorous dipyridyl ^{99m}Tc chelate

Solvents	Log P	Value
Water and n-octanol	P_{WO}	2.34
n-octanol and perfluorohexane	P_{OF}	4.56
water and perfluorohexane	P_{WF}	- 1.41

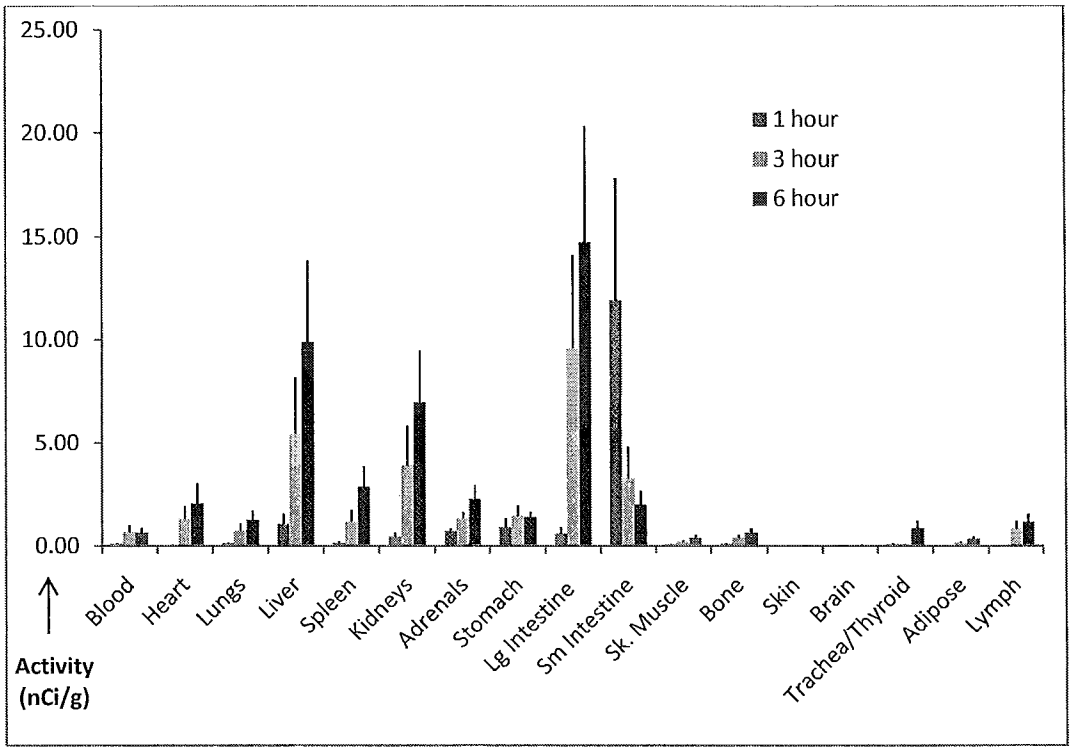

Figure 3.14 – Biodistribution of fluorous ^{99m}Tc chelate in C57 mice

3.10 – Experimental Procedures

Reagents were purchased from Sigma-Aldrich and Fluorous Technologies and were used without further purification. Fluorous solid-phase extractions were conducted using Fluorous Technologies Inc. FluoroFlash® 2 g SPE cartridges. $[^{99m}Tc(CO)_3(OH_2)_3]^+$, and bispyridyl valeric acid (BPV) were prepared according to literature procedures.[17, 36] Compound **5** was prepared as described in section 2.9. Low resolution electrospray ionization mass spectroscopy experiments were performed on a Waters/Micromass Quattro Ultima instrument. Infrared spectra were obtained on a Bio-Rad FTS-40 Fourier transform IR spectrometer. Analytical HPLC was conducted using an Agilent 1100 series HPLC and C-18 Phenomenex Gemini NX column (4.6 x 250 mm). The elution protocols

were: Method A: Solvent A = water (with 10 mM ammonium formate), Solvent B = methanol: Gradient elution 0 min., 20% B; 20 min., 90% B. Method B: Solvent A = water (with 0.1% TFA), Solvent B = acetonitrile (with 0.1% TFA): Gradient elution 0 min., 5% B; 20 min., 60% B. For all experiments the flow rate was 1.0 mL $min.^{-1}$ and monitoring was performed at 254 nm.

3.10.1 – Construction of Microfluidic Apparatus

A Harvard Apparatus PHD 2000 Infusion remote controlled syringe pump was used to push both the radioactive solution and fluorous ligand capture agent (**5**) through 100 μm diameter fused silica capillary tubing. To connect the capillary tubes to the BD plastic syringes, a rubber fitting was placed into a Luer-lock adapter (all plastic HPLC parts were obtained from Upchurch Scientific). At the other end of the tub, a Y-junction was created using a similar rubber fitting, which had two holes, inside of a peek tube end fitting. This piece was then connected through a union to another peek tube end fitting with only one capillary tube exiting. Drops were collected into a 2 mL vial to be loaded onto a 2g F-SPE cartridge. Total volume of the channels was 3.0 μL.

3.10.2 – Microfluidic Fluorous Ligand Capture Method

Compound **6** (t_R = 11.4 min.) was radiolabeled with $[^{99m}Tc(CO)_3(OH_2)_3]^+$ as described in section 2.9. The mixture of **6** and **8b** (t_R = 12.9 min.) was loaded into a 3 mL syringe to 1 mL and connected to the capillary tube. The other tube was then connected to a syringe filled with 3 mg of **5** in 1 mL of 1:1 MeCN/DMF with 4 drops of 1 N HCl. These two solutions were then pumped at 50 μL $min.^{-1}$ for 10 min. and collected into a 2

mL vial (1 mL total volume collected). This blue solution was then loaded onto a 2g F-SPE cartridge and eluted with 4 mL of water to remove any salts. A 12 mL acidic fluorophobic wash of 20% water in MeOH was then used to elute the product followed by an 8 mL fluorophilic wash which removed the entire blue colour from silica. The solvent was removed using the Biotage V10 Rapid Evaporator system and the residue was redissolved into 1 mL of water. A 100 μL aliquot was then added to 900 μL of water for UV and γ HPLC analysis (Method A).

*3.10.3 – Fluorous Ligand Capture of BPV (**6**) Using Preloaded F-SPE Cartridges*

A 1 mL yellow solution containing 20 mg of **5** in 1:1 MeCN/DMF with 4 drops of 1 N HCl was loaded onto a commercially available 2 g F-SPE cartridge by positive pressure from a syringe. The radiolabeling mixture of **6** (t_R = 10.4 min.) and **8b** (t_R = 12.8 min.) was then loaded as a 1 mL solution (1 mg of **6**, in 0.2 mL 50% MeCN/H_2O, 500 MBq of $[^{99m}Tc(CO)_3(OH_2)_3]^+$ in 0.8 mL saline). The cartridge was then washed with 4 mL of water followed by a gradient wash of 10% MeOH in water to 80% (4 mL fractions in 10% steps). After the 80% point was reached, 8 more 4 mL washes were completed at the same percentage of MeOH followed by a fluorophilic wash of 100% MeOH. A 1 mL aliquot was taken from each of the 4 mL fractions for UV and γ HPLC analysis (Method A).

*3.10.3 – Fluorous Ligand Capture of **9** Using Preloaded F-SPE Cartridges*

A 1 mL yellow solution containing 20 mg of **5** in 1:1 MeCN/DMF with 4 drops of 1 N HCl was loaded onto a commercially available 2 g F-SPE cartridge by positive

pressure from a syringe. The cartridge was washed with 8 mL of pH = 10 water and the radiolabeling mixture of **9** (t_R = 13.0 min.) and **10b** (t_R = 15.6 min.) was then loaded as a 1 mL solution (1 mg of **9** in 0.2 mL 50% MeCN/H_2O, 925 MBq of $[^{99m}Tc(CO)_3(OH_2)_3]^+$ (t_R = 13.6 min.) in 0.8 mL saline). The cartridge was then washed with 2 x 4 mL of water followed by 4 fractions of 20% water in MeCN (4 mL each) and a 4 mL fluorophilic wash of 100% DMF (8 mL). A 1 mL aliquot was taken from each of the 4 mL fractions for UV and γ HPLC analysis (Method B).

References

1. P.W. Causey, T.R. Besanger, P. Schaffer, J.F. Valliant. Expedient multi-step synthesis of organometallic complexes of Tc and Re in high effective specific activity. A new platform for the production of molecular imaging and therapy agents. Inorg. Chem. **2008**;*47*,8213.

2. M.G. Pomper. Molecular imaging: an overview. Acad. Radiol. **2001**;*8*,1141.

3. D.J. Yang, M. Chanda, J. Sims-Mourtada, A. Azhdarinia, C.S. Oh, J. Bryant, E.E. Kim. Challenges and opportunities in molecular imaging. Curr. Med. Imaging Rev. **2008**;*4*,46.

4. J.E. Blum, H. Handmaker, N.A. Rinne. The utility of a somatostatin-type receptor peptide radiopharmaceutical (P829) in the evaluation of solitary pulmonary nodules. Chest **1999**;*115*,224.

5. M.J. Paulus, S.S. Gleason, M.E. Easterly, C.J. Foltz. A review of high-resolution X-ray computed tomography and other imaging modalities for small animal research. Lab Animal **2001**;*30*,36.

6. P.F. Daly, J.S. Cohen. Magnetic resonance spectroscopy of tumors and potential *in vivo* clinical applications: a review. Cancer Res. **1989**;*49*,770.

7. X. Gao, Y. Cui, R.M. Levenson, L.W.K. Chung, S. Nie. *In vivo* cancer targeting and imaging with semiconductor quantum dots. Nat. Biotechnol. **2004**;*22*,969.

8. A. Fenster, D.B. Downey. 3-D ultrasound imaging: a review. IEEE Eng. Med. Biol. Mag. **1996**;*15*,41.

9. G.D. Luker, D. Piwnica-Worms. Beyond the genome: molecular imaging *in vivo* with PET and SPECT. Acad. Radiol. **2001**;*8*,4.

10. F.A. Jaffer, R. Weissleder. Molecular imaging in the clinical arena. J. Am. Med. Assoc. **2005**;*293*,855.

11. S.M. Ametamey, M. Honer, P.A. Schubiger. Molecular imaging with PET. Chem. Rev. **2008**;*108*,1501.

12. R.E. Coleman. Single photon emission computed tomography and positron emission tomography in cancer imaging. Cancer **1991**;*67*,1261.

13. H. Levi. George Hevesy and His Concept of Radioactive Indicators - In Retrospect. Eur. J. Nucl. Med. **1976**;*1*,3.

14. M.E. Phelps, E.J. Hoffman, N.A. Mullina, M.M. Ter-Pogossian. Application of annihilation coincidence detection to transaxial reconstruction tomography. J. Nucl. Med. **1975**;*16*,210.

15. T.K. Nayak, M.W. Brechbiel. Radioimmunoimaging with longer-lived positron-emitting radionuclides: potentials and challenges. Bioconj. Chem. **2009**;*20*,825.

16. W.C. Eckelman, S.M. Levenson. Radiopharmaceuticals labelled with technetium. Int. J. Appl. Radiat. Isot. **1977**;*28*,67.

17. S.R. Banerjee, K.P. Maresca, L. Francesconi, J.F. Valliant, J.W. Babich, J. Zubieta. New directions in the coordination chemistry of ^{99m}Tc: a reflection on technetium core structures and a strategy for new chelate design. Nucl. Med. Biol. **2005**;*32*,1.

18. M.M. Ter-Pogossian, M.E. Phelps, E.J. Hoffman. A positron-emission transaxial tomograph for muclear imaging (PET). Radiology **1975**;*114*,89.

19. S.S. Jurisson, D. Lydon. Potential technetium small molecule radiopharmaceuticals. Chem. Rev. **1999**;*99*,2205.

20. G.B. Saba. Physics and Radiobiology of Nuclear Medicine. 3 ed. New York: Springer; 2006.

21. J.R. Dilworth, S.J. Parrott. The biomedical chemistry of technetium and rhenium. Chem. Soc. Rev. **1998**;*27*,43.

22. A.J. Fischman, J.W. Babich, H.W. Strauss. A ticket to ride: peptide radiopharmaceuticals. J. Nucl. Med. **1993**;*34*,2253.

23. I. Dijkgraaf, O.C. Boerman, W.J.G. Oyen, F.H.M. Corstens, M. Gotthardt. Development and application of peptide-based radiopharmaceuticals. Anti-Cancer Agents Med. Chem. **2007**;*7*,543.

24. H.F. Kung, H.-J. Kim, M.-P. Kung, S.K. Meegalla, K. Plössl, H.-K. Lee. Imaging of dopamine transporters in humans with technetium-99m TRODAT-1. Eur. J. Nucl. Med. Mol. Imaging **1996**;*23*,1527.

25. M.M. Alauddin, A. Shahinian, R. Park, M. Tohme, J.D. Fissekis, P.S. Conti. Biodistribution and PET imaging of [18F]-fluoroadenosine derivatives. Nucl. Med. Biol. **2007**;*34*,267.

26. N.G. Butlin, C.F. Meares. Antibodies with infinite affinity: origins and applications. Acc. Chem. Res. **2006**;*39*,780.

27. W.A. Breeman, L.J. Hofland, M. van der Pluijim, P.M. van Koetsveld, M. de Jong, B. Setyono-Han, W.H. Bakker, D.J. Kwekkeboom, T.J. Visser, S.W. Lamberts. A new radiolabeled somatostatin analogue [^{111}In-DTPA-D-Phe1]RC-160: preparation, biological activity, receptor scintigraphy in rats and comparison with [^{111}In-DTPA-D-Phe1]octreotide. Eur. J. Nucl. Med. **1994**;*21*,328.

28. M. Langer, A.G. Beck-Sickinger. Peptides as carrier for tumor diagnosis and treatment. Anti-cancer Agents Med. Chem. **2001**;*1*,71.

29. R.E. Weiner, M.L. Thakur. Radiolabeled peptides in the diagnosis and therapy of oncological diseases. Appl. Radiat. Isot. **2002**;*57*,749.

30. M.J. Welch, C.S. Redvanly. Handbook of Radiopharmaceuticals. Etobicoke, ON: John Wiley & Sons Ltd.; 2003.

31. M. de Jong, D. Kwekkeboom, R. Valkema, E.P. Krenning. Tumour therapy with radiolabelled peptides: current status and future directions. Dig. Liver. Dis. **2004**;*36*,S48.

32. D. Eshima, A.R. Fritzberg, A. Taylor. ^{99m}Tc renal tubular function agents: current status. Semin. Nucl. Med. **1990**;*20*,28.

33. C.J. Anderson, M.J. Welch. Radiometal-labeled agents (non-technetium) for diagnostic imaging. Chem. Rev. **1999**;*99*,2219.

34. D.L. Nosco, J.A. Beaty-Nosco. Chemistry of technetium radiopharmaceuticals 1: Chemistry behind the development of technetium-99m compounds to determine kidney function. Coord. Chem. Rev. **1999**;*184*,91.

35. R.O. Alberto, K.; Wheatley, N.;Schibli, R.; Schubiger, A.P. Synthesis and properties of boranocarbonate: a convenient *in situ* CO source for the aqueous preparation of $[^{99m}Tc(OH_2)_3(CO)_3]^+$. J. Am. Chem. Soc. **2001**;*123*,3135.

36. M.K. Levadala, S.R. Banerjee, K.P. Maresca, J.W. Babich, J. Zubieta. Direct reductive alkylation of amino acids: synthesis of bifunctional chelates for nuclear imaging. Synthesis **2004**;*11*,1759.

37. K.P. Maresca, S.M. Hillier, F.J. Femia, C.N. Zimmerman, M.K. Levadala, S.R. Banerjee, J. Hicks, C. Sundararajan, J. Valliant, J. Zubieta, W.C. Eckelman, J.L. Joyal, J.W. Babich. Comprehensive radiolabeling, stability, and tissue

distribution studies of technetium-99m single amino acid chelates (SAAC). Bioconj. Chem. **2009**;*20*,1625.

38. W.C. Eckelman. Sensitivity of new radiopharmaceuticals. Nucl. Med. Biol. **1998**;*25*,169.

39. W.C. Eckelman. The application of receptor theory to receptor-binding and enzyme-binding oncologic radiopharmaceuticals. Nucl. Med. Biol. **1994**;*21*,759.

40. W.C. Eckelman, M. Bonardi, W.A. Volkert. True radiotracers: are we approaching theoretical specific activity with Tc-99m and I-123? Nucl. Med. Biol. **2008**;*35*,523.

41. R.J. Mairs, M.N. Gaze, D.G. Watson, G.G. Skellern, P. Constable, K. McKeller, J. Owens, G. Valdyarathan, M.R. Zalutsky. Carrier-free ^{131}I meta-iodobenzylguanidine: Comparison of production from met-iodobenzylguanidine and from meta-trimethylsilylbenzylguanidine. Nucl. Med. Comm. **1994**;*15*,268.

42. D.P. Curran. Strategy-level separations in organic synthesis: from planning to practice. Angew. Chem. Int. Ed. **1998**;*37*,1174.

43. D.H. Hunter, Z. Xizhen. Polymer-supported radiopharmaceuticals: [131]MIBG and [123]MIBG. J. Labelled. Compd. Radiopharm **1999**;*42*,653.

44. R. Dunn-Dufault, A. Pollak, J.R. Thornback, J.R. Ballinger. Convenient preparation of no-carrier-added technetium-99m radiopharmaceuticals using solid-phase technology. Bioconj. Chem. **1999**;*10*,832.

45. S. Mundwiler, L. Candreia, P. Hafliger, K. Ortner, R. Alberto. Preparation of no-carrier-added technetium-99m complexes via metal-assisted cleavage from a solid-phase. Bioconj. Chem. **2004**;*15*,195.

46. R.W. Riddoch, P. Schaffer, J.F. Valliant. A solid-phase labeling strategy for the preparation of technetium and rhenium bifunctional chelate and associated peptide conjugates. Bioconj. Chem. **2006**;*17*,226.

47. J. Sui, I.R. Baxendale, R.A. Lewthwaite, Ley, S.V. A phase-switch purification approach for the experident removal of tagged reagents and scavengers following their application in organic synthesis. Organic Biomolecular Chemistry **2005**;*3*,3140.

48. J.A. Gladsyz, D.P. Curran, I.T. Horváth. Handbook of Fluorous Chemistry. Weinhelm , Germany: Wiley-VCH Verlag GmbH & Co. KGaA.; 2004.

49. G. Sanford. Perfluoroalkanes. Tetrahedron **2003**;*59*,437.

50. I.T. Horváth. Fluorous biphase chemistry. Acc. Chem. Res. **1998**;*31*,641.

51. I.T. Horváth, J. Rábai. Facile catalyst separatin without water: fluorous biphase hydroformylation of olefins. Science **1994**;*266*,72.

52. W. Zhang. Fluorous technologies for solution-phase high-throughput organic synthesis. Tetrahedron **2003**;*59*,4475.

53. A.C. Donovan, J.F. Valliant. A convenient solution-phase method for the preparation of meta-iodobenzylguanidine in high effective specific activity. Nucl. Med. Biol. **2008**;*35*,741.

54. R. Bejot, T. Fowler, L. Carroll, S. Boldon, J.E. Moore, J. Declerck, V. Gouverneur. Fluorous synthesis of ^{18}F radiotracers with the ^{18}F fluoride ion: nucleophilic fluorination as the detagging process. Angew. Chem. Int. Ed. **2008**;*48*,586.

55. B. Langstrom, F. Karimi, B. Langstrom, F. KarimiB. Langstrom, F. Karimis. Perfluoro-aryliodonium salts in nucleophilic aromatic ^{18}F fluorination. WO/2009/073273, 2009.

56. W. Erfeld, V. Hessel, H. Lowe. Microreators: Wiley-VCH: Weinheim; 2000.

57. B.P. Mason, K.E. Price, J.L. Steinbacher, A.R. Bogdan, D.T. McQuade. Greener approaches to organic synthesis using microreactor technology. Chem. Rev. **2007**;*107*,2300.

58. T. Thorsen, S.J. Maerkl, S.R. Quake. Microfluidics large-scale integration. Science **2002**;*298*,580.

59. J.M.K. Ng, I. Gitlin, A.D. Stroock, G.M. Whitesides. Components for intergrated poly(dimethylsiloxane) microfluidic systems. Electrophoresis **2002**;*23*,3461.

60. G.M. Whitesides, A.D. Stroock. Flexible methods for microfluidics. Physics Today **2001**;*54*,42.

61. T. Schwalbe, V. Autze, M. Hohmann, W. Stirner. Novel innovation system for a cellular approach to continuous process chemistry from discovery to market. Org. Process Res. and Dev. **2004**;*8*,440.

62. P. Watts, S. Haswell. The application of microreactors for organic synthesis. Chem. Soc. Rev. **2005**;*34*,235.

63. P. Watts, C. Wiles, S.J. Haswell, E. Pombo-Villar, P. Styring. The synthesis of peptides in micro reactors. J. Chem. Soc., Chem. Commun. **2001**;*11*,990.

64. P.D.I. Fletcher, S.J. Haswell, E. Pombo-Villar, B.H. Warrington, P. Watts, S.Y.F. Wong, X. Zhang. Micro reactors: principles and applications in organic synthesis. Tetrahedron **2002**;*58*,4735.

65. H. Song, D.L. Chen, R.F. Ismagilov. Reaction in droplets in microfluidic channels. Angew. Chem. Int. Ed. **2006**;*45*,7336.

66. H. Pennemann, V. Hessel, H. Löwe. Chemical microprocess technology - from laboratory-scale to production. Chem. Eng. Sci. **2004**;*59*,4789.

67. J.P. Rolland, R.M. Van Dam, D.A. Schorzman, S.R. Quake, J.M. DeSimone. Solvent-resistant photocurable "liquid teflon" for microfluidic device fabrication. J. Am. Chem. Soc. **2004**;*126*,2322.

68. Abstracts for International Symposium of Radiopharmaceutical Sciences. J. Labelled. Compd. Radiopharm **2009**;*52*,S1.

69. P.W. Miller. Radiolabeling with short lived PET (positron emission tomography) isotopes using microfluidic reactors. J. Chem. Technol. Biotechnol. **2009**;*84*,309.

70. C.-C. Lee, G. Sui, A. Elizarov, C.J. Shu, Y.-S. Shin, A.N. Dooley, J. Huang, A. Daridon, P. Wyatt, D. Stout, H.C. Kolb, O.N. Witte, N. Satyamurthy, J.R. Heath, M.E. Phelps, S.R. Quake, H.-R. Tseng. Multistep synthesis of a radiolabeled imaging probe using integrated microfluidics. Science **2005**;*310*,1793.

71. J.M. Gillies, C. Prenant, G.N. Chimon, G.J. Smethurst, W. Perrie, I. Hamblett, B. Dekker, J. Zweit. Microfluidic reactor for the radiosynthesis of PET radiotracers. Appl. Radiat. Isot. **2006**;*64*,325.

72. Private communication from Dr. R.W. Simms.: Centre for Probe Development and Commercialization.

73. K. Mikami, M. Yamanaka, M.N. Islam, T. Tonoi, Y. Itoh, M. Shinoda, K. Kudo. Nanoflow microreactor for dramatic increase not only in reactivity but also in selectivity: Baeyer-Villiger oxidation by aqueous hydrogen peroxide using lowest concentration of a fluorous lanthanide catalyst. J. Fluor. Chem. **2006**;*127*,592.

74. J.G. Kralj, H.R. Sahoo, K.F. Jensen. Integrated continuous microfluidic liquid-liquid extraction. Lab Chip **2007**;*7*,256.

75. G. Hu, J.S.H. Lee, D. Li. A microfluidic fluorous solid-phase extraction chip for purification of amino acids. J. Colloid Interface Sci. **2006**;*301*,697.

76. W. Eckelman. Radiolabeling with technetium-99m to study high-capacity and low-capacity biochemical systems. Eur. J. Nucl. Med. **1995**;*22*,249.

77. W.C. Eckelman. Accelerating Drug Discovery and development through in vivo imaging. Nucl. Med. Biol. **2002**;*29*,777.

78. A. Donovan, J. Forbes, P. Dorff, P. Schaffer, J.W. Babich, J.F. Valliant. A New Strategy for Molecular Imaging and Therapy Agents Using Fluorine-Rich (Fluorous) Soluble Supports. J. Am. Chem. Soc. **2006**;*128*,3536.

79. S.R.W. Banerjee, L.; Levadala, M.K.; Lazarova, N.; Golub, V.O.; O'Connor, C.J.; Stephenson, K.A.; Valliant, J.F.; Babich, J.W.; Zubieta, J. {ReIIICl3} Core Complexes with Bifunctional Single Amino Acid Chelates. Inorg. Chem. **2002**;*41*,5795

80. T. Clifford, C.A. Boswell, G.B. Biddlecombe, J.S. Lewis, M.W. Brechbiel. Validation of a novel CHx-A" derivative suitable for peptide conjugation: small animal PET/CT imaging using yttrium 86-CHX-A"-Octreotide. J. Med. Chem. **2006**;*49*,4297.

81. D. Obeymayer, B. Gutmann, C.O. Kappe. Microwave chemistry in silicon carbide reaction vials: separating thermal from nonthermal effects. Angew. Chem. Int. Ed. **2009**;*48*,1.

82. P. Lidström, J. Tierney, B. Wathey, J. Westman. Microwave assisted organic synthesis--a review. Tetrahedron **2001**;*57*,9225.

83. M.A. Ubeda, R. Dembinski. Fluorous Compounds and Their Role in Seperation Chemistry. J. Chem. Ed. **2006**;*83*,84.

84. A.A. Riberio. ^{19}F, ^{13}C Correlations in a Highly Fluorinated Alkyl Chain and Coupling Constant Signs at the Fluorocarbon/Hydrocarbon Interface. Magn. Reson. Chem. **1997**;*35*,215.

85. T. Mathivet, E. Monflier, Y. Castanet, A. Mortreux, J.-L. Couturier. Easy two-step synthesis of new tris(perfluoroalkylphenyl)phosphites. Tetrahedron Let. **1998**;*39*,9411.

86. R.S. Varma, A.K. Chatterjee, M. Varma. Alumina-mediated microwave thermolysis: a new approach to deprotection of benzyl esters. Tetrahedron Let. **1993**;*34*,4603.

87. A.R. Lepley, G.L. Closs. Chemically induced magnetic polarization. New York: Wiley Interscience; 1973.

88. D.H. Busch, J.C. Bailar. The Stereochemistry of Complex Inorganic Compounds. XVII. The Stereochemistry of Hexadentate Ethylenediaminetetraacetic Acid Complexes. J. Am. Chem. Soc. **1953**;*75*,4574.

89. J. Alvarez, F. Cortés, T. Pérez. Rapid estimation of technetium in ^{99}Mo-^{99m}Tc generators. J. Radioanal. Chem. **1979**;*52*,471.

90. X.-F. Wang, M. Birringer, L.-F. Dong, P. Veprek, P. Low, E. Swettenham, M. Stantic, L.-H. Yuan, R. Zobalova, K. Wu, M. Ledvina, S.J. Ralph, J. Neuzil. A Peptide Conjugate of Vitamin E Succinate Targets Breast Cancer Cells with High ErbB2 Expression. Cancer Res. **2007**;*67*,3337.

91. M. Shadidi, M. Sioud. Identification of novel carrier peptides for the specific delivery of therapeutics into cancer cells. FASEB J. **2003**;*17*,256.

92. G. Akabani, S. Carlin, P. Welsh, M.R. Zalutsky. *In vitro* cytotoxicity of ^{211}At-labeled trastuzumab in human breast cancer cell lines: effect of specific activity and HER2 receptor heteogeneity on survival fraction. Nucl. Med. Biol. **2006**;*33*,333.

93. N.E. Hynes, D.F. Stern. The biology of *erbB-2/neu/HER-2* and its role in cancer. Biochim. Biophys. Acta **1994**;*1198*,165.

94. N. Lazarova, S. James, J.W. Babich, J. Zubieta. A convenient synthesis, chemical characterization and reactivity of $[Re(CO)_3(H_2O)_3]Br$: the crystal and molecular structure of $[Re(CO)_3(CH_3CN)_2Br]$. Inorg. Chem. Commun. **2004**;*7*,1023.

95. A. Elizarov. Microreactors for radiopharmaceutical synthesis. Lab Chip **2009**;*9*,1326.

96. C. Wiles, P. Watts, S. Haswell, E. Pombo-Villar. The aldol reaction of silyl enol ethers within a micro reactor. Lab Chip **2001**;*1*,100.

97. S. Liu, D.S. Edwards. 99mTc-Labeled Small Peptides as Diagnostic Radiopharmaceuticals. Chem. Rev. **1999**;*99*,2235.

98. D.M. Goldenberg, R.M. Sharkley. Novel radiolabeled antibody conjugates. Oncogene **2007**;*26*,3734.

99. J. Fichna, A. Janecka. Synthesis of target-specific radiolabeled peptides for diagnostic imaging. Bioconj. Chem. **2003**;*14*,3.

100. L. Kang, B.G. Chung, R. Langer, A. Khademhosseini. Microfluidics for drug discovery and development: from target selection to product lifecycle management. Drug Discovery Today **2008**;*13*,1.

101. G.M. Whitesides. The origins and the future of microfluidics. Nature **2006**;*442*,368.

102. A. Hélène. Positron Emission Tomography (PET) and microfluidic devices: a breakthrough on the microscale? Angew. Chem. Int. Ed. **2007**;*46*,1772.

103. S.-Y. Lu, P. Watts, F.T. Chin, J. Hong, J.L. Musachio, E. Briard, V.W. Pike. Syntheses of 11C- and 18F-labeled carboxylic esters within a hydrodynamically-driven micro-reactor. Lab Chip **2004**;*4*,523.

104. C.J. Steel, A.T. O'Brien, S.K. Luthra, F. Brady. Automated PET radiosynthesis using microfluidic device. J. Labelled. Compd. Radiopharm **2007**;*50*,308.

105. A. de la Hoz, A. Diaz-Ortiz, A. Moreno. Microwaves in organic synthesis. Thermal and non-thermal microwave effects. Chem. Soc. Rev. **2005**;*34*,164.

106. C.-C. Lee, G. Sui, A. Elizarov, C.J. Shu, Y.-S. Shin, A.N. Dooley, J. Huang, A. Daridon, P. Wyatt, D. Stout, H.C. Kolb, O.N. Witte, N. Satyamurthy, J.R. Heath, M.E. Phelps, S.R. Quake, H.-R. Tseng. Multistep Synthesis of a Radiolabeled Imaging Probe Using Integrated Microfluidics. Science **2005**;*310*,1793.

107. P.K. Jörg, C.J. Stephen, J.M. Ramsey. Solid phase extraction on microfluidic devices. J. Microcolumn Sep. **2000**;*12*,93.

108. R.D. Oleschuk, L.L. Shultz-Lockyear, Y. Ning, D.J. Harrison. Trapping of bead-based reagents within microfluidic systems: on-chip solid-phase extraction and electrochromatography. Anal. Chem. **2000**;*72*,585.

109. K.H. Bleicher, H.-J. Böhm, K. Müller, A.I. Alanine. A Guide to Drug Discovery: Hit and Lead Generation: Beyond High-Throughput Screening. Nature Reviews Drug Discovery **2003**;*2*,369.

110. S.A. Sundberg. High-Throughput and Ultra-High-Throughput Screening: Solution and Cell-based Approaches. Current Opinion in Biotechnology **2000**;*11*,47.

111. M. Schena, D. Shalon, R.W. Davis, P.O. Brown. Quanitative Monitoring of Gene Expression Patterns with a Complementary DNA Microarray. Science **1995**;*270*,467.

112. Y. Matsumura, H. Maeda. A New Concept for Macromolecular Therapeutics in Cancer Chemotherapy: Mechanism of Tumoritropic Accumulation of Proteins and the Antitumor Agent Smancs. Cancer Res. **1986**;*46*,6387.

113. J.L. Duffner, P.A. Clemons, A.N. Koehler. A pipline for ligand discovery using small molecule microarrays. Current Opinion in Chemical Biology **2007**;*11*,74.

114. G. MacBeath, A.N. Koehler, S.L. Schreiber. Printing Small Molecules as Microarrays and Detecting Protein-Ligand Interactions en Masse. J. Am. Chem. Soc. **1999**;*121*,7967.

115. N.L. Pohl. Fluorous Tags Catching on Microarray. Angewandte Chemie International Edition **2008**;*47*,3868.

116. E. Kissa. Fluorinated surfactants in blood. Journal of Fluorine Chemistry **1994**;*66*,5.

117. C.J. Mathias, S.R. Bergmann, M.A. Green. Species - dependant binding of Copper (II) *Bis*(thiosemicarbazone) radiopharmaceuticals to serum albumin. Journal of Nuclear Medicine **1995**;*36*,1451.

APPENDIX A: Supplementary Data

A.1 – Benzyl 2,2′-(3-perfluorooctylpropylazaenediyl)diacetate, $C_{29}H_{24}F_{17}NO_4$, (3)

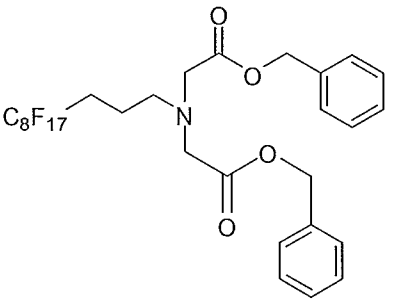

^1H NMR in $CDCl_3$ (600.13 MHz)

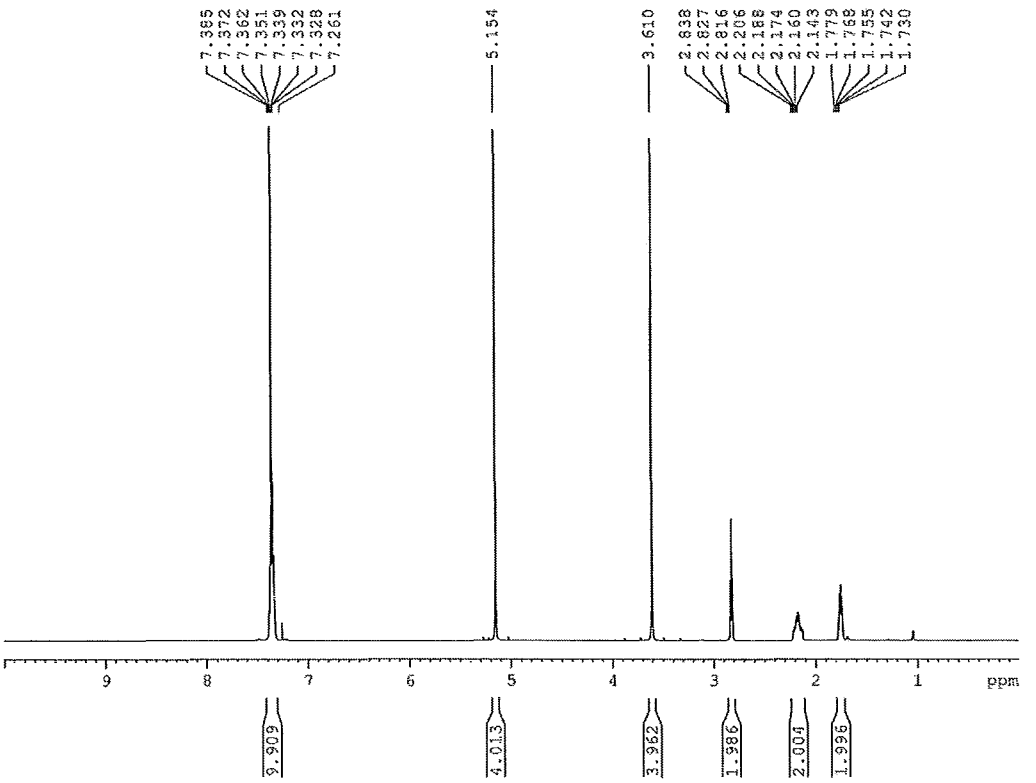

^{13}C NMR in $CDCl_3$ (150.90 MHz)

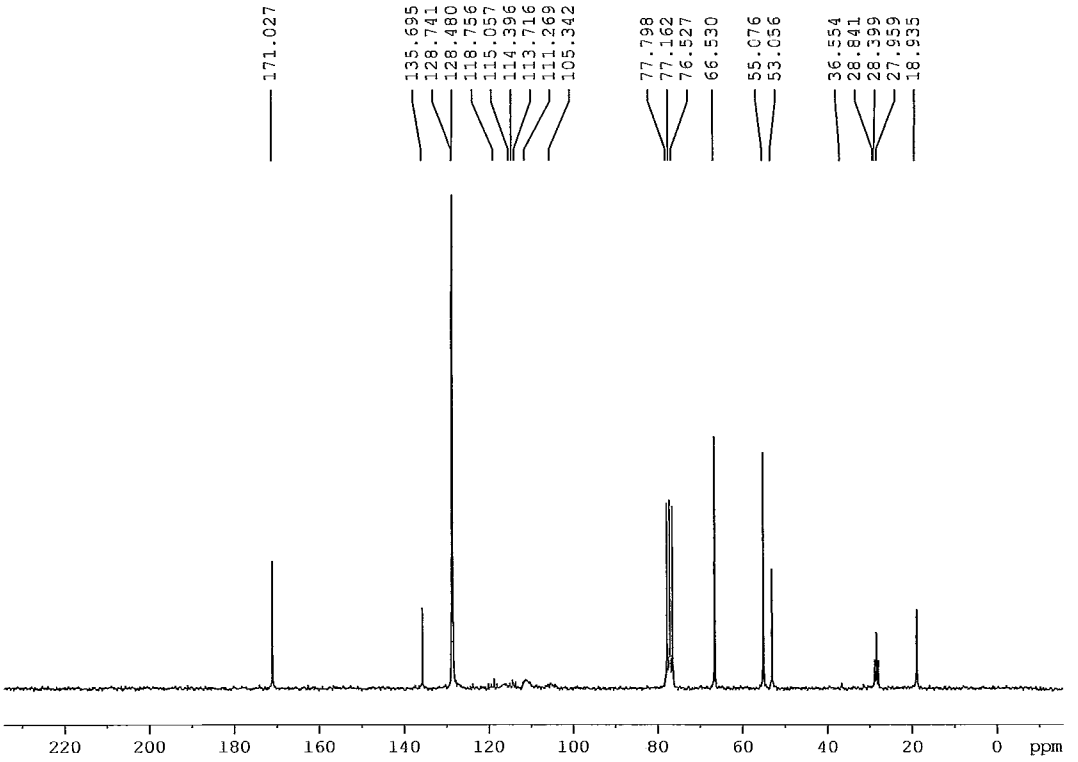

FT-IR on KBr Window

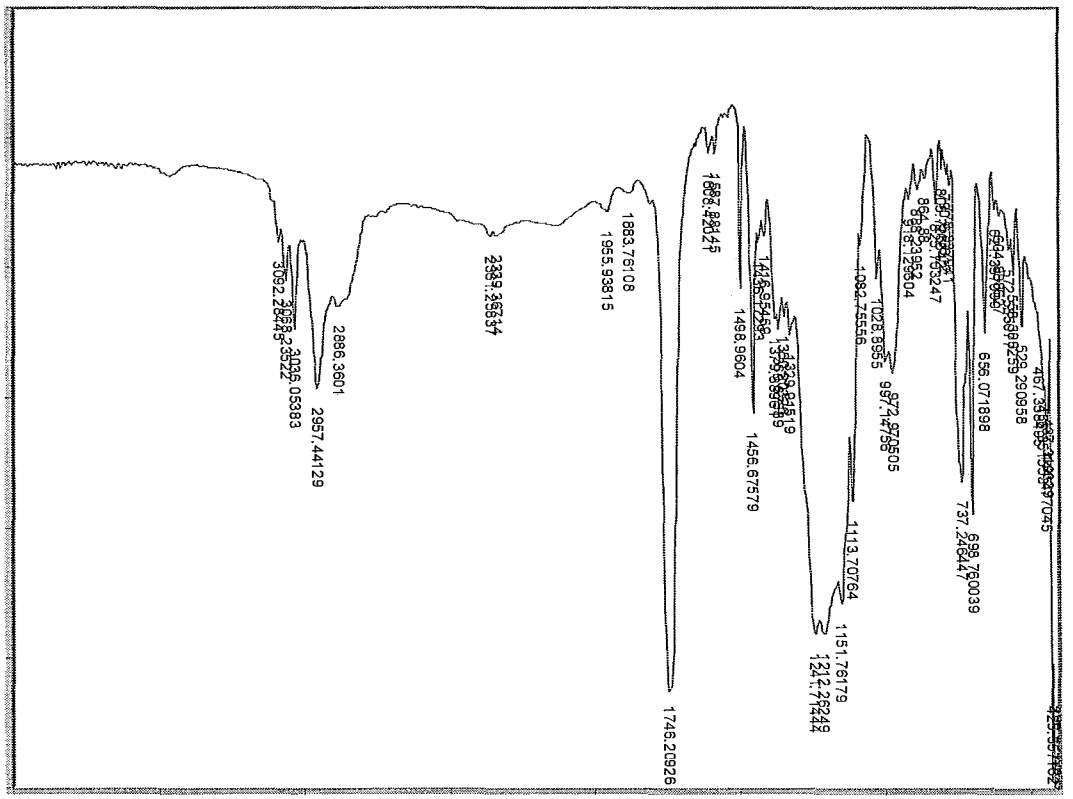

High Resolution ESI-MS

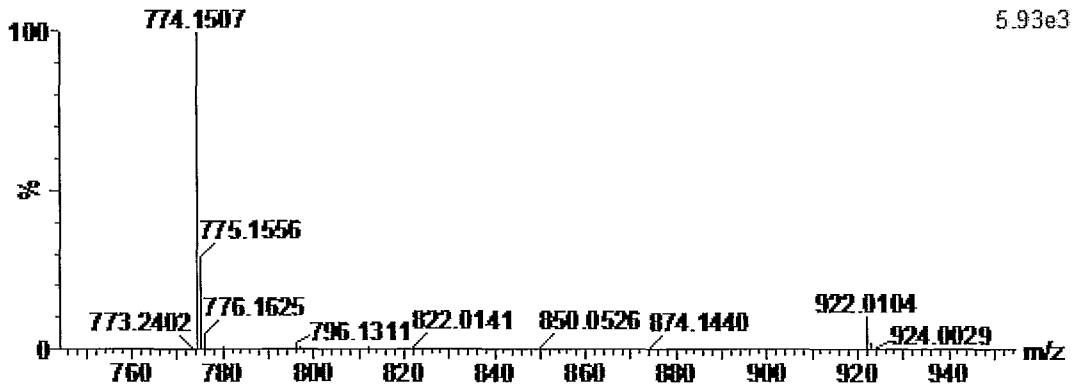

A.2 – 2,2′-(3-Perfluorooctylpropylazanediyl)diacetic acid, $C_{15}H_{12}F_{17}NO_4$, (4)

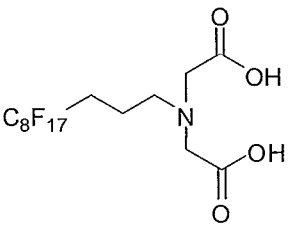

^1H NMR in CD_3OD (600.13 MHz)

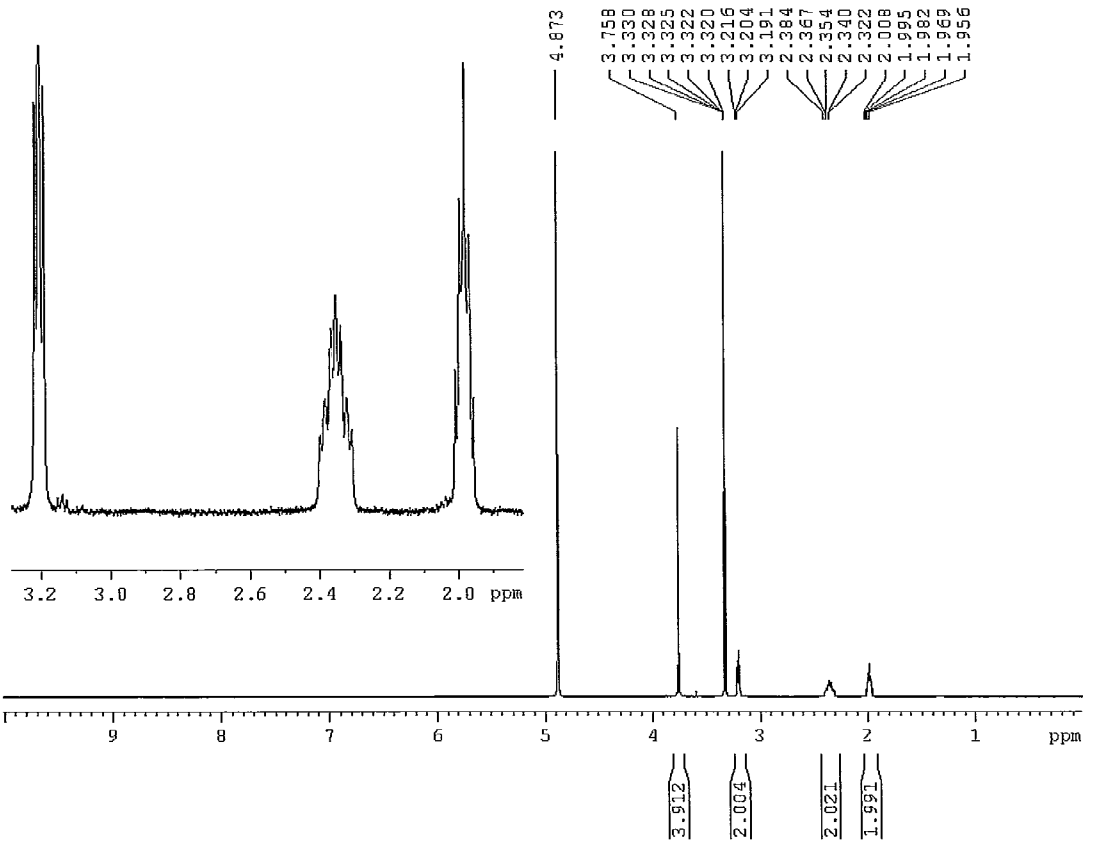

^{13}C NMR in CD_3OD (150.90 MHz)

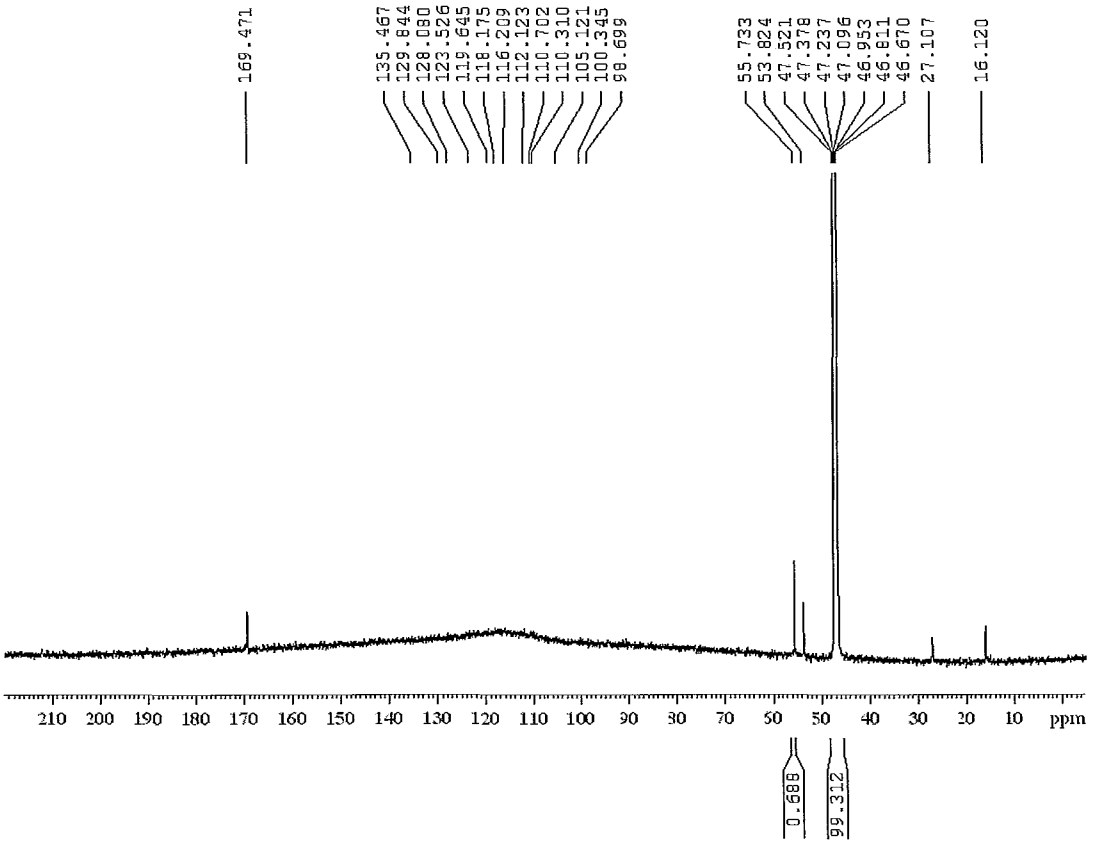

FT-IR in KBr Window

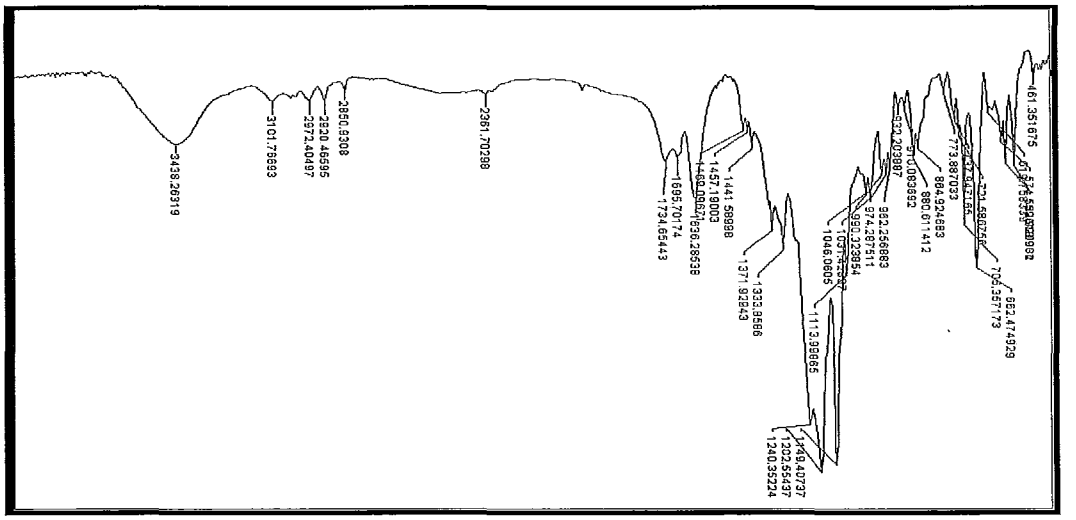

High resolution ESI-MS

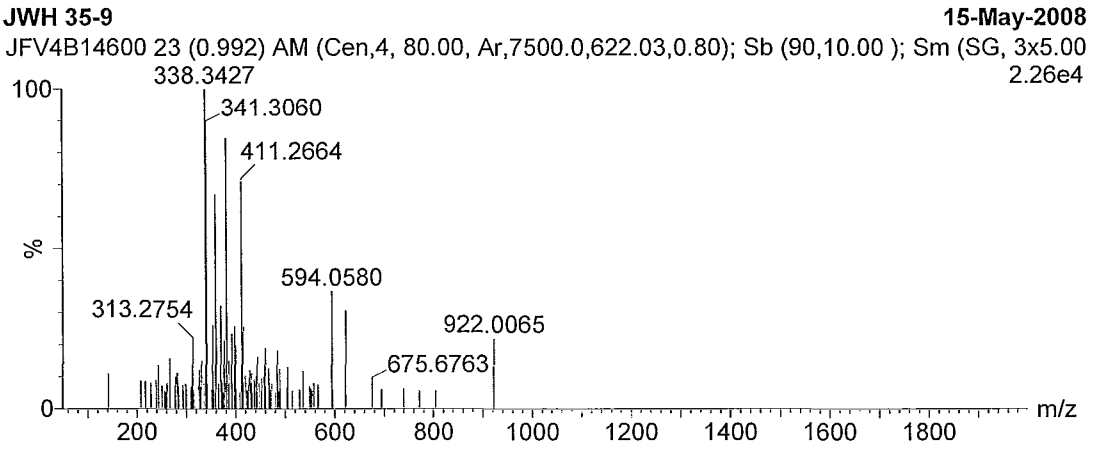

A.3 - Copper II 2,2′-(3-perfluorooctylpropylazanediyl)diacetate, $C_{15}H_{10}F_{17}NO_4\ Cu^{2+}$ (5)

FT-IR in KBr Window

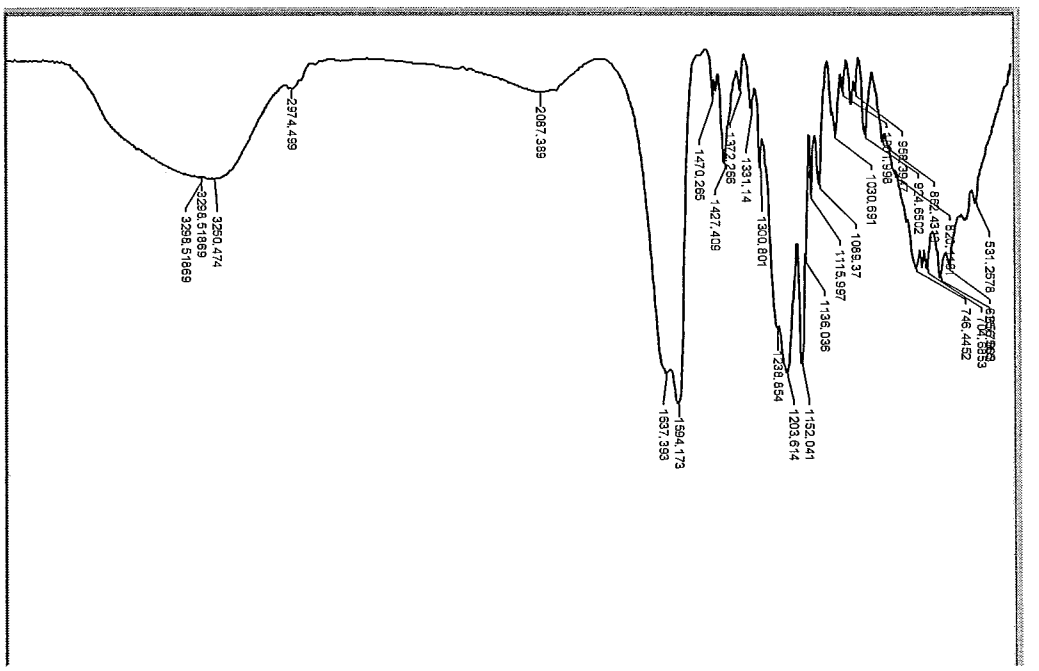

High resolution ESI-MS

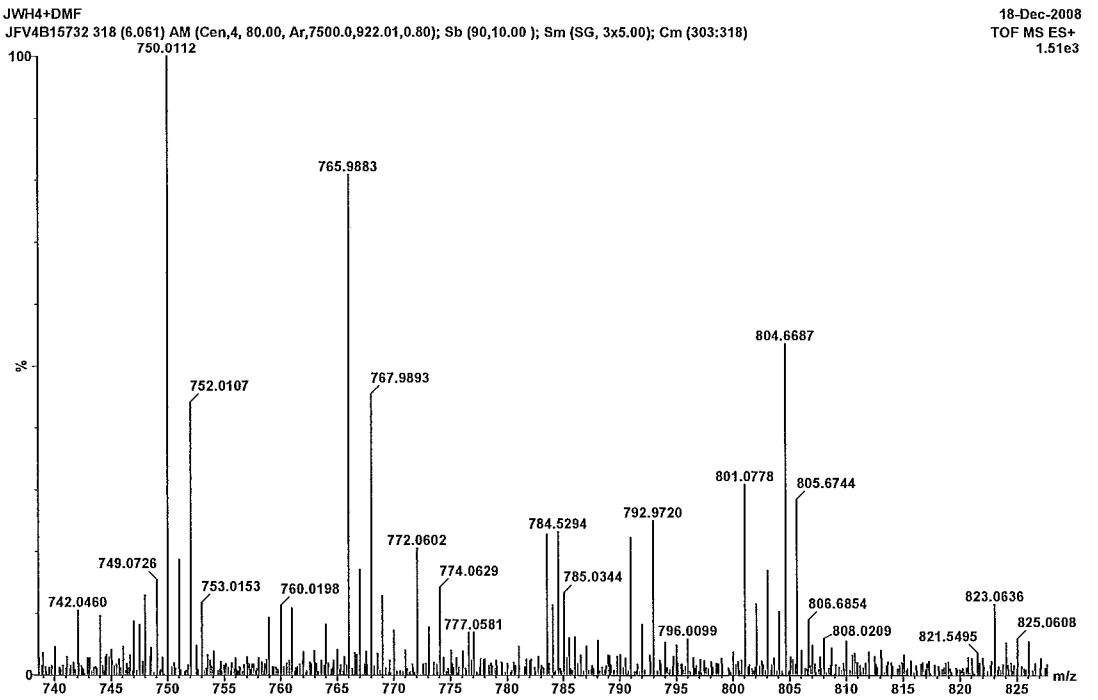

Single Mass Analysis
Tolerance = 100.0 PPM / DBE: min = -1.5, max = 200.0
Isotope cluster parameters: Separation = 1.0 Abundance = 1.0%

Monoisotopic Mass, Odd and Even Electron Ions
10 formula(e) evaluated with 1 results within limits (up to 5 closest results for each mass)

Minimum:				-1.5		
Maximum:		5.0	100.0	200.0		
Mass	Calc. Mass	mDa	PPM	DBE	Score	Formula
801.0778	801.0768	1.0	1.3	2.5	1	C21 H25 N3 O6 F17 Cu